AIM2015: Documentation

Lynnette M. Dray, Corresponding Author
Air Transportation Systems Lab, UCL Energy Institute
14 Upper Woburn Place, London, UK WC1H 0NN
Tel: +44 (0)7886678564 Fax: +44 (0)2076792000; Email: l.dray@ucl.ac.uk

27.1.20

1. Introduction

The Aviation Integrated Model (AIM) is a global aviation systems model which simulates interactions between passengers, airlines, airports and other system actors into the future, with the goal of providing insight into how policy levers and other projected system changes will affect aviation's externalities and economic impacts. The model was originally developed in 2006-2009 with UK research council funding (e.g. Reynolds et al., 2007). Subsequently it was used in a variety of EC Framework 7 projects, including TOSCA, Team_play and MetaCDM (e.g. Dray et al. 2012).

More recently it has been substantially updated as part of the ACCLAIM project (2015-2018) between University College London, Imperial College and Southampton University. The ultimate aim of the ACCLAIM project is to produce a tool which can assess the local and system-wide impacts of adding capacity at constrained airports, with a particular focus on the current challenges facing the London airport system. AIM2015 is related to, but separate from, the airline behaviour model developed by the ACCLAIM project (e.g. Doyme et al., 2019; Evans and Schäfer, 2014)[1]. AIM2015 does not include detailed airline profit optimisation, but does include a number of substantial updates on previous versions of the model, including a 2015 base year, passenger itinerary choice and fare modelling, more detailed fleet representation and integrated externalities modules. Run time has also been substantially reduced: a single model run now takes approximately forty minutes – three hours, depending on the input parameters. The model is open-source; this document is intended to be distributed with the model code.

This version of the documentation is intended to accompany v9[2] of the main AIM code. Changes in v9 over v8 include:

- Updated OD demand, itinerary choice and fare models,
- Aircraft performance model estimates flight time by phase as well as emissions,
- New PM model, based on FOX methodology (Stettler et al. 2013),
- Estimation of NO_2 as well as NOx totals,
- Integration of a climate impacts metamodel,
- Integration of rapid dispersion code (RDC, Barrett & Britter 2008) to calculate the distribution of primary PM and NO_2 from aircraft engines around airports,
- Integration of single-metric noise calculations (SINE, LkAeq and quota count),
- Inclusion of electric aircraft as a technology option, with extension of the technology input data, and

[1] The airline behaviour model (ABM) is an optimisation model which simulates airline profit maximisation, and so can be used to assess system impacts from competition-related phenomena (for example, cost pass-through and scarcity rents at congested airports). Due to the increased complexity and model runtime inherent in simulating competition, the airline behaviour model is more suitable for assessing detailed regional impacts of system changes in a single near-future year, and AIM2015 is more suitable for projecting long-term global impacts.

[2] The version number is updated each time there is a major addition to the codebase. Versions 1-6 corresponded to the original 2006-2009 development of the AIM. Version 7 was the initial code and base year update for the ACCLAIM project; version 8 introduced further improvements in cost, performance and technology modelling.

- The availability of input data files which do not contain confidential data.

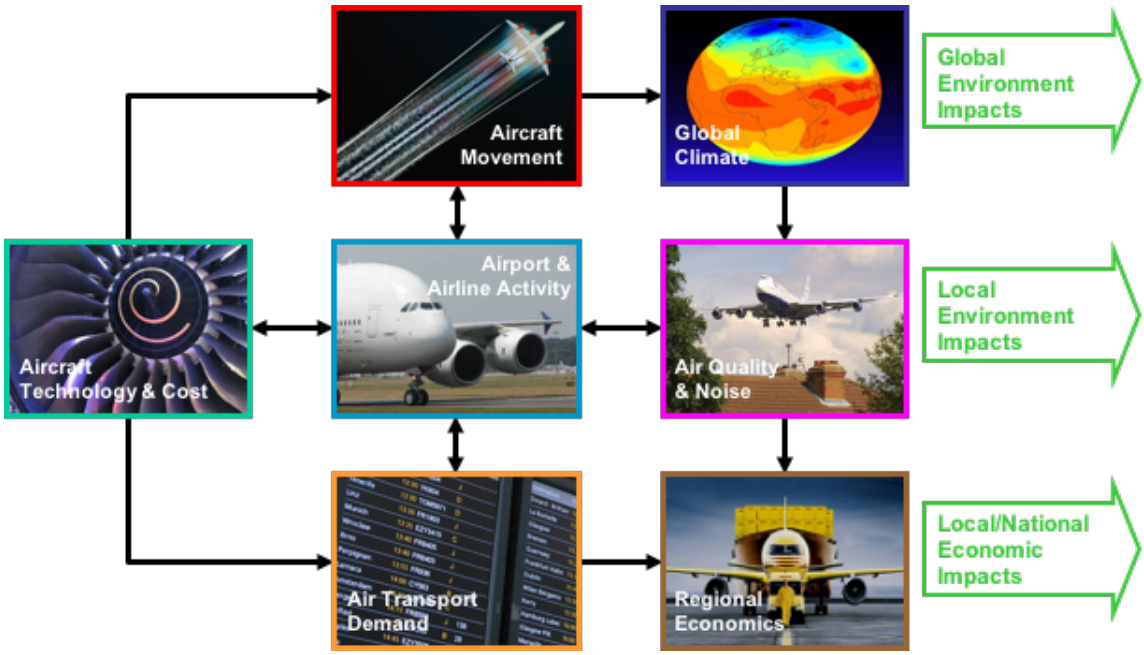

Figure 1. AIM 2015, broad structure.

The basic structure of AIM is shown in Figure 1. AIM consists of seven interconnected modules. The demand module projects true origin-ultimate destination demand between a set of cities representing approximately 95% of global scheduled revenue passenger-kilometres (RPK), and assesses which of the available routes they will use to take these journeys. Fares are simulated using a fare model and based on airline costs and other factors. The airline and airport activity module assesses which aircraft will be used to fly these routes and at what frequency, what the resulting airport-level movements are and how this translates into delay at each airport. The aircraft movement module assesses the corresponding airborne routes and the consequent location of emissions. The aircraft technology and cost module assesses the size, composition, age and technology use of the aircraft fleet, and the resulting costs for airlines and emissions implications. These four modules are run iteratively until a stable solution is reached. Data is then output which can be used in the impacts modules, shown on the right of Figure 1. The global climate module is a rapid, reduced-form climate model which calculates the resulting climate metrics (e.g. CO_2e in terms of global temperature potential (GTP) and global warming potential (GWP) at different time horizons). The air quality and noise module are similarly rapid, reduced-form models which provide metrics by airport for the noise and local/regional air quality impacts of the projected aviation system. The regional economics module looks in more detail at the economic impacts, including benefits such as increased employment as well as costing of noise and air quality impacts. The output data from the first four AIM modules can also be used more generally as input to external impacts models: for example, the model includes the option to produce detailed emissions inventories which can be input into climate models. A more detailed representation of the model structure, including sub-models and data flows, is given in Figure 2. Models which have been added or updated for AIM2015 are shown with a white background. Additionally, as part of the ACCLAIM project the demand, fare and airline activity blocks can be substituted by an airline behavior model which estimates the airline

response to system changes by maximizing airline profit. This model is not included in AIM2015 but more information is available on it on request. Each individual sub-model is discussed in more detail in the sections below.

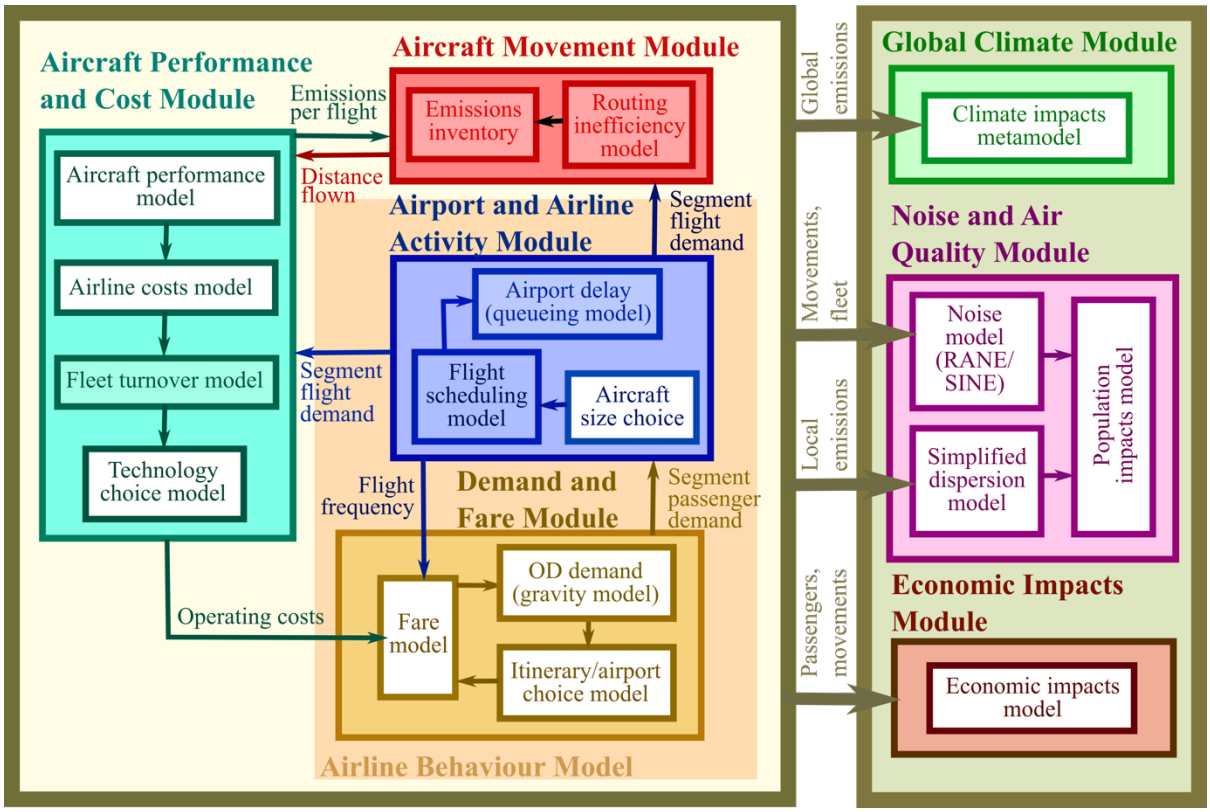

Figure 2. AIM, detailed structure showing sub-modules.

The structure of the rest of the report is as follows. Section 2 discusses the scope of the model, in terms of flights and airports covered, aircraft size classes, passenger types and types of modellable policy. Section 3 discusses the methodology for each module in more detail. Section 4 discusses the future projections that are needed to run the model. In section 5, we show validation outcomes for the integrated model, including outcomes for 2005-2015 using 2005 base year data. In Section 6, we discuss how to run the model, what inputs are needed, and what outputs are produced. The appendices contain parameter estimates for some of the models discussed below.

2. Scope

2.1 Types of flight

There are many different components to the global aviation system. As well as passengers, airlines carry mail and cargo – sometimes in the holds of passenger aircraft, sometimes in separate cargo aircraft. Flights may be scheduled or unscheduled. Military and general aviation are also sources of aviation fuel use and emissions, as are helicopter flights. Whilst a relatively large amount of data is available on scheduled passenger flights, this is not the case with other types of flight. For example, very little information is available about military flights and their fuel use.

Currently AIM models only scheduled passenger flights. It accounts for the weight of hold freight when modelling fuel use, but does not model separate freighter flights[3]. When comparing model outputs with external fuel and emissions inventories that are based on fuel uptake from all sources (e.g. IEA (2017) we would expect AIM to produce output that is somewhat below observed global totals. In particular, freight in 2015 accounted for around 24% of global aviation tonne-km performed (ICAO, 2016). We take account of hold freight in passenger aircraft when modelling aircraft weight load factor, but do not account for dedicated freighter aircraft, which carry around 40-50% of air freight (e.g. FTA, 2008). Unscheduled passenger flights accounted for 5% of global RPK in 2015 (ICAO, 2016), and military aviation has been estimated to be around 7-13% of aviation fuel use (Wilkerson et al. 2010; ICCT, 2019). Therefore we would expect our base year total fuel use to be approximately 20-30% below the IEA total fuel use from all sources, as observed in Section 5.

2.2 Geographic scope

There is no set limit on the number of cities or airports that can be modelled with AIM. However, the year-2015 and year-2005 base year datasets contain data for sets of cities and airports that account for around 95% of global RPK. These flights are modelled in detail, but we also approximate some quantities for flights to and from the airport set from airports outside the set, to get the correct airport movement totals at each airport, which are needed for emissions and delay modelling. The base year 2005 dataset includes 699 cities and 1127 airports, between which 29803 separate flight segments are modelled. The base year 2015 dataset includes 878 cities (including a more detailed set of minor UK airports) and 1169 airports, between which 40265 separate flight segments are modelled. Airports are grouped into cities primarily by a distance-based criterion: we assume two airports are likely to be in the same city region if they are within 31km of each other and there is a straightforward ground connection between them. Other airports are dealt with on a case-by-case basis. We allow city regions to extend across national borders (with the exception of closed borders) as there are numerous global examples of airports serving cities in adjacent countries (for example, Basel airport serves Swiss, French and German demand). We exclude airports which had no scheduled flights in the base year, as derived from global schedule data (Sabre 2017). In the model input databases, the full list of cities is given in the file *CityData.csv* and the full list of airports is given in the file *AirportData.csv*. The base year flight network for 2015 is shown in Figure 3; busier routes are indicated with darker/thicker lines, airports are shown as dots, and cities are filled circles scaled with city population.

[3] Because hold freight flows are estimated in AIM, it is possible to produce simple models of freighter networks in situations where aggregate air freight flows are available (for example, at a country-country level), by subtracting hold freight from total air freight flows and using aggregate data on freighter fleet capacity and load factor. In situations where AIM emissions projections including freight are required (e.g. Dray & Doyme, 2019), this is the approach which has been used.

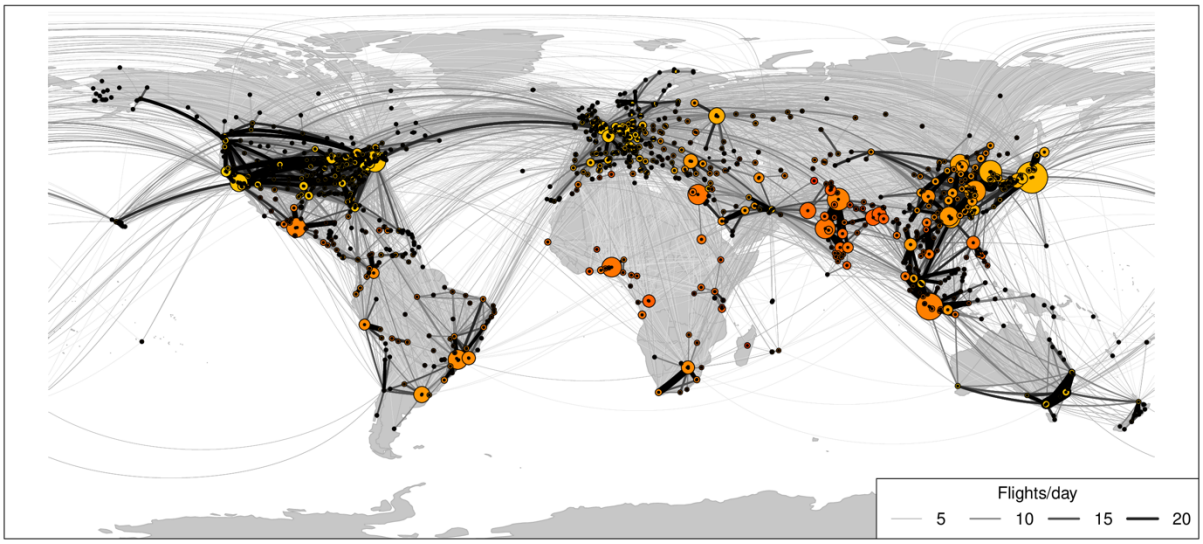

Figure 3. Base year flight network for the 2015 base year model.

There is no absolute requirement to run the full global city or airport set when running AIM – it is possible to run a subset of airports (e.g. just Europe) if a shorter runtime is needed or other regions are not of interest. However, this means that flights into and out of the subset of airports will only be approximately modelled.

2.3 Aircraft size classes

For the current version of AIM, we use nine aircraft size classes. These are adapted from the Sustainable Aviation aircraft size classes (e.g. Sustainable Aviation, 2015). Sustainable Aviation is a collaborative project between major UK airlines, airports, air navigation service providers and manufacturers, aimed at delivering a long-term strategy which allows the industry to grow in a sustainable fashion. This represents a substantial increase in resolution over previous versions of AIM, which used a three-size classification (e.g. Dray et al. 2014), and allows more detailed assessment of noise, fuel use and local air quality impacts. Aircraft are assigned to classes based on number of seats and MTOW. In Figure 4 we show base year classification across all aircraft models (excluding freight and combi aircraft) by typical seat number, MTOW and year 2015 aircraft-km performed (AKM; RJ = Regional jet, SA = Single-aisle, TA = twin-aisle, VLA = very large aircraft).

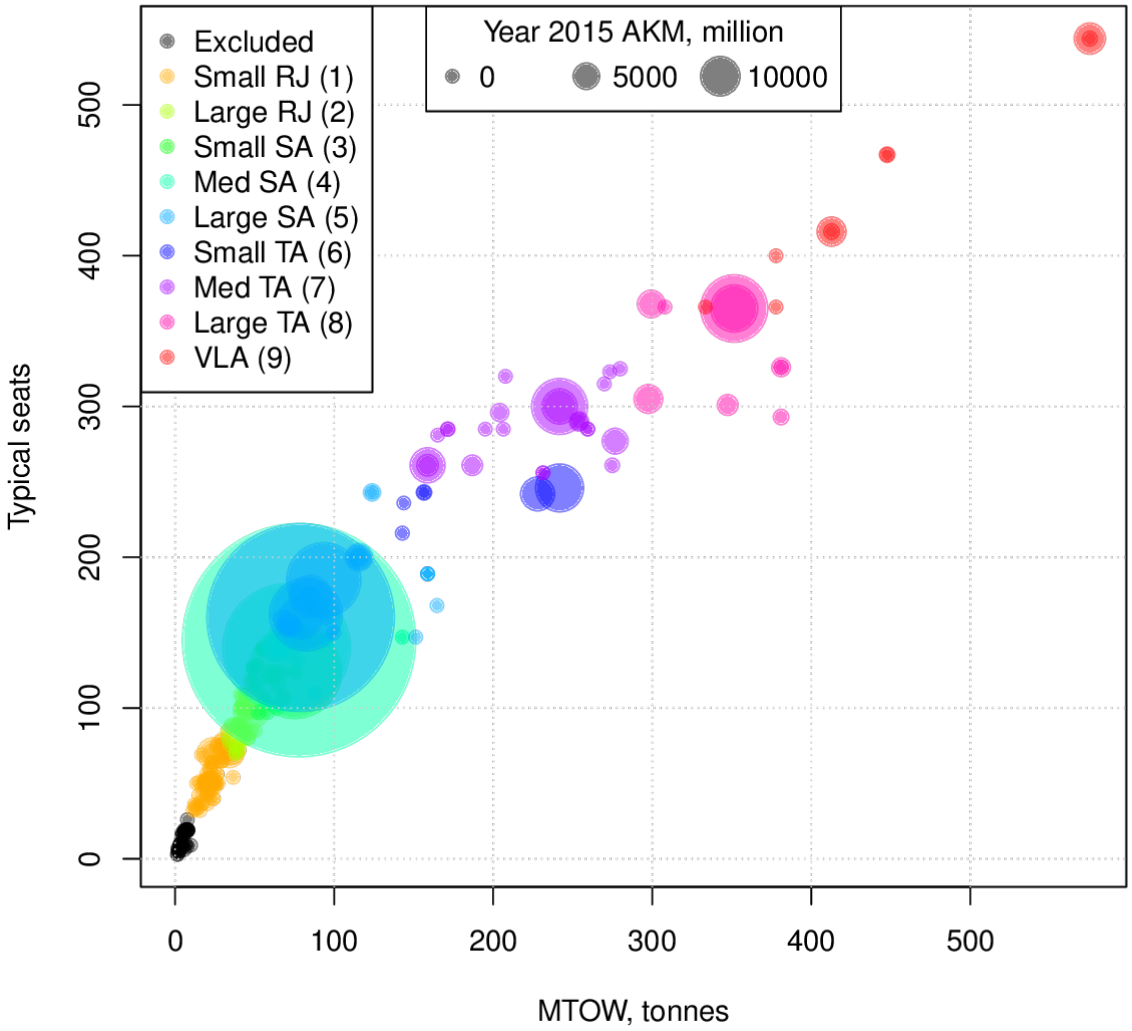

Figure 4. Aircraft size classification by MTOW and typical number of seats.

To model baseline emissions, noise and cost, we need to use a reference aircraft to represent each size category. These are shown in Table 1. Reference aircraft are chosen based on their share of base year AKM in their size class and the need to have a representative spread of different airframe and engine manufacturers. The reference aircraft are primarily used in the aircraft performance and cost models described in the section below on the Aircraft Technology and Cost model. Reference engines are used to derive some engine parameters that are used for emissions modelling, e.g. for PM.

Table 1. Aircraft size classes used in the updated AIM model

Size Category	Approx. seat range	Reference aircraft	Reference engine
1. Small regional jet	30-69	CRJ 700	GE CF34 8C5B1

2.	**Large regional jet**	70-109	Embraer 190	GE CF34 10E6
3.	**Small narrowbody**	110-129	Airbus A319	V.2522
4.	**Medium narrowbody**	130-159	Airbus A320	CFM56-5B4
5.	**Large narrowbody**	160-199	Boeing 737-800	CFM56-7B27
6.	**Small twin aisle**	200-249	Boeing 787-800	GEnx-1B67
7.	**Medium twin aisle**	259-299	Airbus A330-300	Trent 772B
8.	**Large twin aisle**	300-399	Boeing 777-300ER	PW4090
9.	**Very large aircraft**	400+	Airbus A380-800	EA GP7270

2.4 Types of Passenger

Demand models frequently divide passengers according to the purpose of their trip (e.g. business/leisure) and/or by categories such as age, gender or employment status. In the current version of AIM, only a single passenger category is used. We use average fare over all ticket types and do not track whether passengers choose economy or higher-class tickets. This is primarily a reflection of data availability and the current demand model in use (see Section 3.1) and is planned to be addressed in future versions of the model. We anticipate modelling demand at least for economy (including premium economy) and higher (business plus first class) tickets. One consequence of this is that we do not track the different responses of business and leisure passengers to changes in fare (e.g. IATA, 2007; business passengers are typically less price-sensitive).

2.5 Policy Assessment

AIM can be used to assess a wide range of scenarios and policy options. In the past, it has been used to assess the impact of ticket taxes (e.g. Dray et al. 2008); emissions trading (e.g. Dray et al. 2009); alternative fuels (e.g. Krammer et al. 2013); the availability of new aircraft technologies (e.g. Timmis et al. 2015; Dray et al. 2018); the retirement and replacement of older aircraft funded by a carbon tax (Dray et al. 2014); to assess uncertainty due to future uncertainty in global income, population and fuel price trends (e.g. Dray et al. 2019); and to assess carbon leakage due to country-level aviation policy (Dray & Doyme, 2019). Many other policy options are modellable with only minor adaptations. If you are unsure whether AIM is suitable to model a particular policy option, it is best to ask the modelling team via one of the contacts in the contacts section at the end of this report.

3. Methodology

3.1 Demand Module

The demand model contains three major components. True origin-ultimate destination between each pair of cities in the model is projected using an OD demand model. This demand is then distributed between available itineraries using an itinerary choice model. The demand and itinerary choice are influenced by itinerary fares, which are calculated by a fare model which uses airline costs from the Aircraft technology and cost model as an input. These three models are discussed individually below.

3.1.1 OD demand model

The OD demand model projects true origin – ultimate destination demand between a set of global cities. For the updated model, we use a gravity-type model similar to that used in the original AIM (e.g. Dray et al. 2014):

$$\ln N_{od} = \beta_0 + \beta_1 \ln(P_o P_d) + \beta_2 \ln(I_o I_d) + \beta_3 \ln(f_{od} + vot\, t_{od}) + \sum_i \beta_i D_{od}^i,$$

where N_{od} is the total passenger demand by any route between cities *o* and *d*, P_o and P_d are the populations of the greater metropolitan areas of *o* and *d* respectively, I_o and I_d are the per capita household incomes of *o* and *d*, f_{od} is the average fare for passengers travelling between these cities over all routes, *vot* is the passenger value of time, t_{od} is the average time (including delay) to travel between the two cities, D_{od} are dummy variables capturing other elements of the city-city connection (e.g. whether it is a domestic route, whether a road or high-speed rail link exists between the cities, etc.), and the parameters *ß* are estimated. Elasticity parameters by world region-pair and distance (short-, medium- or long-haul) are taken from Dray et al. (2014), including the use of IATA-recommended income elasticities (IATA, 2007). Values of time for air travel are taken from US estimated values and adjusted for different world regions by purchasing power parity (PPP) gross domestic product (GDP) per capita as in INFRAS/IWW (2000). To account for city-city level factors which are not captured in this model (for example, people from city A having a historical preference for taking holidays in City B), we also scale origin-destination flows by the ratio of actual to modelled demand in the base year.

The main parameters used in this model are given in Appendix 1. The code for the demand model is in the file *runDemandModel_v10.java* and OD demand is modelled in the subroutine *ODdemand*. Data on base year city characteristics is given in *CityData.csv*, and on characteristics by city-pair in *DataByCityPair.csv*. Model parameters are included in the file *Elasticities.csv*.

3.1.2 Itinerary choice model

Most air journeys give passengers multiple itinerary options. For example, travel may be direct or via a hub airport. In previous versions of AIM, passenger routing choices were fixed at base year values. However, this fails to take account of how passengers may modify their decisions if the characteristics of one or more routing options change. In this version (v9), we

directly model passenger itinerary choice using a multinomial logit model. The number of passengers between cities *o* and *d* on itinerary *k* in year *y* is modelled as

$$N_{odky} = \frac{N_{ody} e^{V_{odky}}}{\sum_j e^{V_{odjy}}} ,$$

where the deterministic part of the utility, V_{odky}, for an itinerary *k* between cities *o* and *d,* travelling between airport *m* in *o* and and airport *n* in *d*, is:

$$V_{odky} = \gamma_0 + \gamma_1 f_{odky} + \gamma_2 t_{odky} + \gamma_3 \log freq_{odky} + \gamma_4 Nlegs_{odky} + \gamma_5 P_{m,y-1} + \gamma_6 P_{n,y-q} ,$$

and f_{odky} is the itinerary fare as estimated by the fare model (Section 3.1.3), t_{odky} is the total itinerary travel time, $freq_{odky}$ is the itinerary frequency, $Nlegs_{odky}$ is the number of flight legs in the itinerary, $P_{m,y-1}$is the total number of passengers using airport *m* in the previous year, and the parameters γ are estimated. Note that this is a change from version 8 of AIM, as used in Dray et al. (2018), which used origin and destination airport fixed effects. Passenger numbers, schedule and fare data are taken from Sabre (2016). Parameter estimates for major world regions are given in Appendix 2. The code for the demand model is in the file *runDemandModel_v10.java* and itinerary choice is modelled in the subroutine *CalculateItinerary*. Model parameters are included in the file *Elasticities.csv*.

3.1.3 Fare model

In previous versions of AIM, changes in fares from base year values were modelled based only on changes in airline cost. In reality, there are many more factors that affect the fares on a given route. For demand between cities *o* and *d*, passengers will have the option of multiple different airport-airport itineraries *k*, from some airport *m* in *o* to some airport *n* in *d*, and potentially via some number of hub airports. For this version (v9), we have estimated a detailed fare model to calculate the average fare for each available passenger itinerary:

$$\ln f_{odk} = \alpha_0 + \alpha_1 \ln FC_{odk} + \alpha_2 \ln CP_{odk} + \alpha_3 \ln CF_{odk} + \alpha_4 \ln CUI16_{mn} + \alpha_5 \ln AHHI_{mn} + \alpha_6 \ln LHHI_{odk} + \alpha_7 \ln Freq_{odk} + \alpha_8 \ln N_{odk} + \alpha_9 LF_{odk} + \alpha_{10} \ln RS_{odk} + \alpha_{11} Nlegs_{odk} + \alpha_{12} H_{odk} + \alpha_{13}(C_m) + \alpha_{14}(C_n)$$

where f_{odk} is the fare between cities *o* and *d* on itinerary *k*, FC_{odk} is the sum of fuel cost per passenger over all segments on the itinerary, CP_{odk} and CF_{odk} are the sum of per-passenger and per-flight based nonfuel costs over all segments on the itinerary, $CUI16_{mn}$ is the mean of the average 16-hour capacity utilisation index (CUI) for airports *m* and *n*, $AHHI_{mn}$ is the mean airport-level Herfindahl-Hirschmann Index (HHI)[4] over airports *m* and *n*, $LHHI_{odk}$ is the geometric mean of the city-pair HHI for all segments on itinerary *k*, $Freq_{odk}$ is the yearly frequency of the given itinerary, N_{odk} is the number of passengers using this itinerary, LF_{odk} is the geometric mean of passenger load factor over all segments, RS_{odk} is the share of the total origin-destination passengers on this city-pair using the itinerary, $Nlegs_{odk}$ is the number of

[4] The HHI is the sum of the squares of the market shares (in passengers) of all airlines in the given market, and is used to assess the amount of competition in that market.

flight legs in the itinerary, and H_{odk} is the number of major hub airports used on itinerary k. The parameters α are estimated; α_{13} and α_{14} are origin and destination country fixed effects terms. Data on fares by itinerary, schedules and passenger numbers is taken from the Sabre Market Intelligence database (Sabre, 2016). Airline costs are generated by the airline cost model described in Section 2.7. Using the model, we obtain global fare per passenger-km of 0.09 year 2015 US dollars in 2015 and 0.10 year 2015 US dollars in 2016, using the 2015 base year model. These numbers match well to global estimates of total airline revenue per passenger-km performed (e.g. ICAO, 2016b) of around 0.11 year 2015 US dollars in 2015[5].

More information on this model, the estimated parameters, and its validation is given in Wang et al (2017; 2018). Fares calculated by the fare model are combined with passenger shares for different itineraries given by the itinerary choice model (Section 3.1.2) to calculate average fares by origin-destination city pair, which are then used in the demand model (Section 3.1.1). The model used in the current version of AIM has minor changes to that used in the previous version and the cited papers which reflect modest improvements in the input data. A table of main parameters is given in Appendix 3. The code for the demand model is in the file *runDemandModel_v10.java* and fares are modelled in the subroutine *CalculateFares*. Model parameters are included in the file *Elasticities.csv*.

In combination, the gravity, itinerary choice, and fare models project the number of passengers on each airport-airport segment. The three models interact extensively with each other, with the fare model balancing the demand side with the supply components of AIM, here expressed via airline costs. To find a solution, we iterate between all components of the model until segment demand is stable on all modelled segments. The resulting base year demand by airport in the 2015 base year model for the top 50 global airports is shown in Figure 5.

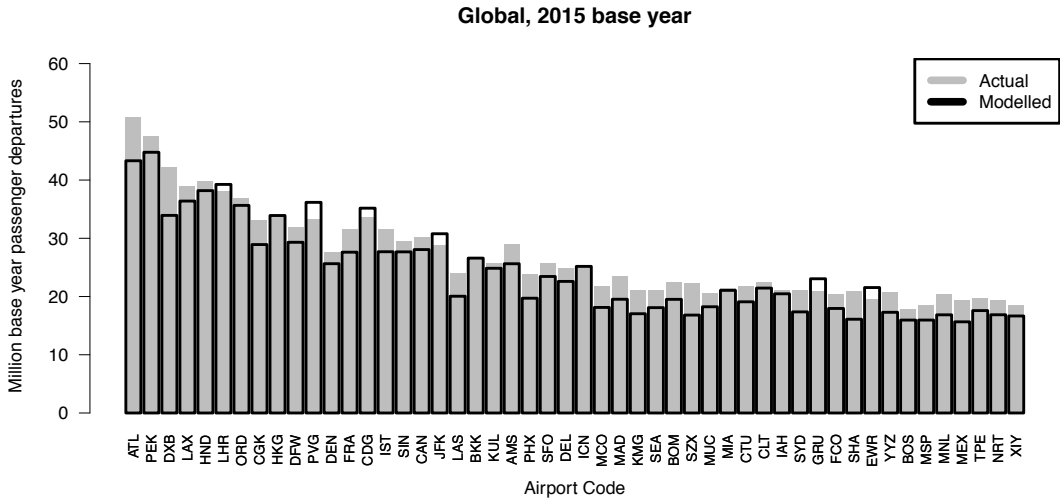

Figure 5. Total demand by airport, top 50 global airports in the 2015 base year.

[55] Note that we do not expect the two numbers to match exactly, as airline ancillary and cargo revenue are not included in our model. Ancillary revenue, which includes items such as food sales and website advertising, was around 3-8% of total revenue for US network carriers in 2011 (Hao 2014), and cargo revenue is around 2% (Stalnaker et al. 2016). Fare per RPK also includes some taxes that do not accrue to airlines. Nevertheless, we expect the two figures to be similar.

Modelled demand is typically within 10% of actual for most airports. Future versions of the model may further address the attraction of routing through of some airports (e.g. DXB) where the hub airport itself is marketed as an attractive destination, which at present is not well-captured.

3.2 Airport Activity Module

The Airport Activity Module takes passenger demand by segment from the Demand Module. It converts this to aircraft movements by segment and per airport, and calculates the resulting delays at a given airport capacity. Movements and delays are passed to the Aircraft Movement Module, which calculates the location and type of emissions; the Aircraft Technology and Cost Module, which uses them to estimate airline costs per route; and the Demand Module, where delays may influence passenger choice.

There are two main components to the Airport Activity Module. First, the proportion of aircraft of each size class (as given in Table 1) used on each route needs to be estimated. In combination with simple assumptions about load factor this gives the flight frequency per route. This is done by an Aircraft Size Choice Model. The flight frequency per route can be used to estimate the yearly number of movements at each airport. Given assumptions about how these movements are distributed through the day, this can be used to estimate airport delays; this is done by the Delay Model. Both are described individually below.

3.1.2 Aircraft size choice model

Once passenger demand per segment is generated, this needs to be translated into a feasible flight schedule. We use a multinomial logit model to project which aircraft types will be used on which segments, based on segment- and airport-specific variables such as segment demand, runway length and number of operating low-cost carriers in the base year. This is similar to the approach used in Reynolds et al. (2007) but has been updated for the current version of AIM to account for an increase in the number of aircraft size classes modelled and to include additional relevant variables. The proportion of aircraft, pr_{mns}, of each size class *s* on each segment between airports *m* and *n* is estimated as:

$pr_{mns} = \frac{e^{U_{mns}}}{\sum_j e^{U_{mnj}}}$, where

$$U_{mns} = \theta_0 + \theta_1 d_{mn} + \theta_2 h_m + \theta_3 h_n + \theta_4 N_{mn} + \theta_5 LF_{mn} + \theta_6 R_m + \theta_7 R_n + \theta_8 NLCC_{mn} + \theta_9 HHI_{mn},$$

and d_{nm} is the distance between airports *m* and *n*, h_m and h_n are dummy variables indicating whether *m* and *n* are major hub airports, N_{mn} and LF_{mn} are the number of passengers and the passenger load factor on the segment, R_m and R_n are the lengths of the longest runways at *m* and *n*, $NLCC_{mn}$ is the number of low-cost carriers operating on the segment, and HHI_{mn} is the segment HHI in terms of airline passenger share. Combined with typical load factors for each segment this allows the overall and size-specific flight frequency to be estimated. Main parameter estimates are given in Appendix 4. In Figure 6, we show the resulting proportion

of aircraft of each size class by distance as projected by the model, compared to actual year 2015 schedule data (Sabre, 2016).

As shown in Figure 6, the implied aircraft fleet by size and distance category is generally reproduced well, but is less accurate for the smallest aircraft size class. Applying the model to the base year flight network, the total global fleet for size classes 2-9 is reproduced to within ten percent in each case, but for the smallest size class we underpredict demand for aircraft by around 30%. This may reflect the specific use patterns of these aircraft and the carriers that use them, e.g. constraints at small regional airports with few facilities and small carriers with limited capital, which are not currently reflected in the model.

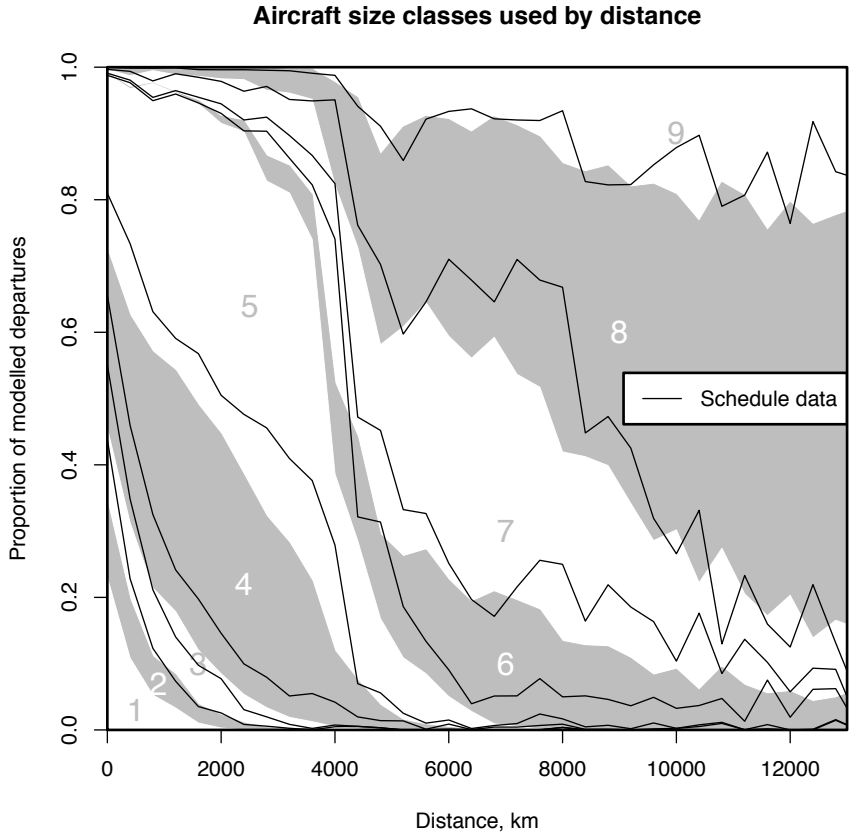

Figure 6. Modelled proportion of aircraft used by distance, compared to year 2015 schedule data.

Figure 7 shows the corresponding distribution of implied fleet by size class and world region, against implied fleet from base year schedule data (Sabre, 2017). As discussed above, the model underpredicts demand for the smallest size class across all regions. Other size class-region combinations are more closely matched. The model does not perfectly capture the split between medium and large single-aisle aircraft (size classes 4 and 5) in Asia and North America. This is primarily a reflection of the strong degree of overlap in the characteristics and use of these size classes. As future technologies are likely to have similar impacts across the narrowbody size classes via closely-related families of narrowbody aircraft (e.g. the Airbus A319/A320/A321 or Boeing 737 families) the overall impact on model outcomes of this is likely to be small.

We assume historical load factor values by airport-airport segment are maintained unless there is a specific intervention to change them (e.g. a new technology or operational measure is introduced which has an effect on load factor). In combination with the typical number of seats per size category and the estimated proportions of aircraft types per segment, this allows flight frequency by aircraft size on a segment to be estimated. It also allows demand for flights by airport to be assessed, so that delays can be calculated using the delay model.

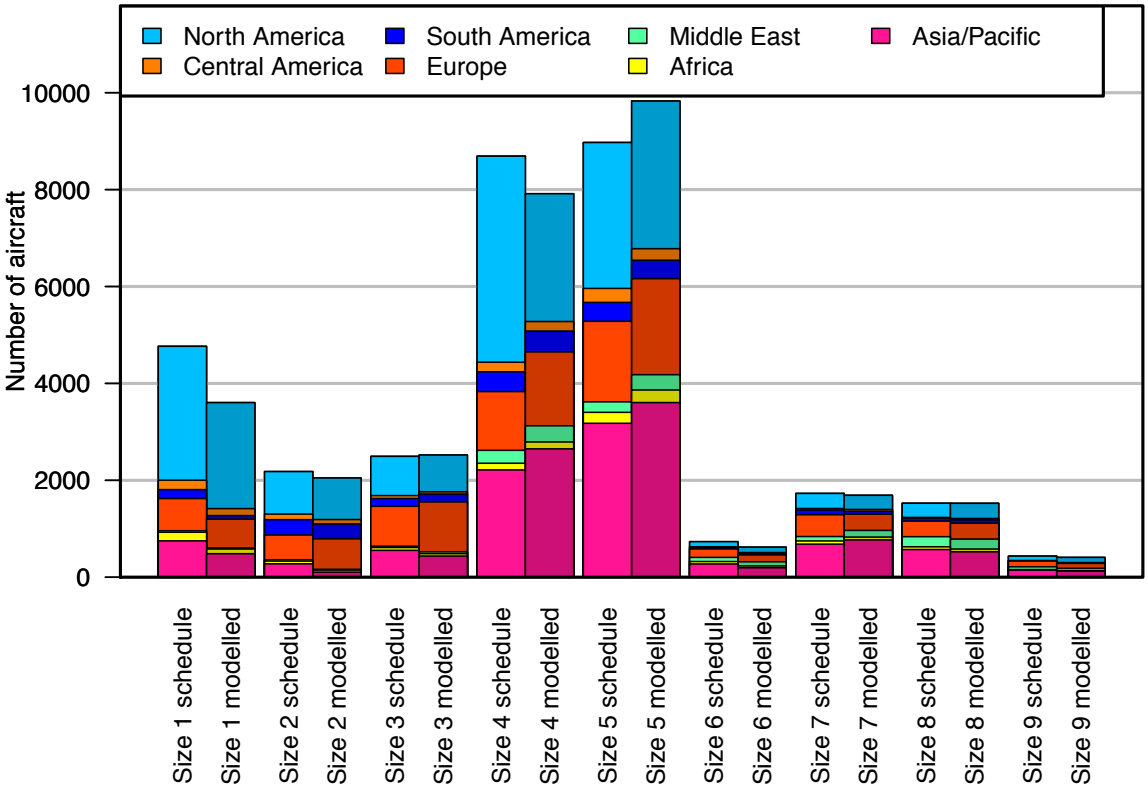

Figure 7. Implied fleet by size class and world region, model versus actual schedule data, for the 2015 base year.

The demand for aircraft by size class and world region is compared to the currently-existing fleet to assess the number of new aircraft required. In the case that more aircraft are already in the fleet than are currently needed, we assume that the excess aircraft are put into storage; aircraft in storage may be reactivated in a subsequent year if demand increases enough that they are needed, or may retire directly from storage, depending on their age and the retirement model parameters (e.g. Dray, 2013). This assumption means that where the model over-predicts aircraft demand for a given size class and region, new aircraft are ordered, but aircraft are not initially removed from the fleet in size classes and regions where the model under-predicts demand. As discussed further in Section 5, this leads to total fleet overestimates in the first few years of a full model run if stored aircraft are not accounted for, which correct themselves over approximately a five-year period due to natural fleet turnover.

The aircraft size choice model is in the file *run_FRSMdl_v8.java*, which is called from the main airport activity module (*run_ArptActMdl_v24_comb.java*).

3.2.2 Delay model

The rapid delay model used in AIM is described extensively in Evans (2008). The aircraft size choice model gives the yearly demand for aircraft movements from each airport. We assume demand is distributed throughout the day similarly to the way it was distributed in the base year (on average). This allows us to get the average demand for arrivals and departures per three-hour time bin for each airport and year.

The rapid delay model uses different approaches depending on whether demand is close to it the airport's declared runway capacity or not. For airports that are well below capacity, delay is modelled using classical steady-state queueing theory, assuming a M/M/1 queue (e.g. Larson and Odoni, 1981). For airports that well exceed capacity, the cumulative diagram approach is used, which projects a linear increase in queue size with time that demand is greater than capacity (e.g. Hansen, 2002). For airports that are close to capacity, delays are calculated using both methods and interpolated between. This modelling approach is shown schematically in Figure 8.

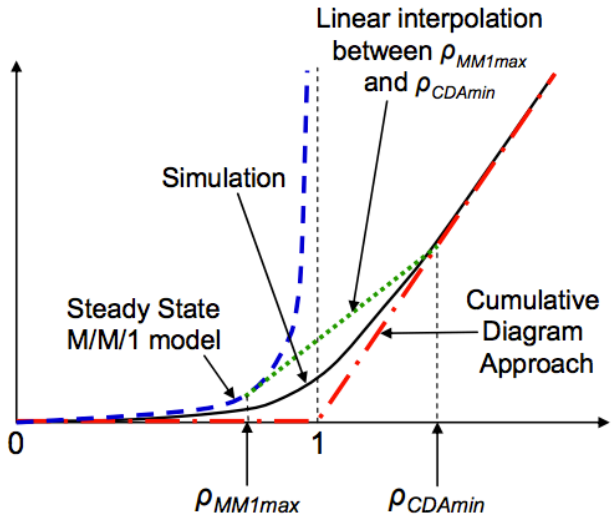

Figure 8. Delay modelling methodology.

Modelled average arrival and departure delay for the top 50 airports by passenger traffic in the 2015 base year is shown in Figure 9 and Figure 10, against data on actual delays from Flightstats (2016), FAA (2016) and BTS (2017). Delay is generally well-reproduced, as was the case also when the model was used with year-2005 data (Evans 2008). Deviations from observed values arise from several sources. First, demand is not perfectly reproduced for all airports, which can lead to delay above or below what is expected. Second, the model overpredicts delay at some airports that are very close to their capacity limits (e.g. London Heathrow (LHR), Istanbul Atatürk (IST), Mumbai Chhatrapati Shivaji (BOM)). This likely reflects that these airports have additional delay management mechanisms that are not included in the current model.

Delays have an impact both on passenger journey times and airline costs. As airlines are operating aircraft for longer on delayed routes, they experience greater per-flight costs,

which in turn may affect ticket prices. Passengers may also respond to increases in journey time on a given itinerary by changing to an alternative itinerary or choosing not to travel.

When the model is used to project future demand, it requires an assumption about how future capacity develops. If capacity is kept at base year values, increasing demand leads to delays that are unrealistically large. Currently, the standard assumption in the model is that capacity is expanded as required to keep delays at base year values. This is a more realistic assumption in parts of the world for which capacity expansion is straightforward. However, in regions where airport capacity expansion is more difficult, it is more likely that passengers and/or airlines will start to switch demand to alternative airports with more space. These issues will be addressed further in future updates of the model, as we move towards a model that can more accurately assess the impact of adding capacity at different airports.

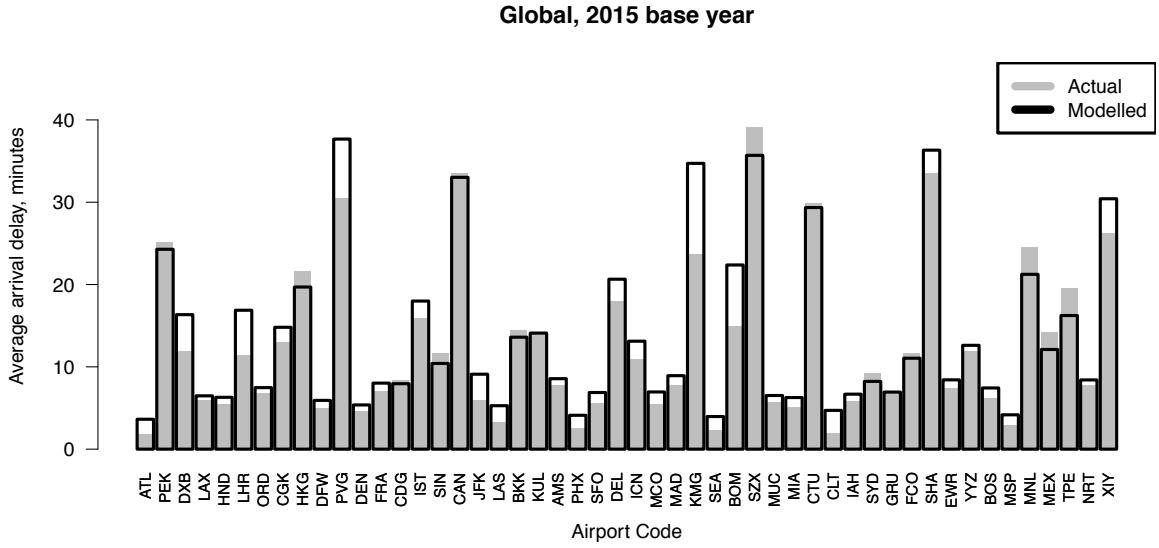

Figure 9. Average arrival delay for the top 50 airports by passenger traffic in the 2015 base year, modelled and actual.

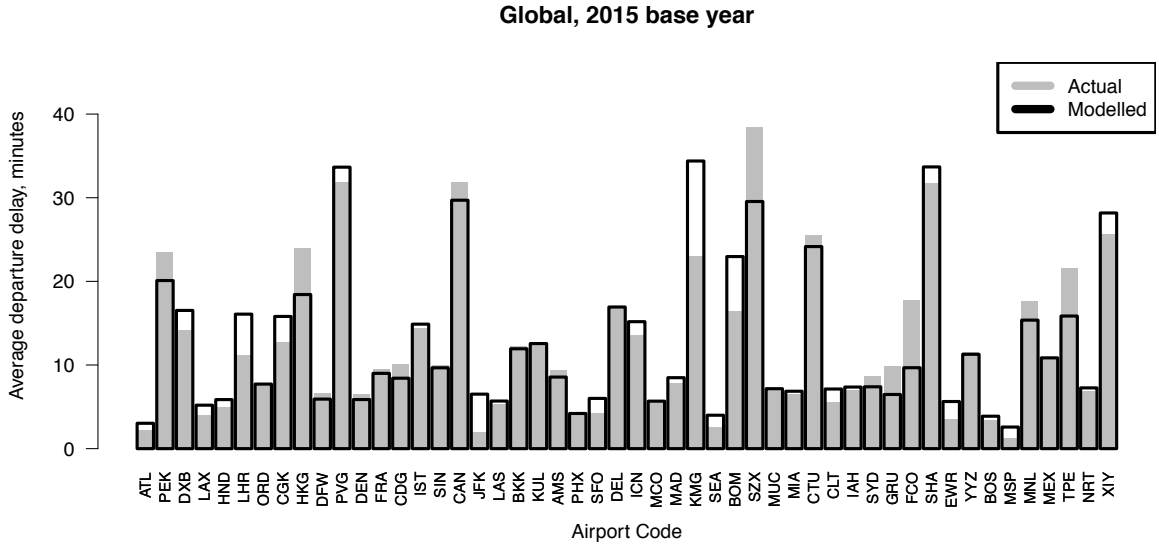

Figure 10. Average departure delay for the top 50 airports by passenger traffic in the 2015 base year, modelled and actual.

The code for the Airport Activity Module is included in the file *run_ArptActMdl_v24_comb.java*; code related to the modelling of LTO operations is in the file *run_LTOOpsMdl_v25.java*, and the code specifically for the delay modelling in the file *surfaceQing_v13.java*. This code also calls *CumDiagSteadyStateQ_Mdl_v9.java* to calculate detailed queueing per airport. Input data parameters by airport come from the file *AirportData.csv*, and those by flight segment are in the file *AirportSegmentData.csv*.

3.3 Aircraft Movement Module

The routes that aircraft take on any given flight segment are not straightforward great-circle routes. Instead, they are affected by multiple factors, including airspace congestion, safety requirements, the relative costs of travelling through airspace belonging to different countries, weather avoidance and wind optimization (Figure 11). The Aircraft Movement Module accounts for increases in fuel use as a result of real-world inefficiencies in routing caused by these and other factors. It can also be used to generate inventories of the location of global emissions that can be used in climate modelling.

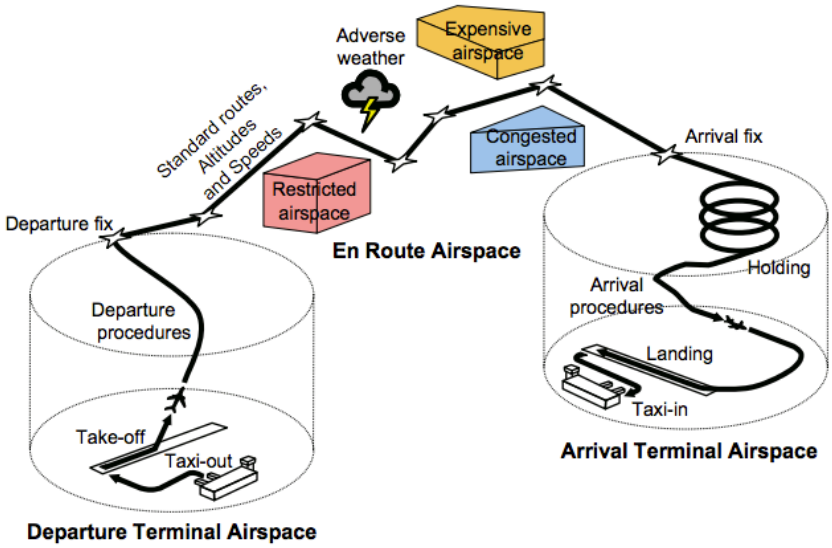

Figure 11. Potential causes of routing inefficiency

The modelling behind the Aircraft Movement Module is described in Reynolds (2009). Based on an analysis of radar track data in comparison to great circle routing, regional efficiency metrics are developed describing the ground track extension resulting from sources of routing inefficiency. Radar track data is derived from a number of sources, as described in Reynolds (2008), including Flight Data Recorder (FDR) data from Swiss Airlines, FAA ETMS data, and routing data from the MOZAIC emissions-measurement project (e.g. Marenco et al. 1998). Lateral route inefficiencies are considered as ground track extension (*GTE*) flown beyond the great circle (*GC*) distance, and are separated into departure terminal area (*DepTA*), enroute and arrival terminal area (*ArrTA*). A schematic description of this division is shown in Figure 12.

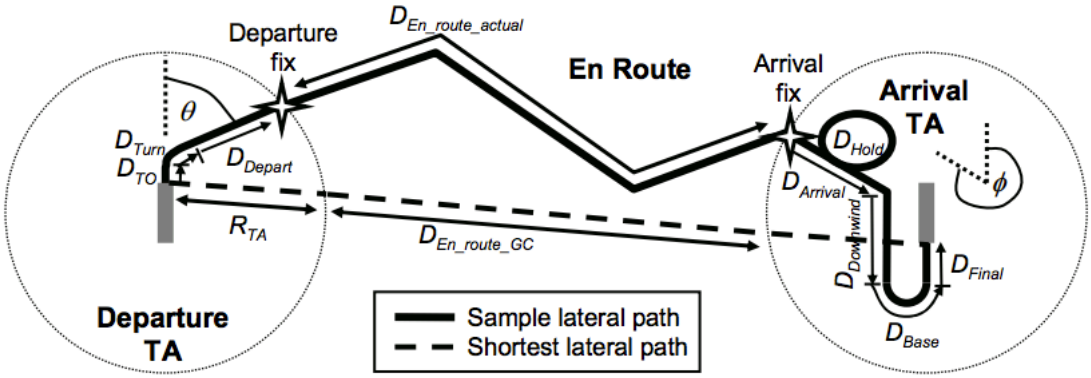

Figure 12. Terminal area and enroute ground track extension definitions.

The lateral inefficiencies are calculated as:

$$GTE_{DepTA} = \left(D_{TO} + D_{Turn} + D_{Depart}\right) - R_{TA},$$
$$GTE_{En\_route} = D_{En\_route\_actual} - D_{En\_route\_GC},$$
$$GTE_{ArrTA} = \left(D_{Arrival} + D_{Hold} + D_{Downwind} + D_{Base} + D_{Final}\right) - R_{TA},$$
and
$$TGTE = GTE_{DepTA} + GTE_{En\_route} + GTE_{ArrTA}.$$

A summary of lateral ground track extension results is given in Table 2.

Table 2. Ground track extension by region, from Reynolds (2008).

Region	Average route length in data (nm)	Average TGTE (nm)	Average TGTE (%)	Flight data source
Intra Europe	415	57	14	FDR (n=4420)
Intra US	635	76	12	ETMS (n=2946)
Intra Africa	489	41	8	Mozaic (n=525)
North Atlantic	3430	176	5	Mozaic (n=3311)
Europe – Asia (typical)	4705	316	7	Mozaic (n=2448)
Europe-Asia (Extreme)	4730	1100	23	Mozaic (n=37)

Based on this analysis, we incorporate a regional ground track extension model into AIM, in which ground track extension is considered as a function of world region-pair (capturing the current weather and airspace constraints existing in each region) and distance (capturing the greater inefficiency applicable to shorter routes, for which a greater proportion of the flight is in the terminal area), i.e.

$$D_{Actual,nm} = \mu_{1,r_n r_m} + \mu_{2,r_n r_m} D_{GC,nm}$$

for distance flown *D* between airports *n* and *m* in regions r_n and r_m.

The ground track extension model addresses the typical extra distance flown by aircraft due to en-route inefficiencies. However, this is not the only source of additional fuel use: flying at non fuel-optimal altitudes or speeds also raises average per-flight fuel use above typical performance modelling outcomes, and may also vary significantly due to individual flight circumstances. The discrepancy between lateral distance-corrected performance modelling and fuel use in practice has been noted by multiple authors. For example, Reynolds (2009) finds lateral inefficiency of 13% but fuel inefficiency of 23% for a sample of European A320 FDR data; Poll (2018) similarly estimate global ATM-related fuel inefficiency to be around 20% (including lateral, altitude and speed-related inefficiencies); Graver & Rutherford (2018) find a similar gap between performance model-generated outcomes and reported fuel use for transatlantic flights; ICCT (2019) estimate an average 9% difference comparing US airline fuel use data with distance-corrected performance modelling outcomes; and Dray & Doyme (2019) find a shortfall of just below 10% in estimated UK departing passenger aircraft fuel uptake after accounting for lateral inefficiency and freight usage. Given the consistency of the fuel discrepancy across samples of flights containing very different mixes of aircraft size and stage length, AIM allows a non-lateral inefficiency factor per aircraft size class to be applied in the file *AircraftPerformanceParams.csv*. In the most recent version of the model, this is set at 9% for all size classes.

The code for the Aircraft Movement Module is in *run_AircraftMovementModule_v25.java*. Regional parameters for the model are included in the data input file *RegionPairData.csv*.

3.4 Aircraft Technology and Cost Module

The Aircraft Technology and Cost Module takes estimates of aircraft movements by route, projections of future fuel, carbon prices and available technology characteristics, and data on the existing fleet. It uses these to project the how the size, age distribution and technological composition of the aircraft fleet will change over time, and what impact this will have on emissions and on airline costs. Airline costs are an output to the Demand Module, where they affect fares and hence passenger demand. Fleet characteristics are used to generate fuel use and emissions by segment, which are a model output and can also be used to generate detailed emissions inventories by location in the Aircraft Movement Module, and as input to the Global Climate and Air Quality Modules.

There are four main components to the Aircraft Technology and Cost Module. The Aircraft Performance Model uses the reference aircraft (Table 1) to estimate fuel use and emissions per flight. The Fleet Turnover Model calculates aircraft retirements and the age distribution of the fleet, and how this affects fuel use and emissions. The Technology Choice Model calculates which of a range of available current and future technologies airlines will adopt, based on their costs and benefits for each size class, aircraft cohort and region. The Airline Cost Model then calculates the corresponding cost to airlines of operating these flights with the given fleet and technology characteristics. These components are described individually below.

3.4.1 Aircraft Performance Model

The original AIM model calculated fuel use by a simple fuel burn rate-based-approach. For this updated version (v9), as well as expanding the number of aircraft size classes, we have also integrated a rapid fuel use and emissions model which calculates performance by flight phase based on a model estimated from the output of the PIANO-X aircraft performance model (Lissys, 2017). Fuel use and NOx emissions and time in stage for the nine reference aircraft are calculated for climb, cruise and descent, for passenger load factors between 0 and 1 and stage lengths between 500 km and each aircraft's maximum range. For each aircraft size class *s*, variable and flight phase *p* for distance *D* and payload *PL* a model of the type:

$$Var_{sp} = \eta_{sp,0} + \eta_{sp,1}D + \eta_{sp,2}D \cdot PL + \eta_{sp,3}D^2 + \eta_{sp,4}PL + \eta_{sp,5}D^2 \cdot PL$$

is estimated. Parameters η_{sp} for these models are stored in *AircraftPerformanceParams.csv*. We assume 100 kg for a passenger with luggage and hold freight average load calibrated against available capacity, global totals and typical passenger-to-freight payload ratios by region-pair (ICAO, 2009; ICAO, 2014; ICCT, 2019). It is assumed that the ratio between passenger and freight payloads per route group will remain similar into the future, with fluctuations in freight demand growth compared to passenger demand growth resulting primarily in changes to the number of freighter aircraft flights flown. This results in an effective switch towards belly freight and away from freighter aircraft over time, as discussed by Boeing (2018).

For the gate, taxi and holding phases we use fuel use and emissions rates as previously. These allow the model to adjust for emissions from delay incurred during taxi with engines on, and for different lengths of the holding phase. For take-off and landing standard fuel use and emissions totals by type are used. The resulting fuel and NOx totals by flight phase are also adjusted by the stock and technology choice models (Sections 3.4.1 and 3.4.2) to take account of the age profile of the fleet and changes in the use of different technologies over time, and by an optional factor to account for non-lateral routing inefficiencies as discussed in Section 3.3, above. Figure 13 shows the block fuel output of the rapid performance model for the nine reference aircraft; more information can be found in Al Zayat et al. (2017). Similarly, Figure 15 shows block NOx by aircraft size class, stage length and load factor.

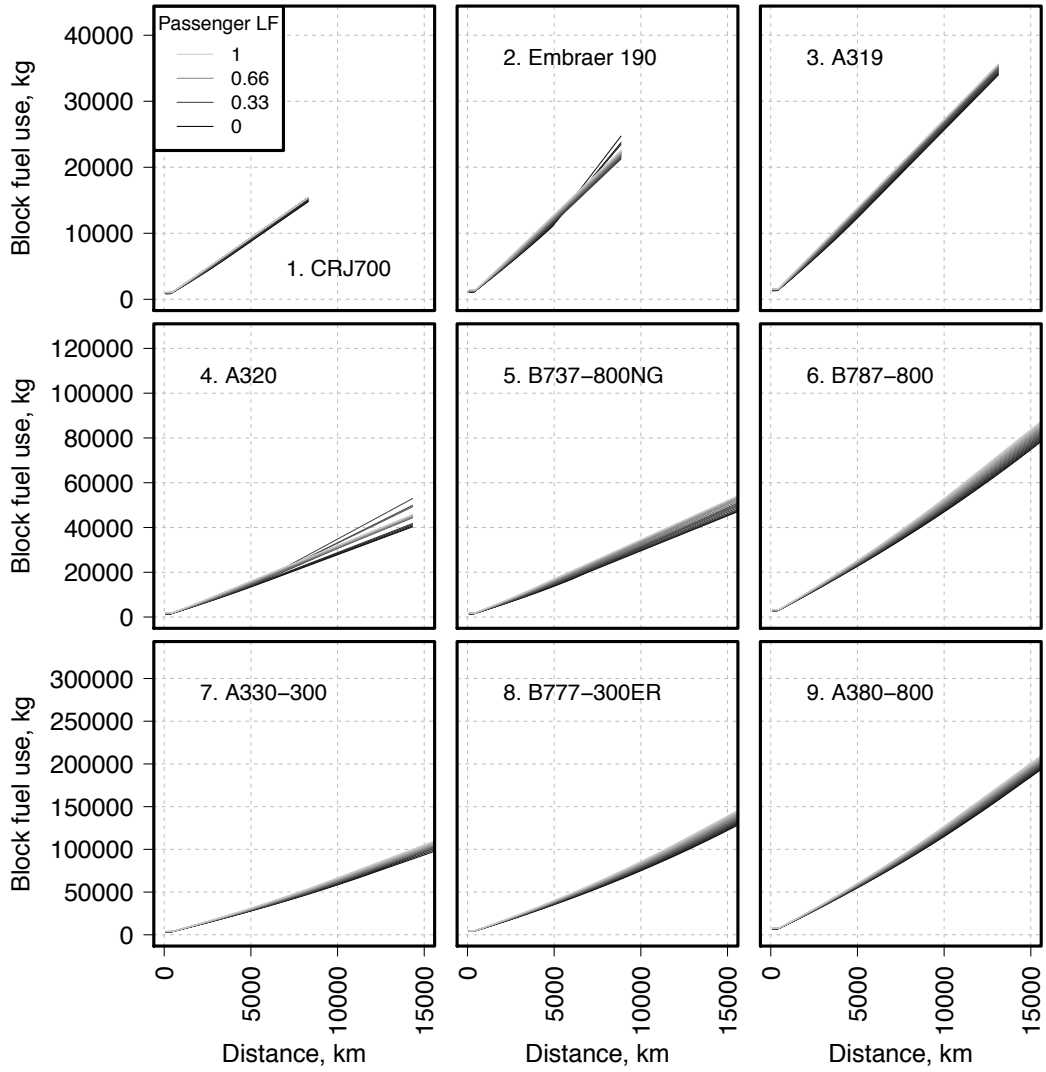

Figure 13. AIM performance model block fuel use for the nine reference aircraft, by passenger load factor (LF) and stage length.

The performance model takes distances flown including ground track extension from the aircraft movement module. The code for the performance model is included in *run_LTOOpsMdl_v26.java* and input parameters are given in *AircraftPerformanceParams.csv*. Due to substantial differences in performance behavior over distance and load factor, electric aircraft are modelled separately in the performance model in the case that they are included as a future technology option, using electric aircraft performance data from Gnadt (2018) and Gnadt et al. (2018) for narrowbody aircraft types and Hepperle (2012) for regional jets. The corresponding data for electric aircraft are given in *AircraftPerformanceParamsElec.csv*.

3.4.1.1 PM modelling in the performance model

To assess air quality and health impacts at airports, we also need to be able to model PM emissions. PM also has an impact on contrail and cirrus formation, although the direct impact on radiative forcing of the particles themselves is small. PM emissions are not included in the output of PIANO. Similarly, although engine certification processes measure smoke number (SN), this does not straightforwardly convert to emissions metrics that are

usable with health or environmental models. Instead, we use methodology based on the emissions inventory code AEIC (Simone et al. 2013). Estimating PM emissions requires several steps:

- Estimating emissions indices for the non-volatile (black carbon/soot) component of PM. These are formed by combustion processes within the engine. We estimate emissions indices using the FOX method (Stettler et al 2013). This requires engine pressure ratios as an input, which are taken from the ICAO engine emissions databank for representative engines for each size class. Fuel flow per engine by flight phase is derived from the performance model and is used as a proxy for thrust setting, as discussed in Stettler et al. (2013).
- Estimating emissions indices for the volatile component of PM (arising from sulfates, unburnt fuel, engine lubrication oil etc.). These are formed in the cooling exhaust gas downstream of the combustor. For these emissions we use the FOA3 method (Wayson et al. 2009). There are three components to this model. The first estimates PM from sulfates given the fuel sulphur content (thus this component will change with ultra low sulphur fuels, including synthetic fuels). The second estimates PM from unburnt hydrocarbons using the hydrocarbon emissions index included in the aircraft performance model. The third part estimates PM from engine lubrication oil; this component is implicityly included in the hydrocarbon calculation.
- Estimating PM emissions on takeoff and landing from brake and tyre wear. These totals are very uncertain, can be significant, and are mainly in the form of PM10. Currently we concentrate on PM2.5 and do not model these emissions, but they may be added in a future version of the model.
- Applying a particle size distribution. Particle size is important for impact modelling, with smaller particles generally having more severe health impacts and longer atmospheric retention times. PM10 refers to all particles with a diameter less than 10 µm, and PM2.5 to all particles with a diameter of less than 2.5 µm. Aircraft engine PM is primarily PM2.5. As we currently do not include brake and tyre wear, we model PM2.5 only.
- For future projections we need to know how the major input variables are likely to change over time. Changes in fuel flow over time are already accounted for in AIM, but we need to project how engine pressure ratios (for conventional-technology aircraft) are likely to alter over time. To project engine pressure ratios we use a linear model over time for pressure ratio relative to the reference aircraft pressure ratio, with parameters estimated from the ICAO engine emissions databank. This relationship is depicted in Figure 13, below. Changes in PM for alternative technologies over and above those projected by this model are handled by the technology choice model.

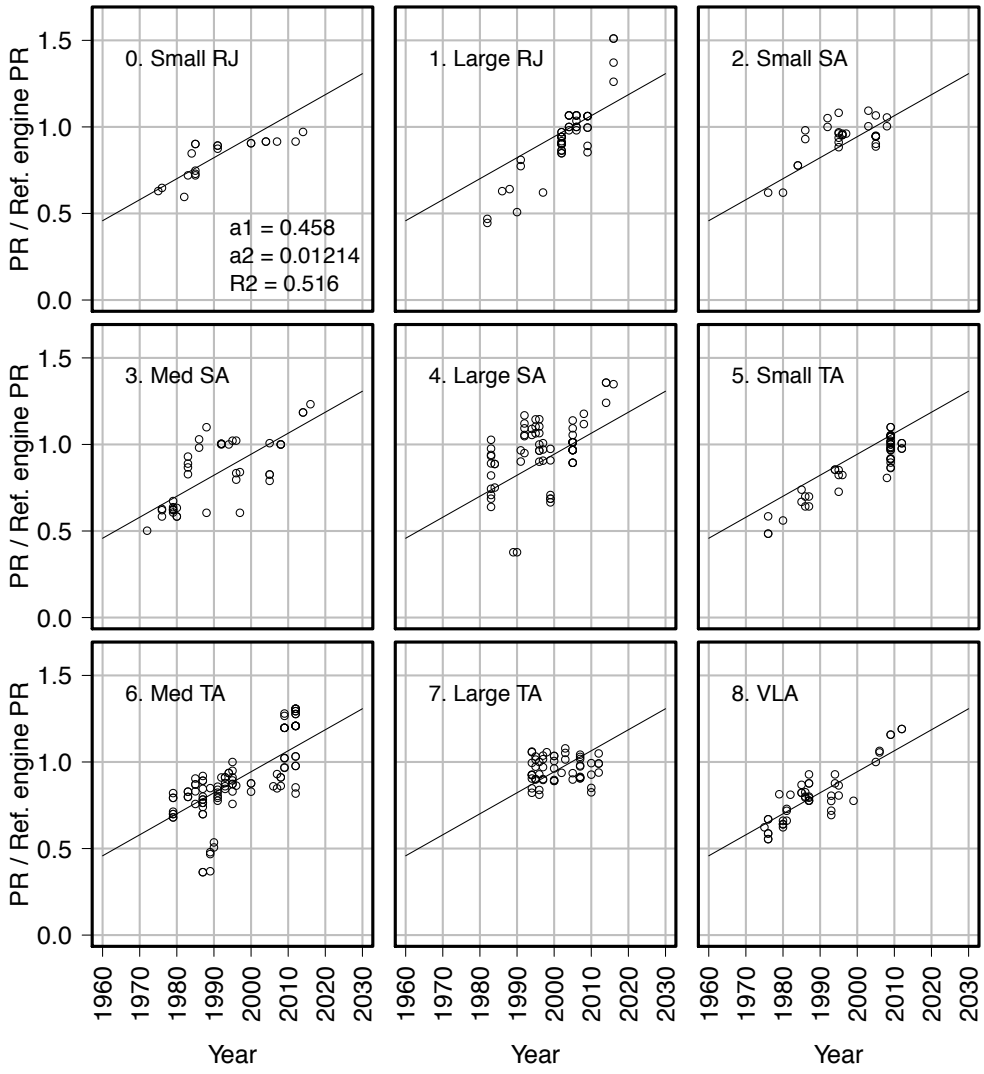

Figure 14. Model for aircraft engine pressure ratio development over time, using data from the ICAO engine emission databank (ICAO, 2017)

The code for PM modelling is included in *run_LTOOpsMdl_v26.java.*

3.4.1.2 NO_2 modelling in the performance model

NOx is the aggregate of NO and NO_2 emissions. However, NO_2 is a more useful metric for projecting human health impacts. The performance model only gives the total NOx emissions. However, studies exist which look at how much of this is released as NOx and how much as NO_2. Wood et al. (2008) find that this ratio is dependent on engine thrust setting, with higher NO_2 at lower thrust settings. We adopt this relationship in our model, using linear interpolation between the points given in Wood et al. (2008) with engine condition. As with the PM modelling, we assume fuel flow as a proportion of maximum as a proxy for thrust setting. The code for NO_2 modelling is included in *run_LTOOpsMdl_v26.java.*

3.4.2 Fleet turnover model

The fleet turnover model is based on the fleet analysis in Dray (2013) and Morrell and Dray (2009), updated with new data from FlightGlobal (2016). The main purpose of the fleet turnover model is to track the composition of the global aircraft fleet in terms of size class, age and world region, and to assess how this affects fuel use and other fleet characteristics that may impact on technology uptake. For the purposes of this model, the fleet is divided into groups by world region (North America, Central America/Caribbean, South America, Europe, Middle East, Africa and Asia-Pacific), size class and year of aircraft age. The base year data for the fleet is taken from two sources. Regional age distributions by size are sourced from the FlightGlobal (2016) fleet database. However, this database does not contain enough information on aircraft use to be sure that each aircraft is within the AIM scope. Therefore we use implied fleet totals per region and size class from an analysis of global schedule data (Sabre, 2017), assuming utilization averages from FlightGlobal (2016) are maintained.

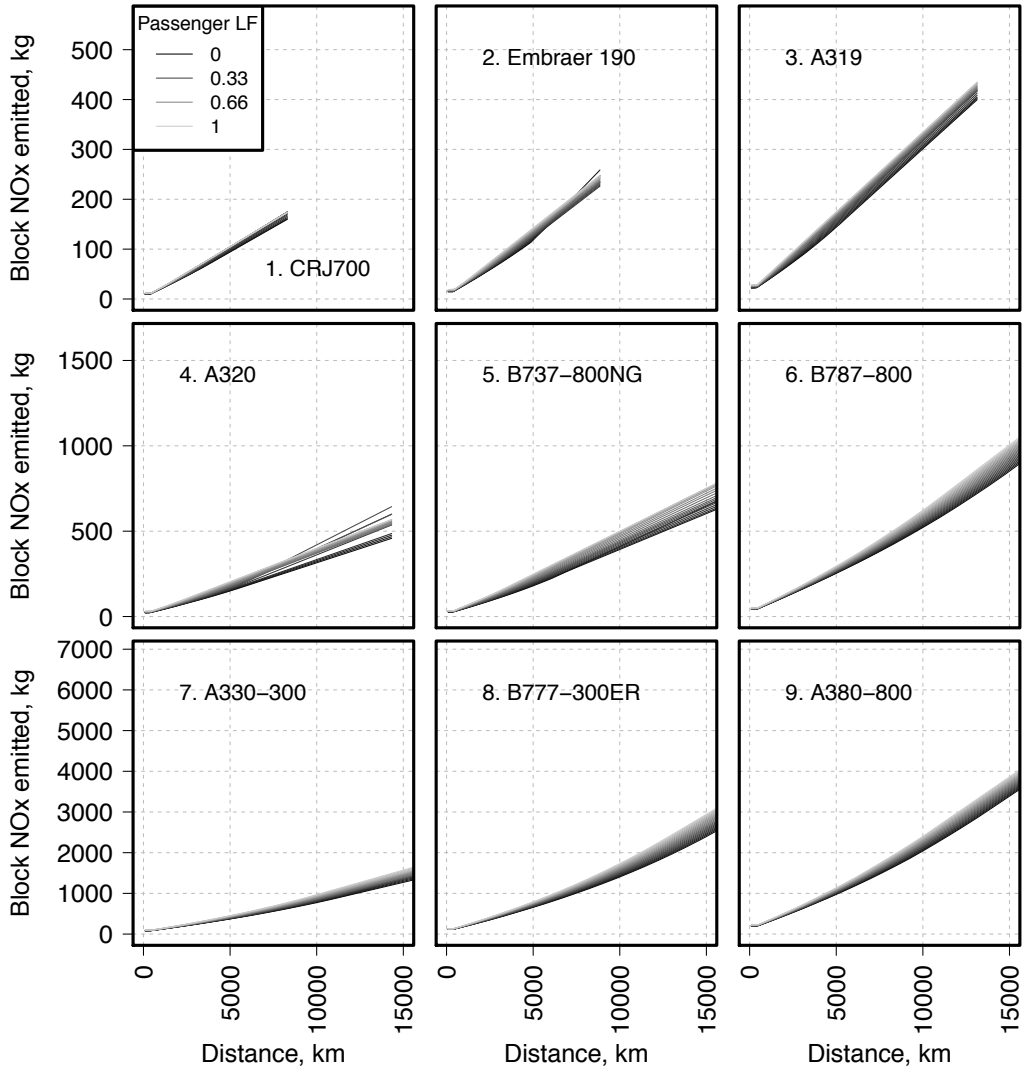

Figure 15. AIM performance model block NOx for the nine reference aircraft, by passenger load factor (LF) and stage length.

For each simulation year, the model assesses how many aircraft would naturally retire in that year. For this purpose, we use retirement curves with age from Dray (2013). As shown in Figure 16, the proportion of aircraft still active or in temporary storage with aircraft age has a relatively consistent S-curve shape over time, with typical age at retirement of around 30 years. We model this with a logistic function,

$$\frac{N_{Active,t}}{N_{Active,t} + N_{Retired,t}} = \frac{1}{1 + e^{-\varphi_1 - \varphi_2 t}},$$

where the active fleet $N_{Active,t}$ at time t is a function only of t and the estimated parameters φ_1 and φ_2. Parameters by aircraft type are given in Appendix 5. This model describes how retirements are carried out under business-as-usual conditions. In the case that AIM is used to model early retirement policies, we typically apply a cut-off age after which all aircraft are retired. For example, a cut-off age of 30 years would automatically retire all aircraft at age 30.

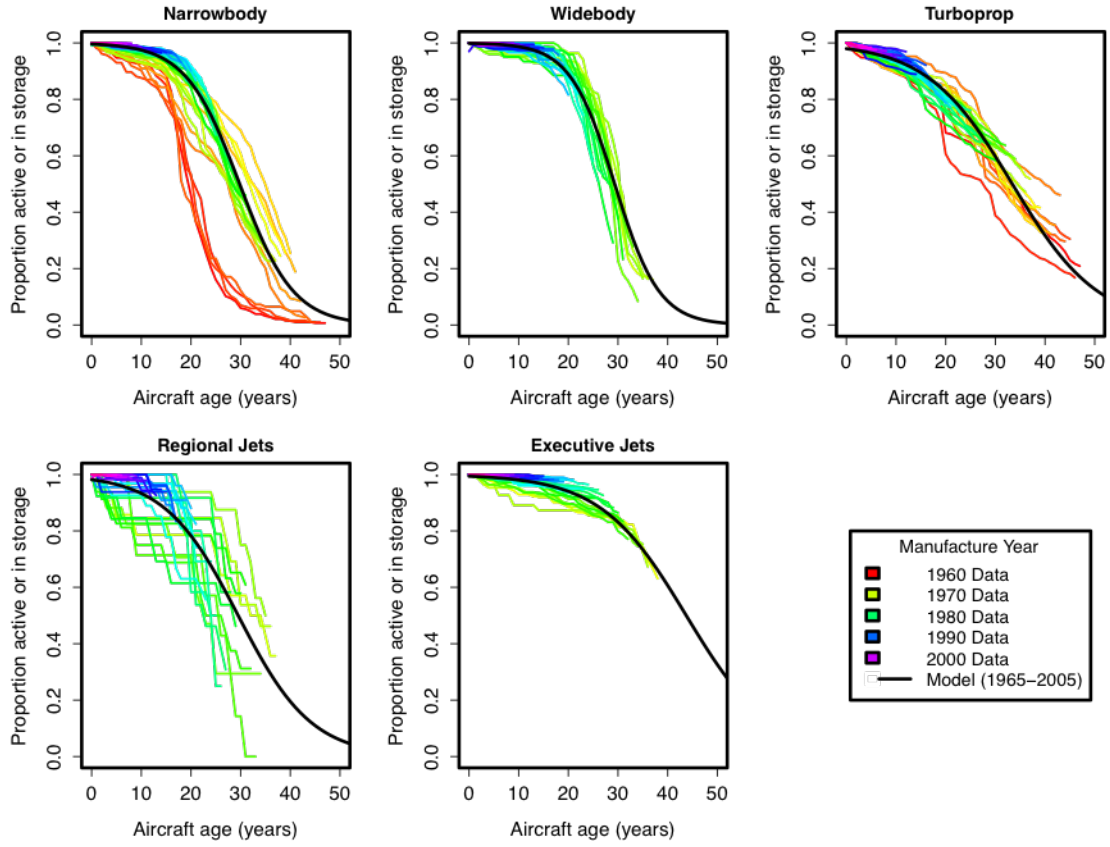

Figure 16. Proportion of aircraft still active or temporarily stored by aircraft age.

Aircraft are assumed to go into storage if supply exceeds demand for aircraft in a given world region and size class, but can be removed from storage if there is demand for them in later years and they have not yet retired. Aircraft may also be removed from the passenger fleet via conversion to freighters. Figure 17 shows the proportion of active aircraft that are freighters by aircraft age, analogously to the retirement curve plot above. Freighter conversion removes a substantial proportion of older passenger aircraft from the passenger fleet and so needs to be corrected for in our model.

As in Dray (2013), we also model freighter conversion with a logistic function,

$$\frac{N_{Freighters,t}}{N_{Active,t}} = \frac{1}{1+ e^{-\omega_1 - \omega_2 t'}}$$

i.e. the proportion of freighters is assumed to be just a function of aircraft age and estimated parameters ω_1 and ω_2. Freighter conversion is typically an economic decision which depends on aircraft depreciation over time, giving a time window during which most conversions by type are carried out, which results in the types of curves seen in Figure 17.

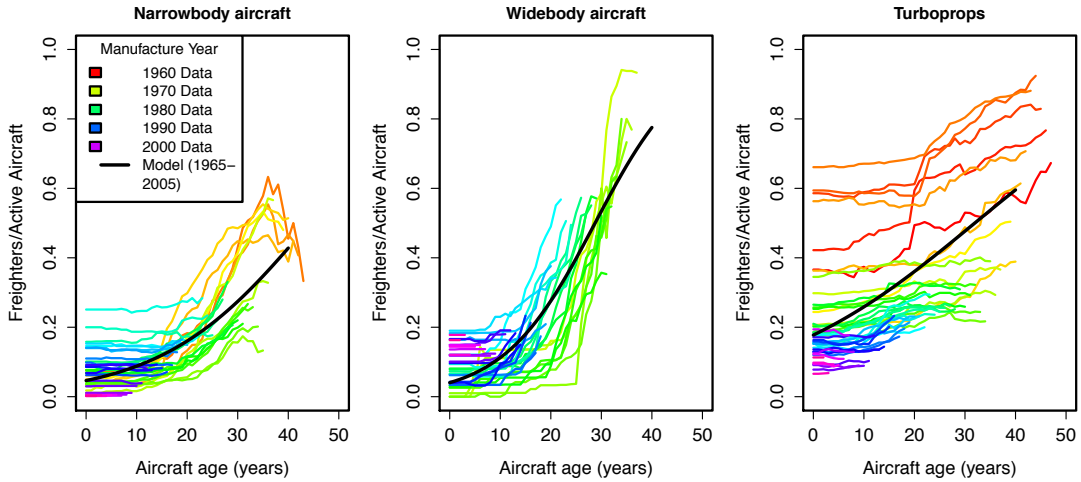

Figure 17. Freighters as a proportion of active aircraft, by aircraft age.

Fleet composition by region can also be affected by region to region aircraft sales. For example, world regions with greater capital constraints may choose to purchase much of their fleet second-hand, leading to older average fleets than would be otherwise projected. We also apply a simple, regional GDP-based model of sales, based on Bosbach (2011).

Once these models have been applied, the resulting fleet by size and region can then be compared to the sum of the regional segment demand for aircraft by size class at typical utilisation. Any shortfall is assumed made up from new aircraft. As discussed above, if supply exceeds demand we assume that excess aircraft are temporarily stored. From storage, they may either be retired or re-enter the fleet, depending on demand developments in subsequent years.

The second purpose of the fleet turnover model is to assess how the age structure of the fleet affects aircraft fuel burn and NOx emissions, in comparison to the reference aircraft. Several factors may affect this. First, aircraft typically become less efficient per year of age. Following Morrell and Dray (2009), we assume an 0.2% increase in fuel burn over the reference aircraft per extra year of aircraft age. Second, older aircraft models typically have higher fuel burn for a comparable mission than newer ones. Third, the fleet in any given size class, region and age cohort is typically diverse, and may contain several different aircraft models. The average fuel burn across this diverse fleet may or may not be equal to the fuel burn of the reference aircraft. To correct for these latter two factors, we follow Dray (2013) in assuming that the typical aircraft purchased in a given year will have performance part-way between the highest- and lowest-available fuel burn models in that year, and modelling the distribution of purchases over this range with a triangular distribution estimated from historical data. For

past aircraft, the upper and lower curves are set by historical data. For future aircraft models, two options are available. Users can set a typical rate of reduction per year in the fuel burn of new aircraft models (e.g. 1%/year). Or this value can be set to zero and new aircraft models can be explicitly modelled via the technology choice model[6].

The code for the fleet turnover model is located in the file *aircraftStockCost_v8.java*. Input data by aircraft size class is given in the file *AircraftData.csv*.

3.4.3 Technology choice model

One major use of AIM is in assessing the uptake and use of new technologies. To do this, we need to know whether airlines would be willing to invest in them or not, given the prevailing economic conditions at the time. New technologies may take several forms, and airline investment strategies may differ for each. We consider new aircraft models, retrofits to existing aircraft, new operational measures and alternative fuels separately.

New aircraft models include updates to conventional technology (e.g. the A320neo and B737 MAX ranges) as well as radical new aircraft technologies such as open rotor engine aircraft, electric aircraft, blended wing body aircraft, etc. This choice can only be made in the aircraft purchase year and any given aircraft cannot be more than one type at once. However, airlines in a given world region and size class may choose more than one aircraft model in the overall fleet, for example if the model associated with the lowest costs has other usage restrictions that mean it cannot be used on all segments. For new aircraft models, we assess the cost-effectiveness of an aircraft of technology *x* using net present value (NPV), i.e.

$$NPV_x = \sum_{t=0}^{T_N} R_{t,x}/(1 + i^t) ,$$

where T_N is the time horizon over which the technology is evaluated, *i* is the discount rate, and $R_{t,x}$ is the cash flow associated with technology *x* in year *t*. The discount rate and time horizon are user input values in AIM. By default they are set at ten percent and seven years. The net present values for each available technology in a given year for a given world region are assessed. Airlines are assumed to choose the technology with the greatest net present value. In practice, because we typically assume equal revenue is available from each technology and look at the differences in cost between the reference and alternative technologies, this is expressed as the difference in discounted airline cost terms between the reference and each alternative technology. If more than one alternative technology is better than the reference technology, and there is a limit on the uptake of the best technology (e.g. it cannot be used on all segments, or is just beginning to percolate into the market) then airlines may also adopt the second-best technology as well.

To model cost-effectiveness, the difference in cost by cost category and in fuel use for each technology from the reference technology is needed as input to the model. These numbers are given in *TechnologyMeasureData.csv* and are described in detail in the comments to the code, for example in *datastructures/DataByTechnologyMeasure.java*. We do not currently

[6] Note that only one of these options should be chosen, or benefits due to new technologies will be double-counted.

assume that airlines are able to foresee future developments in the fuel price: instead, technologies are evaluated assuming that current fuel prices will remain constant over the period of evaluation.

For retrofits, we use a simple payback period model, i.e. we assume a retrofit will be cost-effective if

$$\sum_{t=0}^{T_P} R_{t,x} - R_{t,base} > 0,$$

i.e. the technology is adopted if over a period of T_P years overall cost savings relative to the base technology in use in that aircraft cohort can be made. The payback period is a user input but is three years by default. Base technologies can include new aircraft types as selected by the NPV model, provided that the retrofit is compatible with those aircraft types. The base technologies also include any retrofits that have already been made to a given aircraft cohort in previous years. Major retrofits, such as re-engining, are assumed to be only applicable during a D-check. As with the NPV model, we use cost parameters relative to the reference aircraft, including applicability, maximum uptake and compatibility with already-adopted measures, from the file *TechnologyMeasureData.csv.*

Operational measures and drop-in alternative fuels are also assessed using the payback period model. The primary difference with retrofits is that these measures are assumed easily reversible. Therefore in this case the cost-effectiveness of already-adopted measures is also assessed. If a measure is no longer cost-effective (for example if the cost of biofuels increases significantly, or a different alternative fuel becomes available that costs less) then airlines have the option to stop using it. Parameters for these technologies are also included in *TechnologyMeasureData.csv.* Operational measures can have impacts on mission parameters beyond cost and fuel use. For example, reducing tankering is an operational change which will effectively change the fuel price available to airlines. These parameters are also included for each technology.

The characteristics of future technologies can be highly uncertain. In many cases, estimates of the benefits of technologies depend on engineering breakthroughs that have still to be made. Therefore the technology adoption model also includes the option to use a lens approach to assess the impact of uncertainty in technology parameters (e.g. Allaire et al. 2014). A lens is a set of input parameters which reflect a particular scenario for future technology. For example, we use one lens for a future in which it is particularly hard to reduce aviation emissions through technology; this assumes the reduction in fuel use from new technologies is at the low end of available estimates, costs are at the high end of available estimates, and the date from which the technology is available is at the late end of available estimates. Results for different lenses are discussed further in the validation section, below. Technology parameters, including changes in aircraft operating costs by cost type and changes in fuel burn, are derived from Schäfer et al. (2016) and Dray et al. (2018). A set of tables giving the key assumptions from these papers is given in Appendix 6. Biofuels can be modelled in several different ways by AIM depending on the information available. Assumptions about biofuels are given in Appendix 7.

The code for the technology choice model is in the file *aircraftStockCost_v8.java* (specifically, see the routine *getCosts*). Data for the technology choice model on technology characteristics by size class, technology and lens is given in the file *TechnologyMeasureData.csv*. Data on reference aircraft costs and other characteristics is given in the file *AircraftData.csv*.

3.4.4 Airline Cost Model

A new model for airline direct operating costs is also estimated for the current version (v9) of AIM, based on the same nine aircraft size categories. This model is described in Al Zayat et al. (2017), where it is used for the specific case of estimating costs for electric aircraft against those of more conventional technologies. Costs are calculated on a per-passenger, per-year, per-segment or per-aircraft basis as appropriate and are divided into ownership (e.g. interest, depreciation and insurance), volume-related (indirect cost), landing, en-route, maintenance, crew, fuel and carbon costs. Landing and en-route costs by size category are derived from the RDC airport charges database (RDC, 2017). Landing costs are also divided into international and domestic flights, as substantial differences exist in the charges for these flights. Other costs are derived from a range of sources, including BTS (2017), Flightglobal (2016) and Aircraft Commerce (2017). Fuel and emissions totals are derived from the aircraft performance model described in Section 3.4.1 and adjusted for fleet age and technology composition.

Although aviation fuel is usually subject to limited or no taxation, fuel costs scale slightly differently to oil prices because of the costs associated with producing and transporting the fuel. We account for this via a simple model estimated from historical variation in oil prices and fuel costs:

$$P_{fuel,y} = \zeta_0 + \zeta_1 \cdot \left({P_{oil,y}} \Big/ {P_{oil,base}} \right),$$

for fuel costs in year y in year 2015 dollars per US gallon. Model outcomes are shown in Figure 18 for the 1980-2015 period.

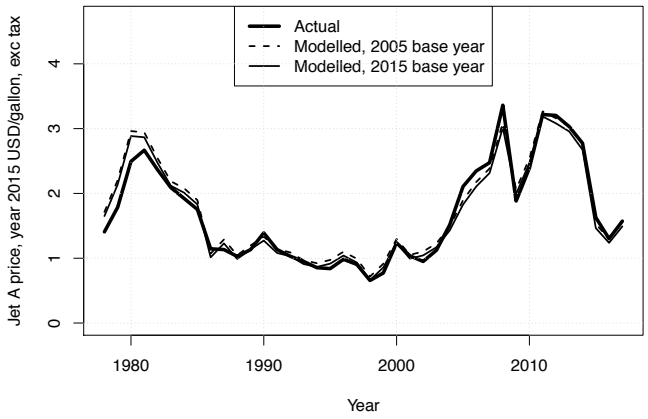

Figure 18. Model for variation in fossil Jet A price with variation in oil price.

Note that we do not model fuel cost hedging. Broadly, this would act as a smoothing factor for oil price trends, as some airlines are paying the previous year's prices for fuel. However,

the extent of hedging varies by airline and is often not publicly available. Additionally, airline hedging strategies can be affected by historical variations in oil price (for example, an airline that has made a large loss by hedging before a fuel price decrease may decide to stop hedging). Parameters for this model are given in the file *CostAndSystemParameters.csv*.

Crew costs, volume-related costs and the labour component of maintenance costs are assumed to vary by world region-pair. The regional scaling factors for these components are derived from ICAO (2009). For the simulations shown here, we assume wage costs of the flight crew and of staff performing maintenance to remain constant in real terms when projecting into the future, but it is also possible to scale wage growth with regional growth in GDP per capita. To illustrate the model outcomes, Figure 19 shows airline per-passenger direct and indirect operating costs by size class for four example flight segments in the base year, assuming a typical load factor per segment. Segment costs are used as input to the fare model described in Section 3.1.3.

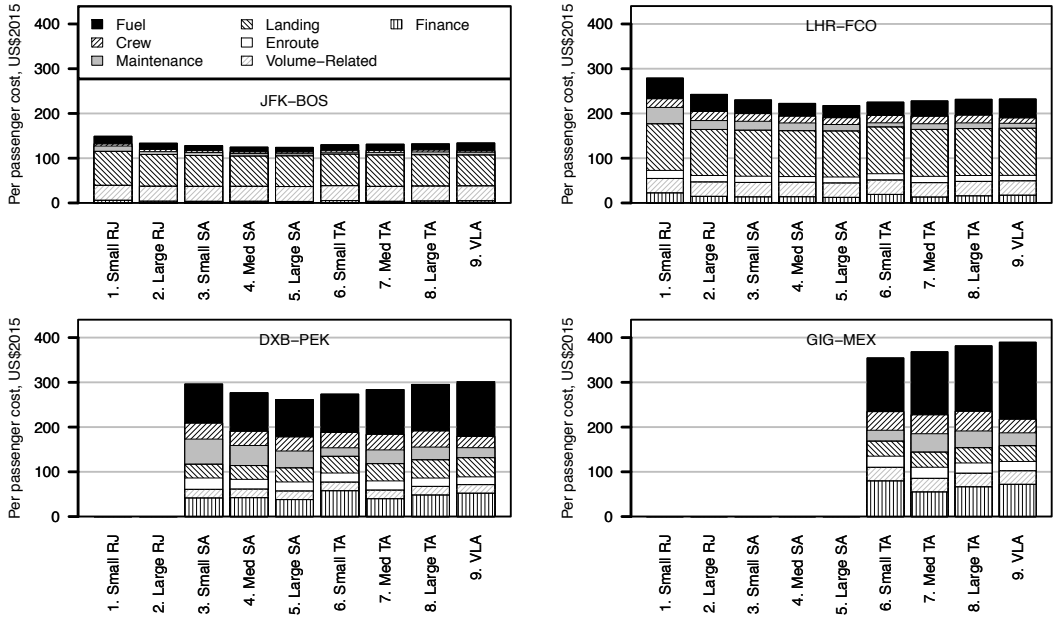

Figure 19. Direct and indirect operating cost model output for four example flight segments. Values are only shown where the stage length is below the maximum range of the reference aircraft[7].

Segment costs are calculated as part of the per-segment, per-size class loop in *run_LTOOpsMdl_v25.java*. Input data for this model which is by aircraft size class is included in the file *DataByAircraftSize.csv*. Input data by region-pair (e.g. the regional scaling factors mentioned above) is included in the file *DataByRegionPair.csv*. Data on per-passenger and per-movement landing costs by airport and size class is in the file *AirportData.csv.* Data on en-route charges by size class is in the file *AirportSegmentData.csv*.

[7] JFK: John F. Kennedy Airport (New York), BOS: Logan Airport (Boston), LHR: London Heathrow Airport, FCO: Fiumicino Airport (Rome), DXB: Dubai International Airport, PEK: Beijing Capital International Airport, GIG: Rio de Janeiro International Airport, MEX: Mexico City International Airport.

The Demand Module, Airline and Airport Activity Module, Aircraft Movement Module and Airline Cost and Technology Module are run iteratively until a solution is reached where there is equilibrium between demand and supply. This is assessed via the change in segment passenger demand per iteration. Iteration parameters and tolerance levels are set in the input file *DimensionsAndSolutionParameters.csv*. This iteration is carried out in the file *AIMController_World_ReqCap_v10_comb.java*.

Once convergence is achieved, the model runs a final iteration in which it calculates a range of output parameters and sets starting data for the next model year. This includes data for the impact assessment modules.

3.5 Global Climate Module

The Global Climate Model takes as input global emissions, fuel use and distance flown by altitude band, which is also output by the model as *AltitudeData_RunID.csv*. It outputs CO_2e from different sources (CO_2, NOx impact on ozone, NOx impact on methane, NOx impact on long-lived ozone and contrails/cirrus) as calculated using a range of climate metrics (pulsed GWP, sustained GWP, pulsed GTP, sustained GTP) and time horizons (currently 50, 100 and 500 years). These are output into the file *ClimateMetrics_RunID.csv*.

The Global Climate Model is a rapid meta-model in which linear approximations are made to the response of a detailed climate model response to perturbations from changes in aviation emissions. It was originally developed by Helen Rogers at Cambridge University during the original AIM project, and is based on a present-day atmosphere. Typically metrics are calculated by integrating radiative forcing from each source over the chosen time horizon, but the option also exists to use approximation equations from the literature for a shorter run time.

GWP and GTP for CO_2 are calculated using formulae from IPCC (2001), Berntsen et al. (2005) and Shine et al. (2005). CO_2 is assumed completely mixed in the atmosphere, i.e. only the global CO_2 total from aircraft is needed as input.

The NOx impact on ozone is calculated using radiative forcing values derived from the p-TOMCAT chemical transport model model and data from the AERO2K emissions inventory. These encapsulate the climate response for to a given level of change in aircraft NOx, which is assumed to be linear. Although AIM can calculate primary NO_2 as an output, we use NOx emissions rather than NO_2 as an input as the p-TOMCAT runs implicitly include the calculation of NO_2-NOx equilibrium concentrations. The -9% impact of the stratospheric adjustment is also accounted for. We model the impact of different NOx emissions indices at different altitudes (due to different typical engine settings, different typical cruise altitudes for different aircraft types, etc.) but do not currently model the impact of the changes in the geographical distribution of NOx.

The fractional change in methane concentrations due to aircraft NOx is derived from changes in methane lifetime, using a present-day global mean mixing ratio to calculate the resulting radiative forcing impact. Methane perturbations are assumed to be well-mixed and forcing is derived from the formula recommended by IPCC (2001). The average impact of methane

perturbations on long-lived ozone is also considered, based on Berntsen et al. (2005) with the results of a multi-model inter-comparison as reported in IPCC (2001).

We calculate the impact of line-shaped contrails based on aircraft distance flown from the AERO2K emissions inventory and the extent of ice supersaturation (ISS) regions, normalised with satellite data. As the internal calculation of metrics is carried out on a per distance flown basis, this effectively assumes a linear response with greater distance flown, i.e. a similar distribution of flights through ISS regions. To account for the impact of aircraft emissions and contrails on 'natural' cirrus, a factor is chosen to scale the line-shaped cirrus radiative forcing. This is a user-changeable parameter ('*contrailFactor*' in *PhysicalAndClimateParameters.csv*) and is currently set at 5. Sausen et al. (2005) suggest a value in the range of 2 – 10. Some example outcomes of the model are shown in Figure 20.

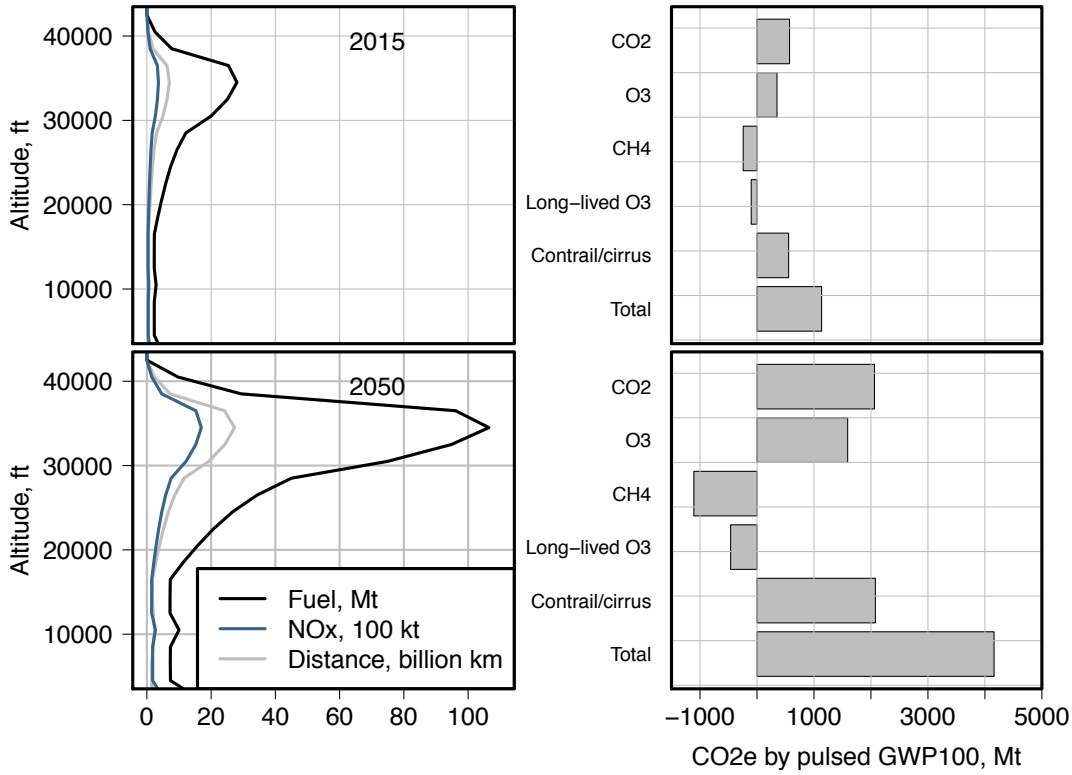

Figure 20. Emissions and distance flown by altitude, and the resulting CO_2e in terms of pulsed GWP_{100}, for a sample model run in 2015 and 2050.

More information about this model can be found in Krammer et al. (2013), where it is used to assess the wider climate impacts of aviation biofuel policy. The code for the climate model is in the file *run_ClimateMdl_v2.java*. Outputs are given in the file *output/runID/GlobalClimateMetrics_RunID.csv*; note that this contains CO_2e for a range of time horizons and metrics. Depending on the choice of time horizon and metric, the results may differ substantially, particularly when considering short-lived effects such as contrails. Key input parameters, including the relative RF impact of cirrus to line-shaped contrails, are given in the file *PhysicalAndClimateParameters.csv*.

3.6 Air Quality and Noise Module

There are three separate parts to this module. The air quality module is a rapid dispersion model which estimates the distribution of primary pollutants from aircraft engines around airports. The noise module can either produce noise outcomes in terms of a single output parameter (SINE; currently integrated) or generate noise contours (RANE; available as a separate code). The population impacts model is an add-on routine in R which takes AIM output and overlays pollutant concentrations, noise contours and global population distributions to estimate population impacts.

3.6.1 Air Quality

The air quality module is a rapid, standalone model approximating the impact of detailed dispersion models for a given set of airports. It is adapted from the open source Rapid Dispersion Code (RDC) made available by MIT's Laboratory for Aviation and the Environment (http://lae.mit.edu). This model has been used in multiple contexts to estimate local pollutant concentrations across a wide range of airports (e.g. Wolfe et al. 2014; Yim et al. 2015) More information about the principles behind the model can be found in Barrett & Britter (2009) and in the documentation to the RDC code (Yim & Barrett 2014). Broadly, the RDC calculates yearly average pollutant concentrations for a given set of point, line and area sources in a computationally efficient manner, allowing it to approximate the output of conventional dispersion models at significantly reduced run time. This allows the model to be run for multiple airports and years on a timescale that is compatible with the rest of the AIM model. As discussed in Yim & Barrett (2014), this approach has been validated against AERMOD runs and demonstrates an error of around 5% for 15 investigated airports where both models were applied.

To use the adapted RDC code in AIM, three types of data are required. First, we need meteorological data for each airport to be modelled. This data is supplied with AIM for a subset of airports (currently the top 20 global airports plus selected others) but can be generated for any airport. Instructions for obtaining and processing the meteorological data are given in Yim & Barrett (2014). Both upper air and surface data are needed. Surface weather station data can be obtained freely from the Integrated Surface Database (NOAA 2008a) and upper air data from the Integrated Global Radiosonde Archive (NOAA 2008b). Once obtained, these data need to be processed using the dispersion models AERMET and AERMOD to produce data in the format needed for AIM input. To do this, we use the matlab script provided with the RDC for this purpose. The output matrices from this script (referred to as 'AA' and 'ss' in the RDC) give an idea of the dispersion that would be expected for a point source in this location, given the typical weather conditions. These are used as AIM input in the file *MeteorologicalData.csv*.

Second, we need layout data for the airport in question. This can include just the runways, or runways, terminals and taxiways, depending on the emissions data that is available. Layout for most of the airports in the database is given in the file *AirportGeography.csv*. Sources are described in terms of width, length, angle and X and Y displacement from an airport central co-ordinate, as well as NO_2 and PM2.5 emissions totals (see e.g. Appendix A of Yim & Barrett 2014). For runways, we also need the distribution of runway usage (for example, a short or

crossing runway may be used substantially less than others). These are used to distribute airport-level emissions between the different runway area sources. The variable *RunGeog* in *AirportData.csv* indicates whether layout data is available for a given airport – if this value is -1, then layout data is not in the airport database and would need to be added (for example, by tracing runway outlines available from global mapping services such as Google Maps). Note that the RDC distributes emissions evenly across the runway, i.e. it does not take account of typical directions of use or airport-area flight tracks.

Finally, we need airport-level NO_2 and PM emissions totals. These are estimated using the routines discussed above in sections 3.4.1.1 and 3.4.1.2. Figure 21 shows the base year total airport-level emissions of primary PM2.5, NO_2 and NOx from aircraft engines, in comparison to airport emissions inventories from the literature on a similar scope (note however that not all literature values shown are for 2015 and some are projections). These emissions are distributed between runways based on the runway use assumptions above.

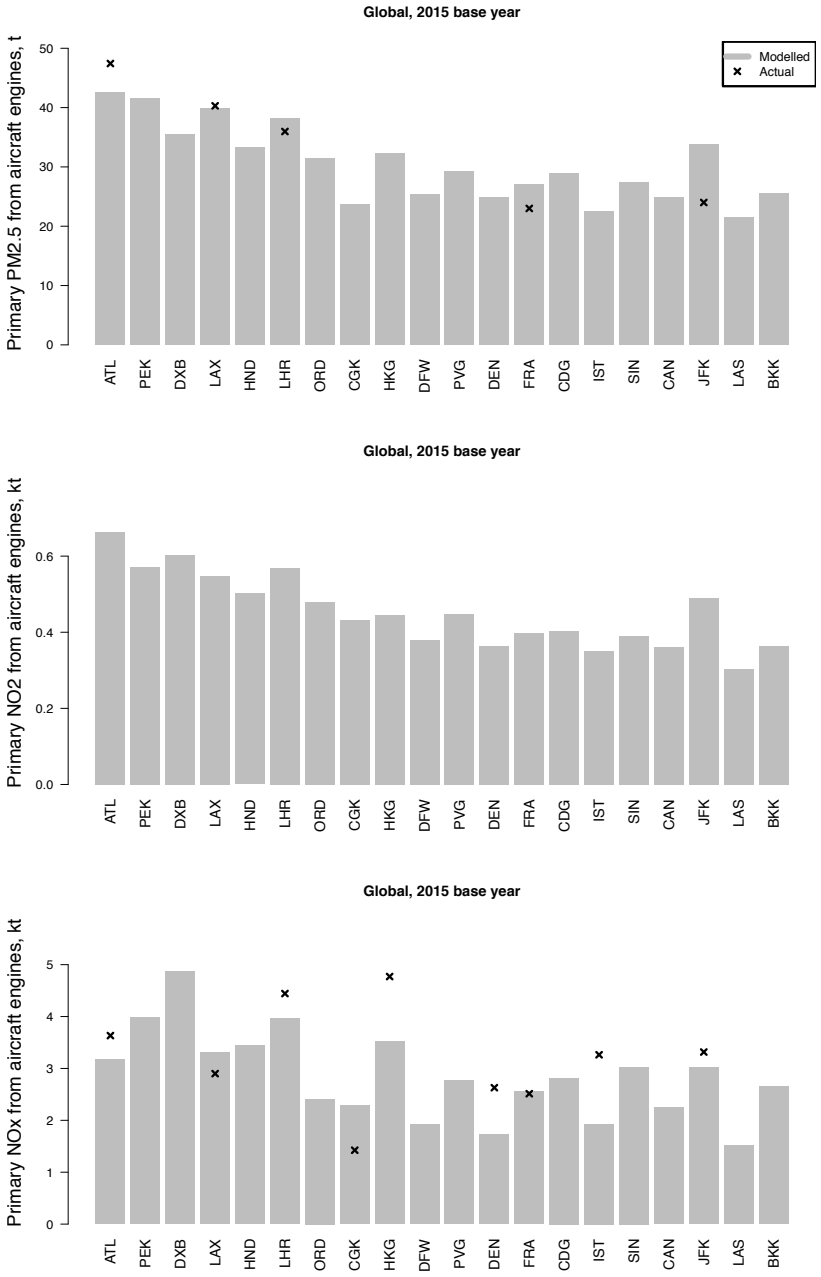

Figure 21. PM2.5, NO_2 and NOx at the top 20 airports, in comparison with literature assessments[8] (where available).

To run the RDC for a given airport for which meteorological and layout data are available, set the variable *RunGeog* for that airport in *AirportData.csv* to 1. User-specified parameters for the size and resolution of the modelled concentration grid are given in

[8] Airport data sources: ATL: sustainable management plan, 2011; LAX: Los Angeles World Airports, Midfield Satellite concourse EIR, 2012; LHR: Heathrow Airport Limited, Local air quality strategy 2011-2020, excluding brake and tyre wear; CGK: Khardi, S. & Kurniawan, J., 2013, Modeling of aircraft pollutant emissions of LTO cycles around Soekarno Hatta International Airport, ESAIJ, 8(1), 22-34; HKG: 2012 Hong Kong government press release LCQ12: Air pollutant emissions from aircraft; DEN: Denver airport emissions inventory, 2005 (projections to 2013); FRA: Fraport abridged environmental statement, 2016; IST: Sen, O. & Durmus, O., 2017, Air pollution caused by aircrafts in 2016 at Istanbul Atatürk airport, EGU general assembly 2017; JFK: Port Authority of New York and New Jersey, 2015 GHG and CAP emissions inventories.

DimensionsAndSystemParameters.csv. Output grids giving the resulting annual average concentration of primary NO_2 and PM2.5 from aircraft engines are written out to *DispersionData_RunID.csv* in the model output directory. The output grid is centred on the latitude and longitude values for the airport in *AirportData.csv* with the y axis aligned North-South, as with the original RDC code output. Figure 22 shows sample outputs for the top 16 airports by scheduled passenger traffic in 2015. The differences between these airports arise from several sources. First, local emissions totals differ based on fleet composition and typical delay (as shown in Figure 21) and are not necessarily higher at an airport with more passengers. Second, airports vary in physical extent, depending on how long and widely-spaced their runways are. Third, different airports have different meteorological conditions, including wind speed, direction, height of mixing layer etc., which affect the size of high emissions concentration areas and how those concentrations decay over time.

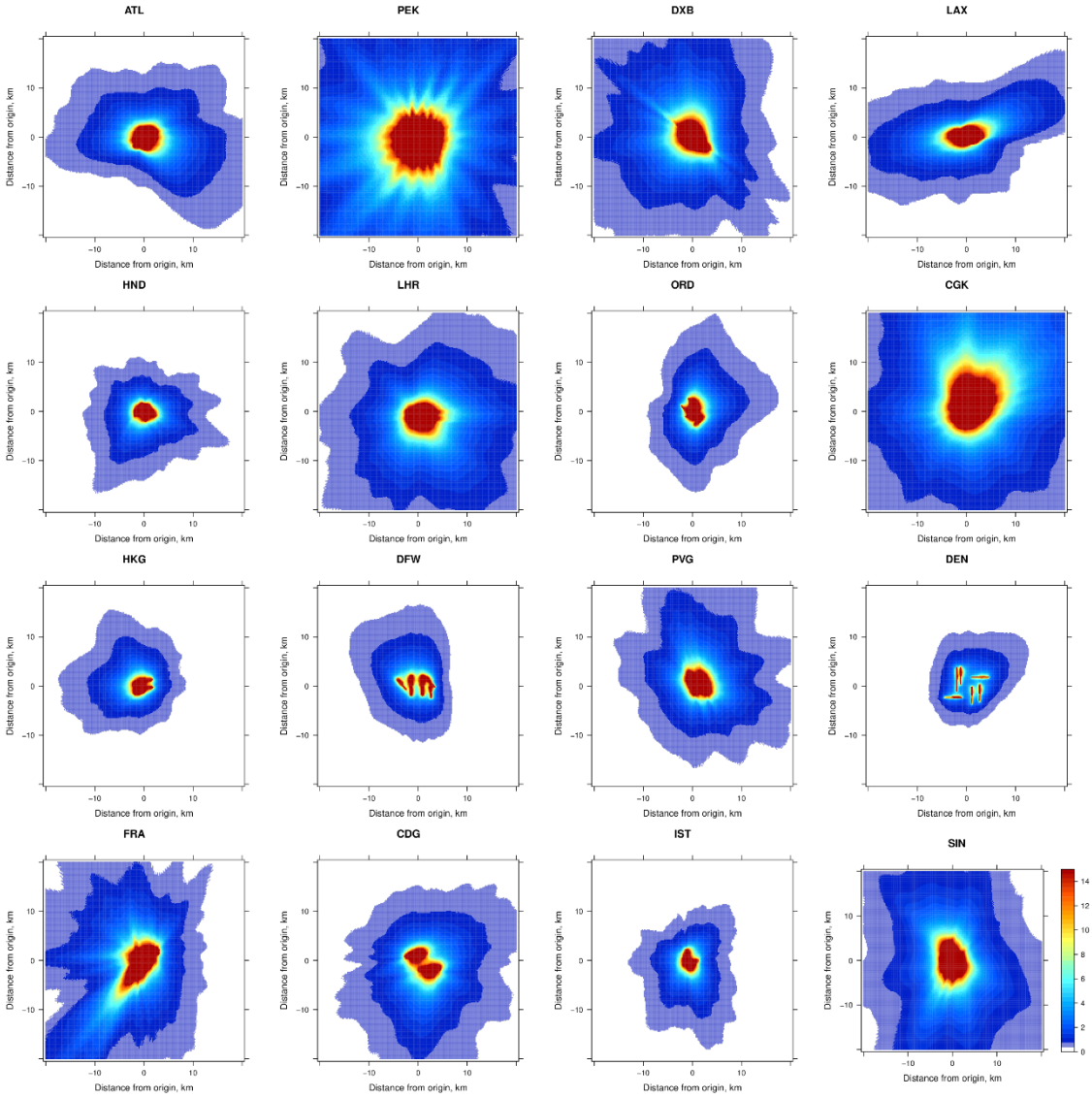

Figure 22. Sample dispersion modelling for the top 16 airports by passenger traffic in 2015: annual average concentration of primary NO_2 from aircraft engines.

Emissions distributions generated using the RDC can be compared to literature ones in several ways. First, Yim & Barrett (2014) report a validation study on the original RDC code in which 14 airports were modelled using both the RDC and AERMOD with the same data inputs. They found differences in model outputs of around 5%, for a significant reduction in run time.

Second, we can compare outputs to other estimates of emissions concentrations due to airports. Heathrow Airport's Air Quality Strategy (2011) presents modelled contours for NOx concentrations due to airport sources. Although not directly comparable to our modelling (the Heathrow contours are for NOx from all airport sources and use input meteorological data from a different year), the absolute concentration values are similar to ours. For example, a 30 μg/m^3 contour in NOx is roughly equivalent to a 4.5 μg/m^3 contour in primary NO_2; we observe these contours a similar distance from the runway to those in the Heathrow report. Finally, ACI (2010) carried out a study looking at the impact of emissions concentrations around European airports of the period during the 2010 volcanic ash crisis when operations were sharply reduced. Because of the short time period of this reduction, the study was unable to draw firm conclusions at many airports. However, it did find a reduction in NOx concentrations of approximately 1/3 at Heathrow Airport on-airport monitoring sites, corresponding roughly to a drop of 30 μg/m^3. As noted above, this is similar to the values found here. It is also notable that no corresponding reduction was seen at off-airport monitoring sites, i.e. fluctuations due to reductions in air traffic were indistinguishable from fluctuations from other sources in background concentrations.

It should be noted that the RDC is not a chemistry transport model and can only calculate the distribution of primary emissions from aircraft engines. Therefore it does not account for secondary PM or ozone. It also does not account for background concentrations or other emissions sources such as local roads. Because of these limitations, it is more useful for looking at changes in concentrations rather than absolute values and, where detailed concentration values are required, an external chemistry transport model should be used.

The dispersion model code is located in *run_DispersionModel_v2.java*. It uses input meteorological data by airport from the file *MeteorologicalData.csv*, and airport layout data from the file *AirportGeography.csv*. By-airport local emissions totals are reported in the output file *AirportData_RunID.csv* and grids of modelled yearly average concentrations in the file *DispersionData_RunID.csv*. Because of its data requirements, the model is typically only run for a subset of airports. Meteorological and layout data is currently available for the top 20 airports plus a subset of smaller airports (including AMS, BOS, LGW, STN, SYD) and is filled in with dummy data for all other airports. Setting the variable *RunGeog* in *AirportData.csv* to 1 will run the RDC yearly for a given airport. The RDC was originally developed by Steven Barrett (sbarrett@mit.edu).

3.6.2 Noise

The Noise Module (RANE/SINE) is a rapid, standalone noise model which can take AIM output as input and produces airport-level noise metrics. Two approaches can be used. Currently, a range of single-metric noise indicators are integrated into the code. Each takes as input the historical and projected noise certification level of aircraft per size class and year (and region in the case that technological trajectories diverge per region) in terms of EPNdB (L_{LTO}). For historical manufacture years this is read in from the input data file *NoiseCertificationData.csv*. Separate data for sideline, flyover and approach noise are used. For future years users can choose a per annum rate of improvement for all aircraft (the user specified variables *noiseTrendSideline, noiseTrendFlyover* and *noiseTrendApproach*) if the technology choice

model is not being run, or use specified changes in noise per technology from the technology characteristics file (*TechnologyMeasureData.csv*) if it is being run; see Section 6 below for more information on the variables in this file. Note that only one of these methodologies should be chosen, or there will be double-counting on improvements.

These metrics generated per airport include:

- The Single Index of Noise Energy (SINE) metric (Torija et al. 2016). To calculate this metric, the sound exposure level (SEL_{LTO}) is estimated for aircraft in each age cohort and size class using each airport, using a linear regression analysis with the EPNdB certification levels of each cohort. For each individual aircraft of manufacture year *y* and size class *s* this is converted into a sound intensity parameter using the equation

$$I_{LTO,sy} = \frac{P_0^2 . 10^{(SEL_{LTO,sy}/10)}}{Z}$$

  where P_0 is the reference sound pressure ($2 . 10^{-5}$ Pa) and *Z* is the acoustic impedence (400 N s/m^3). The SINE parameter is the sum of this sound intensity parameter over the entire fleet operating at an airport *m*, i.e.

$$SINE_m = \sum_{s,y} N_{msy} I_{LTO,sy}$$

  where N_{msy} is the number of aircraft operations of size class *s* and manufacture year *y* at airport *m*. We apply these equations separately for departure and approach operations, treating the departure EPNdB certification level as the average of sideline and flyover certification levels. The SINE metric output in the airport data file is the sum of departure and approach values for each airport. SINE has been historically used for projecting changes in aviation noise with different air traffic demands and technology improvements.
- The L_{kAeq} metric (Torija et al 2016b). This is a noise and number (NNI) type metric in dBA (i.e. frequency-weighted dB) which is also derived from the $SEL_{LTO,sy}$ values generated above. It is similar in definition to L_{Aeq}, which gives the equivalent annual sound level of aircraft noise. However, an additional weighting is given to the number of noise events using the input k parameter, by default set at 15 compared to 10 for L_{Aeq}. A full description of how it is derived is given in Torija et al. (2016b). An overview of L_{Aeq} and NNI metrics is given in Jones and Cadoux (2009).
- The Quota Count (QC) metric. This is a weighted measure of how many aircraft above a set of certificated EPNdB thresholds use the airport (shown in Table 3). More information about quota count is given in White et al. (2003).

The single noise metric approach can be applied for all airports and does not need information on flight routes.

Table 3. Thresholds and classification level for the Quota Count metric, adapted from White et al. (2003).

Qualifying Level, EPNdB	< 87	87-90	90-92.9	93-95.9	96-98.9	99-101.9	> 101.9
QC Classification	0.25	0.5	1.0	2.0	4.0	8.0	16.0

Additionally, AIM outputs can be used with the RANE model (Torija et al. 2017), a rapid model for the computationally efficient generation of noise contours. This model, which is not currently integrated into the main AIM code but is planned to be integrated in future, requires some extra data per airport. In particular, information about airport layout and runway usage (as also used for the dispersion model) and typical flight routes into and out of the airport is needed for detailed contours. These data are only available for selected airports at the moment but could be obtained, for example, from radar track data for the airport. More information on this model can be found in Torija et al. (2017). Southampton University is responsible for this model; for further information contact Antonio Torija Martinez (A.J.Martinez@soton.ac.uk). It is anticipated that the RANE noise approach will be the next component to be integrated into AIM and at that point this documentation will be updated to include model implementation and validation details.

Note that currently AIM can be used to model some future technologies with substantially different noise footprints which may require extra data to be run with this module, for example open rotor engines.

3.6.3 Population Impacts Model

The population impacts model is a standalone add-on to AIM which takes AIM and noise model outputs, including pollutant concentrations and noise contours, and matches them to global population distribution data which can then be used to derive health impacts and related metrics. The current version uses ArcGIS, so users who wish to use the population impacts model to analyse AIM output will need a license to run ArcGIS; however, a version using R, which is freely available, is under development. Example output for Sydney airport is shown in Figure 23. For further information contact Joanna Kulsezo (j.kulsezo@ucl.ac.uk).

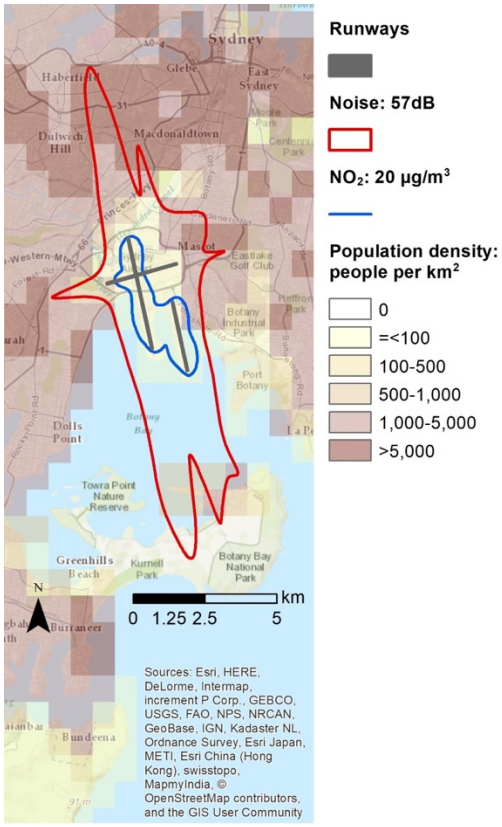

Figure 23. Sample output of the population impacts model for Sydney airport.

3.7 Regional Economics Module

A regional economics module has been developed which uses a metamodel of airport economic impact studies to estimate per-airport employment, GVA, income and TBR impacts of changes to the aviation system. This model is currently at the validation stage and will be added to this documentation as soon as validation has been completed. More information on the costing of externalities is given in Wadud (2009). For further information contact Andreas Schäfer (a.schafer@ucl.ac.uk).

4. Future Scenarios

To use the model to predict future demand we need scenarios which project key input variables into the future. These can be supplied as user input, or you can use the scenarios which are already supplied with the model. In the simplest case, using regional trends only and not modelling electric aircraft, four variables are needed:

- Projected population between 1990 and 2100, as a ratio with population in 1990, by world region (North America, Central America/Caribbean, South America, Europe, Middle East, Africa, Asia/Pacific). Historical values between 1990 and 2015 from Summers et al. (2016) are included in the default scenarios supplied with the model.
- Projected GDP per capita between 1990 and 2100, as a ratio with GDP per capita in 1990, by world region (as above). Historical values between 1990 and 2015 from Summers et al. (2016) are included in the default scenarios supplied with the model.

- Projected, constant-price oil price between 1990 and 2100, as a ratio with oil price in 1990. This is specified by world region but usually the same value is used globally; however, different values can be used if substantial differences in the price paid per region are anticipated. Historical values between 1990 and 2015 are included in the default scenarios supplied with the model.
- Projected carbon price per region, absolute values, in year 2015 US dollars **per tonne of carbon** (not CO_2, i.e. converted using tonnes_C/tonnes_CO_2 = 12 / (12 + 16 + 16)), if modelling carbon trading (otherwise set to 0).

If modelling electric aircraft, two additional variables are needed:

- The projected carbon intensity of electricity generation as a ratio with the value in 1990, by world region (as above). Historical values between 1990 and 2015 are included in some of the default scenarios supplied with the model[9], depending on whether the free or non-free databases are used.
- Industrial electricity price (constant-price) as a ratio with the value in 1990, by world region (as above). Historical values between 1990 and 2015 are included in some of the default scenarios supplied with the model, depending on whether the free or non-free databases are used.

If data is available, it is possible to specify all of these variables at a much finer level. Currently we use country-level data where available in the supplied scenarios. It is also possible to specify smaller region-level data, down to the individual city-level, if required. This works as follows:

- Global regions are always specified in the input data. For variables which are broadly global (e.g. oil price) a single global trend may be specified (world region 0). Otherwise, the world regions used are numbered 10-16 (North America = 10, Central America/Caribbean = 11, South America = 12, Europe = 13, Middle East = 14, Africa = 15, Asia/Pacific = 16) and are sometimes also referred to with region codes (NA, CA, SA, EU, ME, AF, AP with subscript _REG). In the absence of any other data, trends for a given city and/or airport are assumed to follow the regional trends. Airline fleet decisions are also assumed to be made on the basis of typical region-level costs, as airlines will typically operate across different countries within a region. The region each country is in is specified in the file *CountryData.csv*.
- Countries are numbered from 100 to 100 + $N_{countries}$, where $N_{countries}$ is the number of countries in the database and may vary depending on the base year dataset. They may also be referred to by their two-letter ISO country code. If input scenario data is specified at a country level, this is used in preference to the regional-level data apart from when assessing fleet decisions, as discussed above. The numbering for each country is given in the file *CountryData.csv*.
- In the file *CityData.csv* it is also possible to specify a further region code for each city, LocalRegion, with separate forecasts (currently dummy values are set which are unique to each city). For example, previous runs with AIM using UK-based forecasts specified population and GDP per capita growth rates in England, Scotland, Wales and

[9] Note that these values in the non-free database are derived from IEA data and hence users must have a license for this data to use this input.

Northern Ireland separately. For this, LocalRegion in *CityData.csv* was set to 1001, 1002, 1003 and 1004 respectively, and trends in *ScenarioData.cs*v were specified for regions 1001, 1002, 1003 and 1004. Where data is specified by local region, this is used in preference to country-level data apart from when assessing fleet decisions, as discussed above.

A recent range of scenarios for future GDP and population is available from O'Neill et al. (2013). These scenarios, SSP1-SSP5 in Figure 24, were developed for the IPCC fifth assessment report and cover a wide range of internally consistent futures. We use these scenarios in the supplied *ScenarioData.csv* file for population and GDP per capita trends. For oil prices we use fossil fuel price projections from DECC (2015; panel (c)). We use the central oil price projection with scenario SSP2. We pair the higher GDP growth scenarios, SSP5 and SSP1, with the DECC low oil price projection, to obtain scenarios in which we would expect particularly rapid growth in aviation demand. Similarly, we pair SSP3 and SSP4, which have the lowest GDP growth, with the high oil price projection, to make scenarios in which we would expect low growth in aviation demand and emissions.

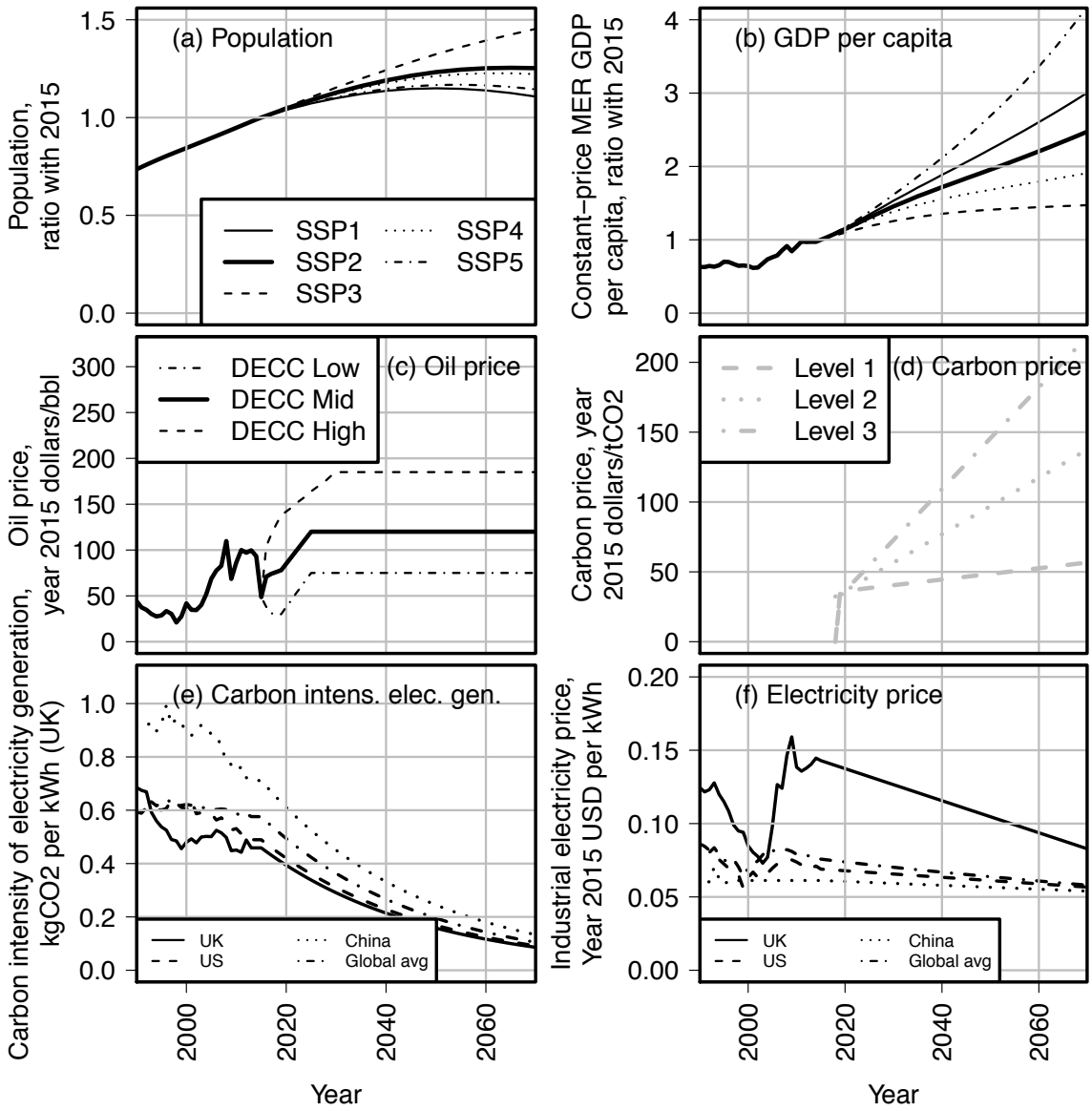

Figure 24. Model input scenario data.

These scenarios without carbon price input are referred to as base scenarios in the scenario data file (see the variable *ScenarioName*). For example, Scenario 1 is called SSP1base and uses the SSP1 population and income trends, DECC low oil price, and zero carbon price. Scenario 2 is called SSP2base uses the SSP2 population and income trends, DECC central oil price, and zero carbon price. These scenarios are also available with different carbon price trends, as shown in panel (d) of Figure 24. For example, Scenario 6 is called SSP1_cprice1 and includes the same variables as SSP1base but with the Level 1 carbon price trends shown in Figure 24. The other scenarios in *ScenarioData.csv* follow the same naming convention.

Currently, the same trends for carbon intensity of electricity generation and electricity price are included with all scenarios. These are intended to reflect a slow transition to greater use of renewables in the electricity sector. Prices trend linearly from year-2015 actual values by country towards a value of 5 US cents per kWh (in year 2015 cents) by 2100. The carbon

intensity of electricity generation is assumed to decrease by three percent per year from current values by country. Examples of the trends used can be seen in the bottom two panels of Figure 24. Note that in the free database supplied with the model only a single global trend for electricity carbon intensity and electricity prices is included per scenario, because the country-level data makes use of non-free (IEA) data.

As discussed in Dray et al. (2019), the baseline input scenario data has a strong impact on the final model outcomes. In particular, projected GDP/capita is perhaps the largest source of variability in projected emissions and demand, absent transformational change in the aviation sector, and this also interacts with uncertainty in income elasticities (e.g. Intervistas, 2007). Ideally any policy option evaluated in AIM should be assessed under multiple different scenarios.

5. Model validation and baseline projections

Model validation can take several forms. It may include validation of the model input data; validation of the assumptions and/or functional forms within the model; and testing the model output data against real-world outcomes. As the sub-models, their input data and assumptions have already been extensively tested (see discussion and individual references above for each model), we concentrate on the third form of validation. This section is based on the validation analysis and baseline projections carried out in Dray et al. (2019). To validate the integrated model, we use two approaches. First, we take a hindcasting approach to test its predictive power: using a 2005 base year dataset, we project demand from 2005 to 2015 and compare to actual 2015 values. Second, we use a 2015 base year and look at how this model matches to 2015 data, how it projects demand and emissions into the future, and how sensitive it is to key input variables. These approaches are separate to the validation processes for individual model components, which are discussed in the sections above and the references for each component cited above.

5.1 2005 base year projections to 2015

We use 2005 base year data from the previous version of AIM (e.g. Dray et al. 2014), recalculated where necessary to accommodate the new models and increased range of aircraft size classes. For projecting into the future, the model requires estimates of population and income growth and oil and carbon prices. For the 2005-2015 period we source these values from Summers et al. (2016) and IEA (2016), on a country-level basis. Modelled passenger enplanements and revenue passenger-kilometres (RPK) are shown in Figure 25, compared to observations from World Bank (2016).

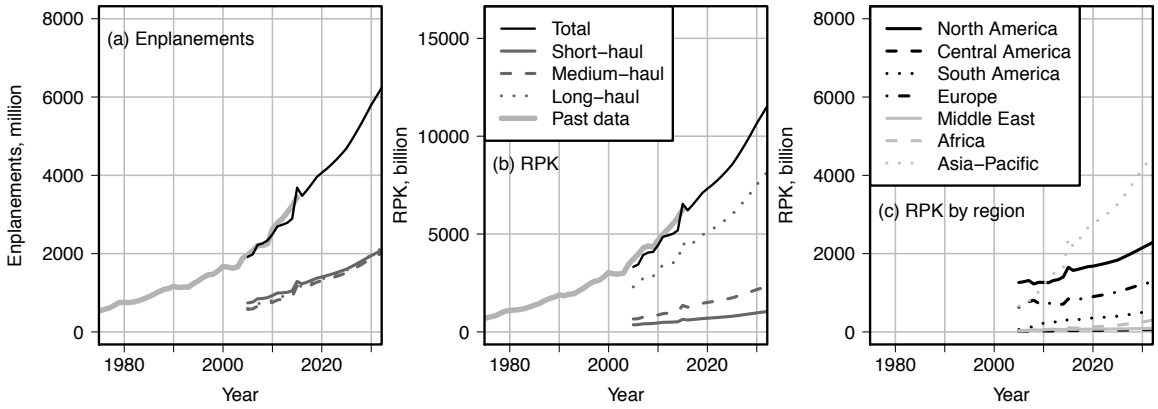

Figure 25. Enplanements and RPK from the 2005 base year hindcasting model.

Running AIM with 2005 base year data predicts 2015 total demand well. For example, projected global enplanements are 3,631 million compared to an actual value of 3,441 million, a difference of just over five percent. The model also projects the larger growth in long-haul travel compared to short-haul. Average regional growth rates are broadly as expected (Figure 7 (c)); for example, ICAO (2016) give year 2015 RPK totals for the North American and Asia-Pacific regions as 1,629 billion and 2018 billion respectively; we project 1,651 billion and 2,399 billion, a difference of 1% and 18% respectively. The small peak in modelled demand in 2015 reflects the large variations in oil price over the 2014-2016 time period and their impact on modelled ticket prices. We do not model the impact of hedging on airline fuel costs or time lags between fuel price rises and ticket price rises, both of which will act to smooth out the impact of fluctuations in the oil price over time.

In Figure 7 we compare the actual and modelled flight networks for 2015. The upper-left hand panel shows the 2015 network modelled by the 2005 base year model, in comparison to the modelled network in 2005 (lower left-hand panel), the 2015 base year model in 2015 (upper right-hand panel) and actual network in 2015 (lower right-hand panel). Although overall total demand is at a similar level, the 2005 base year model tends to concentrate more demand on busy routes than the actual 2015 network, particularly in Asia and South America. This may be a consequence of the network model used; although we allow passengers to shift between different itineraries, we currently do not allow airlines to add new segments to the network. This means the model does not catch the opening up of new routes, instead routing these passengers via hubs on existing routes[10].

[10] The addition of new direct routes when projected OD demand exceeds a given threshold (for example: the equivalent of two flights a day using typical equipment for the segment distance) is a likely addition in the next AIM update. Our analysis of schedule data between 2000 and 2015 shows that around 20% of passengers in 2015 are travelling on routes that did not exist in 2000, i.e. network development can have a significant impact over the long term.

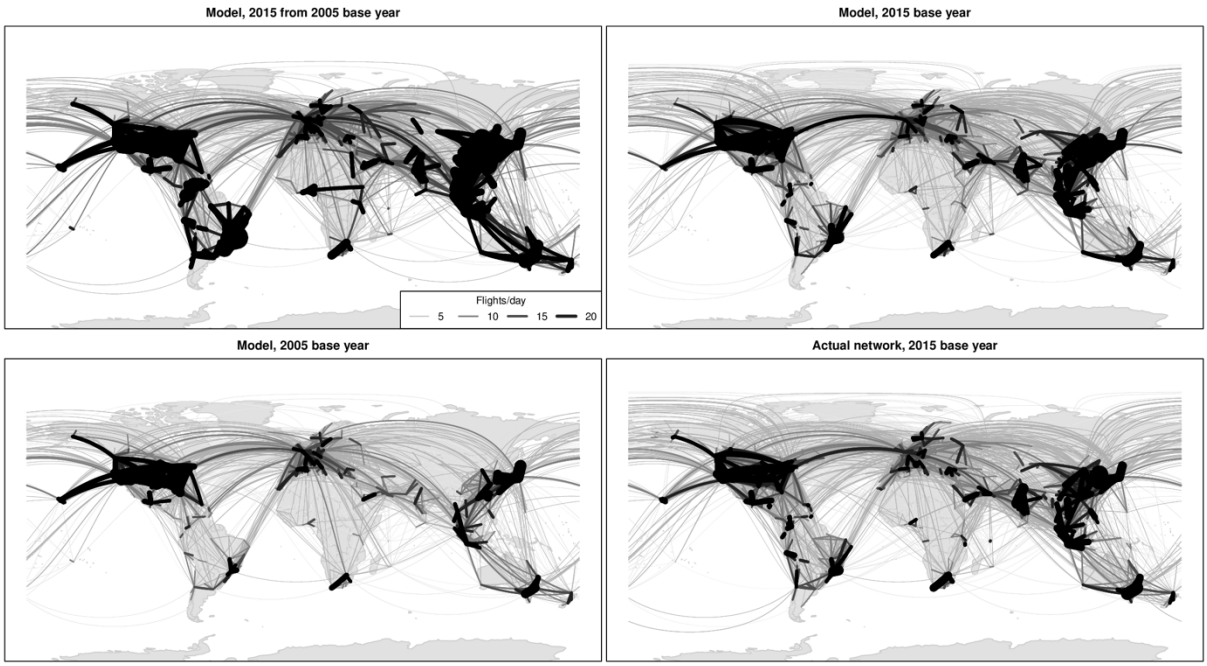

Figure 26. Modelled and actual flight networks.

5.2 2015 base year model

We obtain 2015 base year data from a variety of sources; major data sources include Sabre (2016) for schedule and passenger demand-related data, BTS (2017) for airline cost data, FlightGlobal (2017) for fleet data, RDC (2017) for en-route and landing charges, FlightStats (2016) for data on passenger delays and ICCT (2019) for freight load factors by region-pair. Figure 26 shows the model base year flight network in comparison to actual values. A comparison of the year 2015 base year model airport demand to observations was also made in Figure 2. We project base year global scheduled passenger enplanements and RPK of 3,400 million and 6,200 billion respectively, within 2.5% and 1% of the actual values (ICAO, 2016).

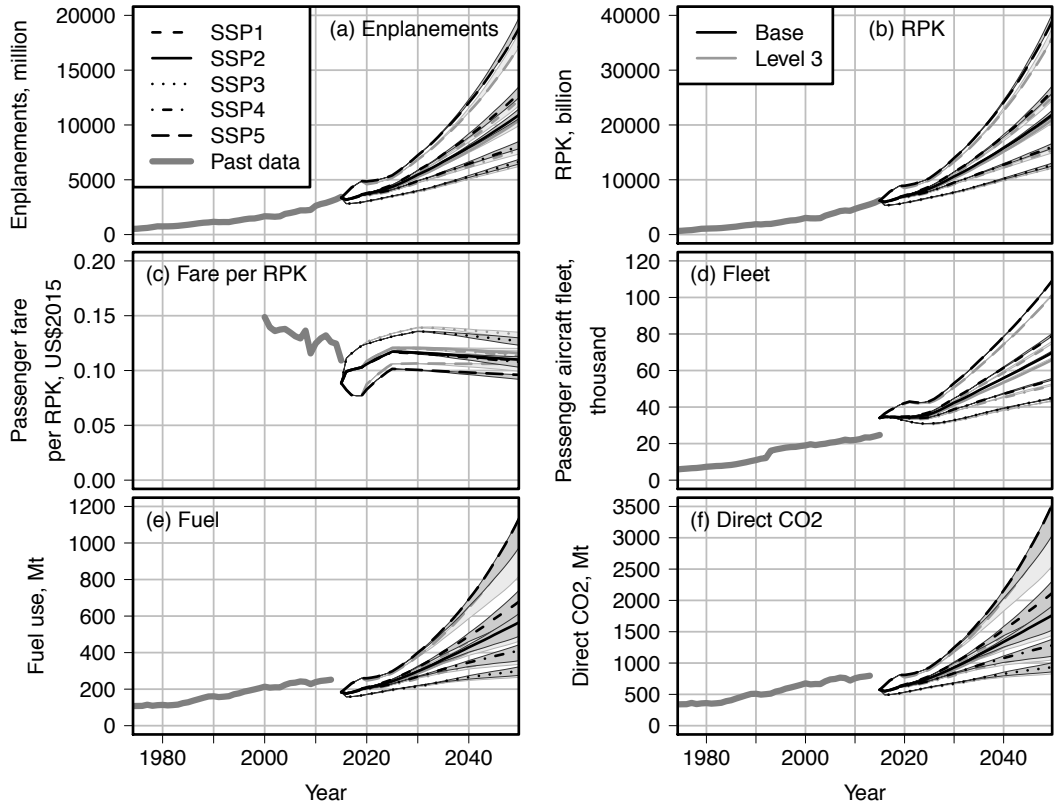

Figure 27. Enplanements, RPK, average system fare, fleet, fuel use and direct CO_2 emissions for the grid of model runs over baseline scenario, carbon price and technology lens for the world aviation system.

To use the model to project demand into the future, we use the scenarios discussed above in Section 4. Note that the scenarios run here differ from those supplied in the data input file in that SSP1 and SSP4 are paired with the DECC central oil price, although it is easy to reproduce input for these scenarios in the scenario input file if required. The baseline input scenario data is one source of variability in the final model outcomes. Another is the application of policy levers to the future system. Panel (d) in Figure 24 shows a range of hypothetical global carbon price scenarios, which we use to assess the model's response to increasing the airline cost of carbon emissions. A third source of variability in the outcomes is uncertainty in the model input parameters. As discussed in Section 2.8, for uncertainty in the characteristics of future technology measures we use a lens approach[11], with a central lens using mid-range characteristics plus two additional lenses chosen to reflect futures in which it is particularly easy or difficult to reduce emissions using technology. We omit the electric aircraft in these runs as at the time of validation only speculative parameters were available for a single size class.

To assess the variability in model outcomes absent any radical societal, technological or operational change, we therefore carry out model runs on a grid over SSP scenario, technology lens and carbon price scenario. The global-level results are shown in Figure 27. The grey bands beneath each line show the range of variability due to technology lens. For

clarity, we show only the baseline (zero carbon price) and Level 3 carbon price runs, over the full range of baseline scenarios.

Panels (a) and (b) of Figure 27 show enplanements and RPK in comparison to historical data from World Bank (2016). Panel (c) shows global system average passenger fare per RPK, in comparison to historical passenger revenue per RPK data from ICAO (2007, 2016; note as discussed in Section 3.1.3 that we do not expect these numbers to be exactly equal). Fare trends largely reflect the underlying trends in fuel cost and passenger numbers. Increasing passenger numbers allows airlines to take advantages of economies of scale, reducing ticket prices. Therefore average modelled fares initially fluctuate as fuel prices change, and then gradually decrease once the input oil price stabilises (panel (c) of Figure 27). Panel (d) shows the global fleet over all size classes compared to historical fleet data from FlightGlobal (2016). As discussed in Section 3.2.1, the fleet model initially over-predicts total fleet but adjusts to more feasible values over around a five-year period. This is the result of our assumption that for each size class and world region, aircraft are stored rather than directly retired if supply temporarily exceeds demand. Panels (e) and (f) show fuel use and emissions, in comparison to past data from all aviation sources from IEA (2017). As we model only scheduled passenger traffic, we expect the model to produce lower base year fuel use and emissions than the observed values for all aviation. In particular, as discussed in Section 2, freight in 2015 accounted for around 24% of global aviation tonne-km performed (ICAO 2016). We take account of hold freight in passenger aircraft when modelling aircraft weight load factor, but do not account for dedicated freighter aircraft, which carry around 40-50% of air freight (FTA 2008). Unscheduled passenger flights accounted for 5% of global RPK in 2015 (ICAO 2016), and military aviation has been estimated to be around 7-13% of aviation fuel use (Wilkerson et al. 2010; ICCT, 2019). For the runs carried out in Dray et al. (2019) we also omit the impact of non-lateral fuel use inefficiency, as discussed in Section 3.3. Therefore we expect our base year totals to be approximately 20-30% below the IEA totals, as observed.

Several outcomes are apparent from the projections of future trends. First, there is a large range of variability in aviation outcomes by 2050. Although demand grows in all scenarios, the projected year 2050 global RPK ranges between 12,150 billion and 40,660 billion, 2 and 6.6 times the year-2015 values respectively. Considering only central lens, zero carbon price scenarios, the highest-RPK scenario in 2050 has 3.1 times the RPK of the lowest-RPK one. If considering all scenarios, this ratio is 3.4, i.e. the most important source of the variability in outcomes is the scenario used for future trends in socioeconomic variables.

The impact of uncertainty in future technology characteristics is somewhat smaller in these runs, with, e.g. the SSP2 high and low lens scenarios differing by 5.4% in year 2050 RPK and 26% in year 2050 fuel consumption. This is partially an outcome of the relatively short time horizon: the technologies with the biggest impact on emissions per RPK are typically new aircraft models, which take a long time to percolate into the fleet. Technology characteristics which are uncertain include fuel use and cost; their impact on enplanements and RPK results from the impact these variables have on ticket prices and hence demand.

Carbon price also has a relatively limited impact at the levels modelled in this paper. Lines in light grey show scenarios in which the highest carbon price shown in Figure 8 is applied globally, reaching 150 dollars per tonne of CO_2 by 2050. This results in reductions in fuel use

and emissions of around 4-16% across scenarios. This is a relatively high carbon price: for example, the highest carbon price in the EU emissions trading scheme to date occurred in 2008 and was equivalent to around 36 (year 2015) dollars (European Climate Exchange, 2017). However, it has little effect on fares and demand compared to the baseline scenario. For example, for an Airbus A320 flight of 2,000 km with an 0.7 load factor, around 0.18 tCO_2 per passenger is emitted; therefore the cost to the airline per passenger for this flight is around 27 dollars. However, the ticket price elasticity for changes in fuel-related costs is typically close to 0.3 (Wang et al. 2017). This gives a fare per RPK increase of only around 0.01 dollars at base year fuel prices, as shown in Figure 27.

These scenarios can also be compared to other projections. Airbus (2016) project average demand growth over the 2015-2035 period of 4.5% per year in RPK, resulting in 32,000 new passenger aircraft of 100 or more seats by 2035 over the 2015-2035 period, around 20,000 of which are to serve new growth rather than replacing retiring aircraft. Boeing (2016) predict average global growth in RPK of 4.8% per year over the same time period, with fleet growth of around 23,000. We project average yearly demand growth of between 1.8% and 5.6% per year over this time period, with the central SSP2 scenario having a 3.8% growth rate; around 13,000 to 40,000 new aircraft of 100 or more seats would be needed to serve new growth over this time period, with the central SSP2 scenario requiring 25,000 new aircraft. Although the Airbus and Boeing projections are broadly central in these ranges, we typically project a larger requirement for aircraft per RPK, most likely because we project a slightly smaller average aircraft size.

6. Running the model

AIM is suppled as java code. It is cross-platform and the main code has no dependencies. However you will need to install java and a program that supplies a java compiler to compile and run it. We have tested AIM on Mac, Windows and Linux systems and have been able to run the model in each case. At least 8GB memory and several GB of disk space is preferable, depending on the number of model runs required and the type of data that the model is set to output.

Model run time is usually around one-three hours for a run from a 2015 base year to 2050, depending on the scenario, output and policy options chosen (further from baseline may take longer to converge, running to a later end year will take longer, producing inventories and dispersion modelling will take longer).

Currently, there are two versions of the year-2015 base year databases. The original version of the databases used some confidential data in the input passenger, fare, aircraft movement and scenario data variables for model initialization and calibration. Because we anticipate model users will not always have access to licenses for this data, we have produced a set of alternate databases for the model which do not contain this data, but instead initialize these variables from a set of baseline estimates from sub-models within AIM. These databases are freely available with the model but produce less accurate base year estimates on an individual route basis. However, system-wide aggregate totals (for example, RPK and CO_2) are typically reproduced to within 2% of the values with the non-free databases.

To run the model, it first needs to be complied. Any recent java compiler should be suitable for compilation. For example, the Java Development Kit (JDK), which is a free download from Oracle (see e.g. http://www.oracle.com/technetwork/java/javase/downloads/index-jsp-138363.html), contains the compiler javac. In MAC OS X or Linux, opening a terminal, navigating to the main AIM code directory (v9) and typing 'javac –classpath . AIMModel_v9.java' should compile the whole program. Another option is to use a GUI-based development environment such as NetBeans (https://netbeans.org), which is also a free download.

To run the model, you will first need to set the input parameters for the runs that you want to carry out. This includes, e.g. specifying the socioeconomic scenario to project demand into the future (Section 4) and any policy and technology options to include. The main user input file is AIMRunParameters.csv, in the code root directory (*v9*). The parameters in this file and typical input values are discussed in
Table 4, below. You may also want to change some values in the other model database files, for example to run only a subset of cities or a different set of technology options (discussed in Appendix 8). These files are stored in directories corresponding to the model base year, e.g. *v9/data_2015baseyea*r for year 2015 base year data and *v9/data_2005baseyear* for year 2005 base year data. The files and variables that users may want to edit are described below in Section 6.2.

Once the input values are set, the model can be run. Assuming java is installed, on Mac OS X and Linux this can be done by typing 'java AIMModel_v9' in the terminal (in the code root directory, *v9*). If using NetBeans or a similar development environment, the option to run the code should also be prominently available (e.g. 'Run' button in NetBeans). The 'verbose' variable in AIMRunParameters.csv sets the amount of information (about convergence and what is running at any given time) that the program prints out as it runs. Output location is determined by the 'RunID' variable in AIMRunParameters.csv: the model creates a directory *output/RunID* for each model run (note that this means rerunning a model with the same RunID will overwrite the output from the first run). The model output data files are described in Section 6.3.

6.1 Code Structure

The structure of the model code is not identical to the broad model structure diagram shown in Figure 1. The code structure is shown in Figure 28. This code is located in the code root directory (*v9*). Object definitions for storing different types of input data are included in the directory *v9/datastructures*. All routines are extensively commented including definitions of input and output parameters. The code comments are probably the best place to find the definition of a given variable, its dimensions and units.

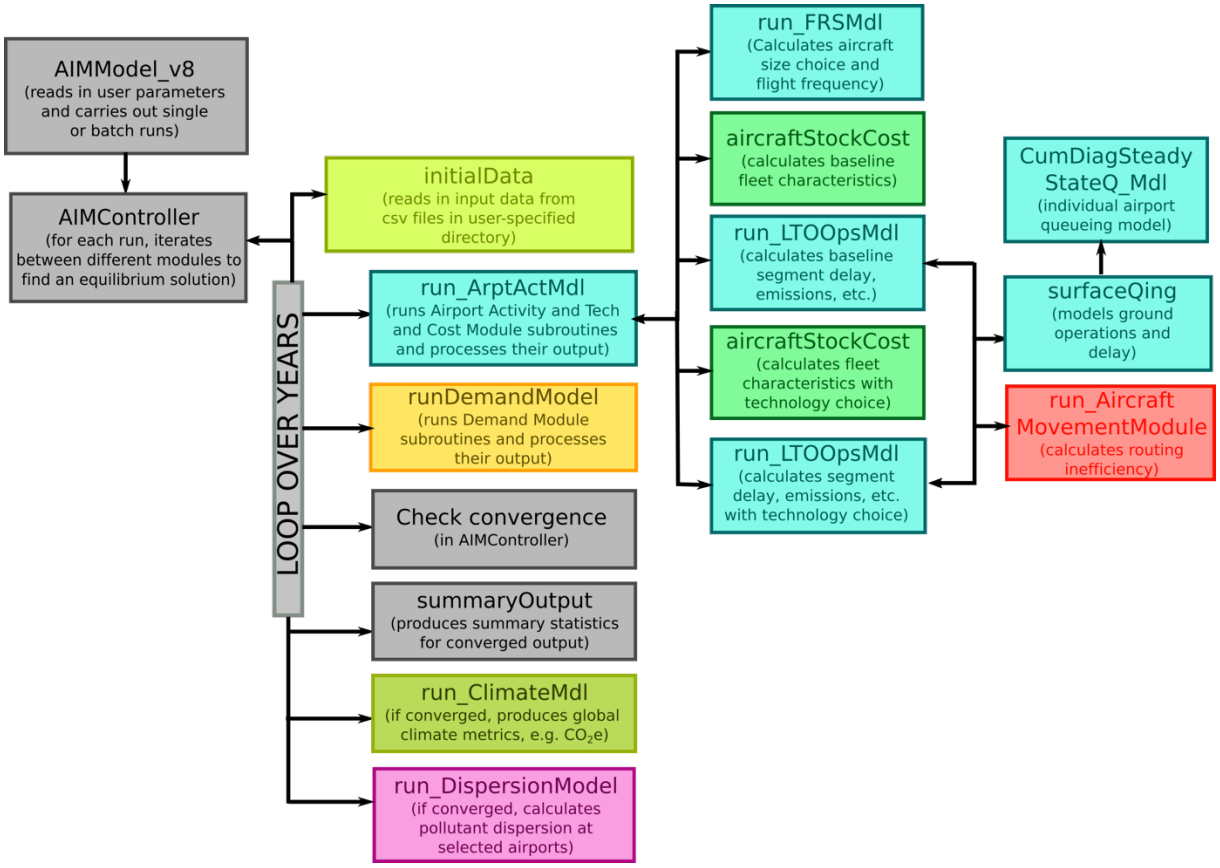

Figure 28. Code structure, AIM 2015 v9.

6.2 Input data

The main user input file is AIMRunParameters.csv, in the main directory. This file contains a selection of variables that affect how the model is run, e.g. which socioeconomic and technology scenarios to run, which year to run to, and how the cost-effectiveness of new technologies is assessed. Each line in the file gives parameters for a single model run. The variables are as follows:

Table 4. AIM model, main user input variables

Variable Name	Description	Typical values
RunNumber	Gives an ID number for each run (for user reference only)	1,2,3, etc.
RunID	The name of the run. This is used to name the run output directory and individual output files, to distinguish them from the output of other runs. If two model runs have the same RunID, the second one will overwrite the output of the first.	Text value, e.g., ScenarioSSP2_NoNewTech
DataInputDirectory	Directory in which to look for the model input databases.	By default this is data_2015baseyear
SocioeconomicScenario	The scenario to run for population and income. A number of scenarios are supplied with the model, based on the	The name of the scenario, e.g. "SSP2". The names and numbers of scenarios are given in the data file ScenarioData.csv: see also

	IPCC SSP scenarios, and more can be added as required (see Section 4).	Section 4 for the input variables used in each scenario.
UrbanisationScenario	A corresponding scenario to run for urbanisation, which is applied only to cities and not to airport groups in rural regions. A scenario based on the UN World Urbanisation Prospects is supplied with the model, and more can be added as required (see Section 4).	The name of the scenario, e.g. "UN_WUP". The names and numbers of scenarios are given in the data file ScenarioData.csv: see also Section 4 for the input variables used in each scenario.
OilPriceScenario	A corresponding scenario to run for oil price. Scenarios from DECC (2016) are supplied with the model, and more can be added as required (see Section 4).	The name of the scenario, e.g. "DECC_MID". The names and numbers of scenarios are given in the data file ScenarioData.csv: see also Section 4 for the input variables used in each scenario.
CarbonPriceScenario	A corresponding scenario to run for carbon price. Test scenarios from Dray et al. (2018) are supplied with the model, and more can be added as required (see Section 4).	The name of the scenario, e.g. "BASE". The names and numbers of scenarios are given in the data file ScenarioData.csv: see also Section 4 for the input variables used in each scenario.
CarbonIntensityOfElectricity GenerationScenario	A corresponding scenario to run for the carbon intensity of electricity generation. Only makes a difference to model outcomes if modelling electric aircraft. Test scenarios are supplied with the free database, and more can be added as required (see Section 4).	The name of the scenario, e.g. "EMF27_FULLTECH". The names and numbers of scenarios are given in the data file ScenarioData.csv: see also Section 4 for the input variables used in each scenario.
ElectricityPriceScenario	A corresponding scenario to run for electricity prices. Only makes a difference to model outcomes if modelling electric aircraft. Test scenarios are supplied with the free database, and more can be added as required (see Section 4).	The name of the scenario, e.g. "BASE". The names and numbers of scenarios are given in the data file ScenarioData.csv: see also Section 4 for the input variables used in each scenario.
BiofuelCharacteristicsScenario	A corresponding scenario to run for aviation drop-in biofuel lifecycle emissions and maximum supply to the aviation sector. These are only used if the biofuel model selected is one which needs scenario input: see BiofuelModelToUse, below.	The name of the scenario, e.g. "EMF27_FULLTECH". The names and numbers of scenarios are given in the data file ScenarioData.csv: see also Section 4 for the input variables used in each scenario.
TechDataFile	Gives the file (in DataInputDirectory) to use for future technology characteristics. Different technologies can be turned on or off for different aircraft size classes in this file. Therefore it is possible to use different input files here to create different technology futures (e.g. with or without electric aircraft, with or without blended wing body aircraft,etc.)	The default input file is TechnologyMeasureData.csv. See Section 3.4.3 for more detail.
TechScenario	To account for the high uncertainty in some technology characteristics we use a lens approach. Three lenses are available: one in which all technology characteristics are mid-range (2), one with pessimistic characteristics (late	0 to turn off the technology adoption model (in this case use the fuel and NOx trend variables specified below to model the impact of future technology changes). 1, 2 or 3 for the

	availability date, high cost, low benefit; 1) and one with optimistic characteristics (early availability date, low cost, high benefit; 3). This variable allows you to choose the technology characteristic lens for this run.	technology adoption model with pessimistic, mid-range or optimistic characteristics.
BiofuelModelToUse	This specifies what the characteristics of any drop-in biofuel should be (see Section 6.3 and Appendix 7 for information on the biofuel characteristics input).	0 to exclude biofuel. Otherwise set to the ID number of one of the options in the file BioFuelCharacteristics.csv (in DataInputDirectory) to use those fuel characteristics (e.g. 1, 2, 3).
CapScenario	The scenario for how airports respond to constrained future capacity when demand is rising. For the current version of AIM we recommend setting this to 1. This assumes that airport capacity will generally expand as required at a rate that maintains present-day delay levels.	1
EarlyRetirementScenario	If > 0, mandates aircraft retirement after a specific age. This option does not provide any extra incentive for airlines to do this – retirement is assumed to be mandatory.	0 to not use this option 1 for early retirements from age 30, 2 from age 25, 3 from age 20. This can be used in parallel with the technology lenses, above.
EndYear	The year to run the model to. Needs to be at or higher than the base year. The maximum EndYear without extending the scenario input data is 2100.	Typically between 2015 and 2100, e.g. 2050. Later EndYears are subject to greater levels of model uncertainty.
MakeInventories	Specifies whether the model should output detailed emissions inventories (i.e. grids of fuel use, NOx and PM by latitude, longitude and altitude) or not. Inventory files are large (around 20MB/year) and generating them will add a few minutes to the run time of the model, so if not needed this option should be turned off.	0 to not output inventories. 1 to output just the base and end year inventories. 2 to output base and end inventories plus one inventory per decade (e.g. 2020, 2030, 2040). 3 to output inventories for all years.
AmortizeTimeframe_years	This gives the timeframe over which purchasing decisions in the stock and technology models should be evaluated when using NPV, in years.	Currently we use 7 years for this value.
AmortizeDiscountRate_percent	The discount rate to use when evaluating purchasing decisions using NPV, in percent.	Currently we use 10 percent for this value.
PaybackTimeframe_years	The timeframe over which to evaluate purchasing decisions that are made on a payback period basis, in years.	Currently we use 3 years for this value.
GlobalExtraKMTax	Allows the user to specify a global extra per-km tax on airline tickets, in year 2015 US dollars, applied after the base year.	Default is 0.
GlobalExtraFlightTax	Allows the use to specify a global extra per-flight tax on airline tickets, in year 2015 US dollars, applied after the base year.	Default is 0.
GlobalExtraItineraryTax	Allows the user to specify a global extra per-itinerary tax on airline tickets, in year	Default is 0.

	2015 US dollars, applied after the base year.	
GlobalNOxAirportCharge_ Year2015DollarPerKG	Allows the user to specify a global extra landing charge for local NOx, in year 2015 dollars per kg NOx, applied after the base year.	Default is 0.
UpliftFactor	Gives a multiplicative factor that can be applied to direct aviation CO_2 to simulate the impact of non-CO_2 climate impacts. Typically this is set to 1.0 (i.e. no uplift) and the output of the climate module is used to more fully assess non-CO_2 impacts.	Default is 1.0, i.e. no uplift.
UseHSR	Model the impact of future planned high-speed rail developments, where data is available on them (note this is a very simple model, and only accounts for whether high-speed rail exists between two cities, not its characteristics). 250 km/h is used as a cutoff point for high speed.	1 to include, 0 to exclude.
MaxBiofuelBlend	Gives the maximum proportion of drop-in biofuel that can be blended with fossil Jet A. This value might be set below 1 to simulate supply constraints or certification requirements, for example.	Currently set to 0.5, i.e. maximum blend of 50% drop-in biofuel, 50% fossil Jet A. This reflects current certification limits (e.g. Zschocke, 2012)
RunCarbonTaxFleetRenewal	Runs a specific policy option where early retirements and aircraft replacement by the best available new technologies is funded by a carbon tax (see Dray et al., 2014). For the other input data files needed to run this model see Section 6.3.	1 to run, 0 to exclude. The retirement years and applicable world regions are set in separate data files, see Section 6.3. Note that EarlyRetirementScenario, above, should be set to 0 when using this option as the policies are not compatible.
FuelTrend20	If we are not modelling alternative technologies (i.e. TechScenario==0), we still need to make assumptions about how the fuel burn and emissions of new technologies change into the future. FuelTrend20 is the assumed percent/year improvement in fuel burn for new aircraft models between the base year and 2020.	A value of 1.0 would give a 1.0% per year reduction in typical fuel use for new technology models. Set to 0.0 to avoid double-counting improvements if running with TechScenario > 0.
FuelTrend50	As FuelTrend20, but for 2020 until the simulation end year.	As FuelTrend20. Should also be set to 0.0 if TechScenario > 0.
AirborneNOxYear20	As FuelTrend20, but for NOx emissions above 3000 feet.	As FuelTrend20 (e.g. 1.0 gives a 1%/year decrease in comparable-mission airborne NOx for new aircraft models). Set to 0.0 if running with TechScenario > 0.
AirborneNOxYear50	As AirborneNOxYear20, but for 2020 until the simulation end year.	As AirborneNOxYear20. Should also be set to 0.0 if TechScenario > 0.
LTONOxYear20	As AirborneNOxYear20, but for emissions below 3000 feet.	As AirborneNOxYear20 (e.g 1.0 gives a 1%/year decrease in comparable-missions LTO NOx for new aircraft models). Set to

		0.0 if running with TechScenario > 0.
LTONOxYear50	As LTONOxYear20, but for 2020 until the simulation end year.	As LTONOxYear20. Should also be set to 0.0 if TechScenario > 0.
NoiseTrendSideline	This variable gives a yearly decrease with future manufacture year for the certified sideline noise level, in EPNL. At the moment we do not directly link future technologies to changes in EPNL, so this value needs to be set manually if projecting these metris into the future.	A value of 1.0 would give a 1.0% per year reduction typical certified sideline EPNL for new technology models.
NoiseTrendFlyover	Same as NoiseTrendSideline, but for flyover noise.	As NoiseTrendSideline, above.
NoiseTrendApproach	Same as NoiseTrendSideline, but for approach noise.	As NoiseTrendSideline, above.
ETSPercentGrandfathered	If modelling emissions trading, this gives the percentage of emissions (from ETSBaseYear, below) which are grandfathered (i.e. airlines only have to purchase emissions allowances on emissions above this level).	A value of 80 assumes that 80% of emissions from ETSBaseYear are grandfathered (i.e. airlines must purchase allowances for any emissions above 0.8 * ETS base year emissions).
ETSBaseYear	This gives the year to use when calculating grandfathering of emissions, see above. Note that it is assumed no grandfathering is applicable before ETSBaseYear, even if nonzero carbon prices are in place.	A value of 2020 assumes emissions grandfathering post-2020 is based on the 2020 emissions level.
RunExternalDemandProjections	This variable allows users to bypass the internal demand model to put in external projections of demand. Note that in this case, there is no feedback between ticket prices and changes in demand.	1 to run external demand projections, 0 to use the inbuilt demand model. External demand projections are specified by world region-pair and can be set in RegionPairData.csv in DataInputDirectory.
WageGrowthModel	Gives the methodology to use for growth in pilot/flight attendant salaries over time. This can make a substantial difference to airline costs in high GDP growth scenarios.	If 0, assume salaries remain constant in real terms. If 1, assume salaries grow in line with GDP per capita.
WriteOutCityData	If 1, the program writes out data on a city-pair basis (e.g. demand, fares). These are large files, so set to 0 if you do not need data at this level of disaggregation.	1 to write city-pair data out, 0 to not do this.
Verbose	If 1, outputs more data to STDOUT about what the program is doing as it runs.	1 for more information, 0 for less.

In addition, the model requires various input data files in DataInputDirectory. These files can be edited if required to simulate a particular policy (e.g. changes in landing fees) but under normal operation users will not usually interact with them. There are several different versions of the data input directory files, including those for 2005 and 2015 base years, and (for the 2015 base year) a database that contains confidential data and one where the confidential data is replaced by values derived from models within AIM (i.e., instead of initializing fares as actual baseline values, they are initialized as baseline estimates from the fare model). The database version that is supplied with the model is the 2015 one without

confidential data. The main differences between model runs with and without the confidential data are:

- Base year individual route-level demand and fare may be less accurate (although they are still typically within 20% of actual values).
- There may be small differences in global aggregate demand and emissions totals (typically under 2% in model test runs).
- If using electric aircraft, baseline and scenario carbon intensity of electricity generation and electricity prices are approximate global-level values rather than country-level ones (note however that electric aircraft are unlikely to enter the system in significant numbers before 2050, by which time accuracy in baseline values will be less important than scenario assumptions about how these values change 2015-2050).
- Run time can be slightly longer.

All files are in csv format. Data read-in is done in the file *initialData_v22.java* and further explanation of the variables which are read in is given in the comments to this code. Most data is read into custom objects collecting together data which is specified on a similar basis: the code defining these objects is in the directory *datastructures* and the relevant object is given in each case below. The files are as follows:

- *AircraftData.csv*, which contains data which is specified by aircraft size class (e.g. reference aircraft utilisation, crew costs, takeoff fuel etc.). This data is read into a *DataByAircraftSize* object.
- *AircraftData_params.csv,* which contains parameters for the aircraft size choice model (Section 3.2.1).
- *AircraftPerformanceParams.csv,* which contains values for the aircraft performance model (Section 3.4.1) to calculate fuel use and emissions for reference technologies. This data is read into an *AircraftPerformanceData* object.
- *AircraftPerformanceParamsElec.csv,* which contains comparable values for electric aircraft, where appropriate. These values are derived from the TASOPTe model at MIT and were generated for the SAECA project on electric aircraft. They are also read into a separate *AircraftPerformanceData* object.
- *AircraftReplacementPolicyData_global.csv*, which contains assumptions used when running the RunCarbonTaxFleetRenewal policy option discussed in Table 3 above. For each year and world region, a manufacture date before which all aircraft are retired is given. See also Dray et al. (2014).
- *AirportData.csv,* which contains data which is specified by airport, e.g. latitude, longitude, base year capacity, landing fees, etc. This data is read into a *DataByAirport* object. This also contains the variable *RunGeog*, which determines whether the dispersion model is run for a given airport.
- *AirportGeography.csv*, which contains layout information and dummy emissions totals for the majority of airports in *AirportData.csv* (Where there is no layout information available, the variable *RunGeog* in AirportData.csv is set to -1).
- *AirportSegmentData.csv,* which contains data by airport-airport segment, e.g. base year flight frequency and enroute costs (either actual baseline values or, in the free database, estimated ones). Data is only stored for segments with nonzero demand, not for all airport-pairs. The data is read into a *SegmentArray* object.

- *AltitudeData.csv,* which contains data which is specified by altitude, e.g. distributions of typical cruise and holding altitudes. This is read into a *DataByAltitude* object.
- *BioFuelCharacteristics.csv,* which contains data on different drop-in biofuel options, e.g. year of first availability and fuel lifecycle emissions, that can be modelled using the input value BiofuelScenario discussed in Table 3 above and in Appendix 7. This includes explanatory notes about the data and its typical use. This is read into a *BiofuelData* object.
- *BiofuelCostCurveModelData.csv,* which contains data on biomass resources and costs for North America which can be used to model biofuel costs with a cost curve based on the year and amount of fuel needed – see appendix 7. The data is also read into the *BiofuelData* object if the cost curve model is in use for a given run (whether the cost curve model is in use or not is set in *BioFuelCharacteristics.csv* for each specific biofuel type).
- *CityData.csv*, which contains data that is specified by city, e.g. base year population and income, list of airports, etc. This file also specifies if a subset of cities is to be run. If the '*RunThis*' variable for a city is set to 1, it will be run; if 0, it will be omitted (though flights to and from the city may still be included if they run to or from a city which is being modelled). Sample files with RunThis = 1 for all cities (*CityData_RunAll.csv*) and with RunThis = 1 for North American cities only (*CityData_runNA.csv*) and European cities only (*CityData_RunEU.csv*) can also be provided. This data is read into a *DataByCity* object.
- *CostAndSystemParameters.csv,* which contains individual parameters which affect cost and operational modelling (mainly estimated model parameters, e.g. for the delay model, but also including assumptions on aircraft scrappage, deterioration per year and per passenger weight). This data is read into a *Params* object.
- *CountryData.csv,* which contains data by country, including region, assumed electricity price in the base year, and fixed effects parameters where specified by country (e.g. for the fare model). This dataset differs between the free and non-free versions: the non-free version contains data from IEA energy prices and taxes, so users should have a license for this data to use this file. However, these values are only needed if running the electric aircraft technology option. If not running this, these values can be replaced with dummy input (as in the free version). This data is read into a *DataByCountry* object.
- *DataByCityPair.csv*, which contains data that is specified by city-pair (including all feasible city-pairs in the dataset, i.e. N_{cities} *x* N_{cities}). This includes base year average journey time, existence of a road link, etc. Estimated fare data is used for initialisation, and estimated demand data is used as part of the interim demand model. This data is also read into the *DataByCity* object.
- *DimensionsAndSolutionParameters.csv,* which contains data on the size of various input datasets (e.g. maximum number of cities available to model, number of aircraft size classes) and data that is used in the model solution routines (e.g. maximum number of iterations to run, convergence tolerance). This data is also read into the *Params* object.
- *Elasticities.csv,* which contains estimated parameters used in the OD demand, fare and itinerary choice models (section 3.1). These are currently specified by distance and world region-pair and are read into a matrix.

- *FleetData.csv,* which contains data on total aircraft fleet by world region, size class and age. How we derive this data is discussed in Section 3.4.2 above. It is read into the *DataByAircraftSize* object.
- *LinkChange.csv,* which contains data on which city-city ground links are projected to change in future, e.g. if bridges or high-speed rail links are projected to be constructed. This data is used in the OD demand model. This is read into a *LinkChange* object.
- *MeteorologicalData.csv,* which contains data derived from surface and upper air meteorological databases per airport which describes how emissions from a point source would disperse under typical weather conditions. Further information on how this data is derived is given in Section 3.6.1. Note that currently only the top 20 airports and a small number of selected other airports (e.g. AMS, BOS, SYD, LGW, STN, LTN, PER) have this data available; currently other airports use dummy data.
- *NoiseCertificationData.csv*, which contains typical noise certification level in EPNL for sideline, flyover and approach noise by aircraft size class and historical manufacture year (up to the base year).
- *PhysicalAndClimateParameters.csv,* which contains individual physical and climate modelling-related parameters, for example the assumed density and specific energy of Jet A and the kg CO_2 released by burning 1kg jet fuel. This data is also read into the *Params* object.
- *RegionPairData.csv,* which contains data which is specified by region-pair, e.g. regional cost scaling factors. This is read into a *DataByRegionPair* object.
- *RoutingData.csv,* which contains sets of feasible (airport-airport, potentially via multiple hubs) routings used to get between each city-pair in the base year, and estimated initialisation parameters for these routes. Data for each city-pair is read into a *RoutingData* object, which are stored in a N_{cities} *x* N_{cities} matrix.
- *ScenarioData.csv,* which contains data on future projections of population, GDP per capita, oil prices etc., as discussed in Section 4. Data for the user-selected scenario only is read into a *DataByScenario* object.
- *TechnologyMeasureData.csv,* which contains data on alternative technologies that airlines can choose to adopt, e.g. the time from which they are available, any limitations on uptake, their impact on fuel use, NOx and PM by flight phase, etc. This includes new aircraft models, retrofits and operational measures. All measures can be turned on or off via the *'RunMeasure'* variable. They are specified by aircraft size class and lens, as discussed in section 3.4.4. Data for the user-specified lens is read into a *DataByTechnologyMeasure* object. The name of the file to use here is specified in the user input data so that users can batch run different technology scenarios, e.g. with technologies of interest turned on and off, using versions of this file with different names. See appendix 8 for more details on changing technologies.

6. 3 Output Data

The location of model output data is governed by the user-specified variable *runID*, as discussed above. Data for a given run is written to the directory *output/runID.* Currently, model output is as follows:

- *AirportData_RunID.csv*, which contains output data by airport. The code governing this output is located in the *DataByAirport* object code, i.e. in

datastructures/DataByAirport.java. This contains data by airport and model year for airport arrivals and departures (totals and by three-hour time bin), average delays by location of delay, cancellations, local NOx, NO_2, CO_2 and PM emissions, noise metrics, demand for fuel by fuel type and capacity utilisation index.

- AltitudeData_RunID.csv, which contains output data on global fuel use, distance travelled and emissions by 2000-foot altitude bin and year. This data is primarily used as input data for the global climate module. The code governing this output is located in the *DataByAltitude* object code, i.e. in *datastructures/DataByAltitude.java*.
- *CityData_RunID.csv*, which contains output data on OD demand and modelled average ticket price by city-pair and year. This is only output if requested by the user (variable *WriteOutCityData* in *AIMRunParameters.csv*) as, depending on the number of city-pairs modelled, these files can be rather large. The code governing this output is located in the *DataByCity* object code, i.e. in *datastructures/DataByCity.java*.
- *CountryData_RunID.csv,* which contains summary output data by country, including aircraft movements, enplanements, RPK, fuel use by type and CO_2 emissions on domestic and international levels. Note that international RPK is assumed to be divided equally between the countries of origin and destination (i.e. metrics are effectively on a departing flights basis). There are multiple ways that passengers, flights, fuel use and emissions may be attributed to different countries, and the methodology chosen will affect outcomes (e.g. Dray & Doyme 2019) – if this data is compared against country-level data that is specified on a different basis, then the totals differ somewhat. The accuracy of these totals will vary by country: for example, in a case where a country has two airports but only one is modelled in the simulation, the model may significantly under-predict totals. The code governing this output is located in the *DataByCountry* object code, i.e. in *datastructures/DataByCountry.java*.
- *DispersionData_RunID.csv,* which contains data on the projected annual average concentration of NO_2 and PM2.5 around airports for which the dispersion model was run (selected by the variable *RunGeog* in AirportData.csv). Not output if the dispersion model is not run. The size and resolution of the output grid is governed by the variables *dispXDist*, *dispYDist* and *dispDeltaDist* in *DimensionsAndSystemParameters.csv*. Currently these are set to output a square grid up to 20km away from the airport, at 200m intervals. The code governing this output is in the *DispersionData* object code, i.e. in *datastructures/DispersionData.java*.
- *FleetData_RunID.csv*, which contains summary output on a fleet basis, by world region, year and size class. This includes the fleet size, number of new aircraft, uptake of technology options, fleet age distribution and emissions and fuel use. The code governing this output is located in the *DataByAircraftSize* object code, i.e. in *datastructures/DataByAircraftSize.java*.
- *GlobalClimateMetrics_RunID.csv,* which gives CO_2e from different emissions sources in terms of different metrics (e.g. GWP, GTP on timescales from 50 to 500 years). The code governing this output is located at the end of *run_ClimateMdl_v2.java*.
- *Inventory_RunID_Year.csv* (one file for each year for which an inventory was requested, see the input variable *MakeInventories* in AIMRunParameters.csv, above). This gives gridded CO_2, NOx and PM2.5 by latitude, longitude and altitude, which can be used as input to a detailed climate model. Altitude resolution is the same as in AltitudeData.csv, above, i.e. 2000-foot bins. The resolution by latitude and longitude is specified by the variable *samplRateMap* in *DimensionsAndSystemParameters.csv*

and by default is 1 degree by 1 degree. The code governing this output is in the file *summaryOutput_v2.java* (specifically the routine *WriteInventory*). Inventories data is calculated in *run_LTOOpsMdl_v25.java* (specifically the routine *calculateInventory*). These files are large and generating them is time-consuming, so they should not be generated if they are not needed.

- *SegmentData_RunID.csv*, which contains output on a flight segment basis by origin airport, destination airport and year. This includes demand, load factor, flight frequency by aircraft size class, delay by location, route extension, emissions, fuel use by fuel type and effective flight frequency for some key technologies. The code governing this output is located in the *SegmentArray* object code, i.e. in *datastructures/SegmentArray.java*.
- *SummaryData_RunID.csv,* which contains a wide range of global and region-level summary data by year. This includes RPK, OD demand, enplanements, direct and fuel lifecycle emissions and fuel use, airline revenues and costs, the short-, medium- and long-haul split of demand, average carbon prices, and the number of iterations to reach convergence. The code governing this output is in the file *summaryOutput_v2.java*.

6.4 Plotting code

AIM is also supplied with some simple R scripts to visualise outputs. To use these you will need to have the (free) software R installed (https://www.r-project.org). These scripts are in the directory *plotting.* In general they are intended to be used for making sure that the model is behaving as anticipated. They are supplied on an 'as-is' basis. Note that to use these scripts you will need to edit the text at the beginning of each to supply various details about the model run you want plotted. The scripts included are:

- *Check_baseyear_byairport.R* – this plots base year segment and airport totals against database values, to check that the base year is well-established.
- *Check_baseyear_bycountry.R* – this plots country-level international and domestic RPK on a departing flights basis. It should be noted that there are several ways country-level flights, passengers and emissions can be attributed. When checking against country-level data, care should be taken that it is not reported on a different basis (for example, ICAO reports RPK by airlines based in a given country).
- *Projected_system_chars.R* – plots (for a grid of models or a single run) a set of projected system metrics including number of passengers, RPK, ticket price per RPK, total fleet, totals fuel use, and fuel lifecycle CO_2 (note that under the accounting used in AIM, direct CO_2 from drop-in biofuels is equal to that from fossil jet A).
- *Plot_fleet.R* – this plots the fleet by technology group for a given run over time. Note that if you change the selection of technologies available you will need to edit this script to make sure it includes all of the available options.
- *Map_system.R* – this generates a map of the global aviation system for a given year and model run. It requires some additional R packages to be installed (geosphere, rworldmap and colorRamps). Note that the pdf files this generates can be large (50 MB or so), because they contain a vector representation of the entire yearly flight segment data. If you need a smaller file at a given resolution these pdfs should be converted to bitmap format (e.g. png).

Output from each script is in the form of pdf files, written to the same directory as the plotting code. The output filenames include the run name in each case (for grid-based plots, the run name of the central run).

6.5 Licensing

AIM is distributed under a MIT license (https://opensource.org/licenses/MIT). This license allows use of the software under the following conditions:

"Permission is hereby granted, free of charge, to any person obtaining a copy of this software and associated documentation files (the "Software"), to deal in the Software without restriction, including without limitation the rights to use, copy, modify, merge, publish, distribute, sublicense, and/or sell copies of the Software, and to permit persons to whom the Software is furnished to do so, subject to the following conditions:

The above copyright notice and this permission notice shall be included in all copies or substantial portions of the Software.

THE SOFTWARE IS PROVIDED "AS IS", WITHOUT WARRANTY OF ANY KIND, EXPRESS OR IMPLIED, INCLUDING BUT NOT LIMITED TO THE WARRANTIES OF MERCHANTABILITY, FITNESS FOR A PARTICULAR PURPOSE AND NONINFRINGEMENT. IN NO EVENT SHALL THE AUTHORS OR COPYRIGHT HOLDERS BE LIABLE FOR ANY CLAIM, DAMAGES OR OTHER LIABILITY, WHETHER IN AN ACTION OF CONTRACT, TORT OR OTHERWISE, ARISING FROM, OUT OF OR IN CONNECTION WITH THE SOFTWARE OR THE USE OR OTHER DEALINGS IN THE SOFTWARE."

6.6 Contacts

The AIM model was originally developed at Cambridge University and is now under active development in the Air Transportation Systems Lab at UCL (http://www.atslab.org). This webpage contains recent news and copies of/links to group publications. For further information about the Air Transportation Systems Lab, contact Andreas Schäfer (a.schafer@ucl.ac.uk). For further information about the AIM code in general, contact Lynnette Dray (l.dray@ucl.ac.uk). For more information about the population impacts model, contact Joanna Kuleszo (j.kulsezo@ucl.ac.uk).

ACCLAIM also links with more detailed demand modelling currently being undertaken at Imperial College. For further information on this modelling, which is currently in progress, contact Aruna Sivakumar (a.sivakumar@imperial.ac.uk).

The noise model was developed at Southampton University and is part of a range of noise models which account for different data requirements and modelling needs. For more information on this model, contact Rod Self (rhs@stoton.ac.uk) and Antonio Torija (A.J.Martinez@soton.ac.uk).

The air quality model was developed at Cambridge University and further refined at MIT. For further information contact Steven Barrett (sbarrett@mit.edu).

The regional economics model is under development at UCL, and is currently at the validation stage. For more information on this model, contact Andreas Schäfer (a.schafer@ucl.ac.uk).

7. References

(see also www.atslab.org/publications for copies of AIM/ACCLAIM group publications)

Airbus. Global Market Forecast 2016-2035. Airbus: Toulouse, 2016.

Aircraft Commerce, 2017. Maintenance and Engineering section. http://www.aircraft-commerce.com/articles/browsearticles.asp?cID=36461852&path=true

Airports Commission, 2015. Airports Commission: Final Report. https://www.gov.uk/government/uploads/system/uploads/attachment_data/file/440316/airports-commission-final-report.pdf

Airports Council International (ACI) 2010. Effects of Air Traffic on Air Quality in the Vicinity of European airports. ACI Europe Environmental Strategy Committee report, Autumn 2010.

Allaire D, Noel G, Willcox K and Cointin R. Uncertainty quantification of an Aviation Environmental Toolsuite. *Reliability Engineering and System Safety*, 2014; **126**:14-24.

Al Zayat, K., Dray, L., Schäfer A., 2017. A Comparative Analysis of Operating Cost between Future Jet-Engine Aircraft and Battery Electric Aircraft. 21st ATRS Conference, Antwerp, 5-8 July 2017.

Barrett, S. and Britter, R., 2009. Algorithms and analytical solutions for rapidly approximating long-term dispersion from line and area sources. Atmospheric Environment 43, 3249-3258.

Berntsen, T. K., Fuglestvedt, J. S., Joshi, M. M., Shine, K. P., Stuber, N., Ponater, M., Sausen, R., Hauglustaine, D. A., Li, L., 2005. Response of climate to regional emissions of ozone precursors: sensitivities and warming potentials. Tellus B, 57(4), 283-304.

Bhadra D. Choice of Aircraft Fleets in the US NAS: Findings from a Multinomial Logit Analysis, *3rd AIAA ATIO Conference*, Denver, CO, 2003.

Boeing. "Current Market Outlook 2016-2035". Boeing: Seattle, 2016.

Bosbach, W. Airline fleet acquisition decisions in the global market for commercial aircraft, TU Munich graduate thesis, 2011. http://www.aimproject.aero/Documents/GraduateThesis_Bosbach.pdf.

BTS, 2017. Form 41 airline costs and on-time performance databases. https://www.transtats.bts.gov/.

Coldren GM, Koppelman FS, Kasturirangan K and Mukherjee A. Modeling aggregate air-travel itinerary shares: logit model development at a major US airline. *Journal of Air Transport Management*, 2003: **9(6)**; 361-369.

DECC, 2015. Fossil fuel price projections: 2015. https://www.gov.uk/government/publications/fossil-fuel-price-projections-2015

Department of Energy. US Billion-Ton Update. ORNL/TM-2011/224. Oak Ridge National Laboratory, 2011.

Doyme K., Dray L., O'Sullivan A., and Schäfer A.W., 2019. "Simulating Airline Behavior: Application for the Australian Domestic Market", *Transportation Research Record,* 2673(2), 104-112

Dray, L., Evans, A., Vera-Morales, M., Reynolds, T. G. and Schäfer, A., 2008. Network and environmental impacts of passenger and airline response to cost and delay. 8th AIAA Aviation Technology, Integration and Operations Conference, Anchorage, AK, September 14-19.

Dray, L., Evans, A., Reynolds, T. G., Rogers, H., Schäfer, A. and Vera-Morales, M., 2009. Air transport within an emissions trading regime: a network-based analysis of the United States and India. 88th Transportation Research Board Annual Meeting, Washington DC, January 11-15.

Dray, L., 2013. An analysis of the impact of aircraft lifecycles on aviation emissions mitigation policies. Journal of Air Transport Management, 28, 62-69.

Dray, L., Schäfer, A. & Ben-Akiva, M., 2012. "Technology Limits to Reducing Transport Sector Greenhouse Gas Emissions", *Environmental Science and Technology*, **46(9)**, 4734-4741.

Dray, L., Schäfer, A. & Al Zayat, K., 2018. The global potential for CO_2 emissions reduction from jet engine passenger aircraft. *Transportation research Record*, 2672(23), 40-51.

Dray L., Krammer P., Doyme K., Wang B., Al Zayat K, O'Sullivan A., Schäfer A., 2019. "AIM2015: Validation and initial results from an open-source aviation systems model", *Transport Policy,* 79, 93-102.

Dray, L. and Doyme, K., 2019. "Carbon Leakage in Aviation Policy", *Climate Policy,* 19 (10), 1284-1296.

European Climate Exchange, 2017. Carbon prices on the European Climate Exchange. http://www.ecx.eu/

Evans, A., 2008. "Rapid Modelling of Airport Delay". 12th Air Transport Research Society (ATRS) World Conference, Athens, Greece, July 6-10.

Evans A. D. and Schäfer A, 2011. The Impact of Airport Capacity Constraints on Future Growth in the United States Air Transportation System. *Journal of Air Transportation Management*, **17**, 288-295.

FlightGlobal, 2016. Ascend Online Fleet Database. http://www.ascendworldwide.com/what-we-do/ascend-data/aircraft-airline-data/ascend-online-fleets.html.

FAA, 2016. Aviation System Performance Metrics (ASPM) database. https://aspm.faa.gov/apm/sys/main.asp.

Flightstats, 2016. Global Cancellation and Delay Database. http://www.flightstats.com/go/Media/stats.do.

FTA, 2008. The role of air freight in the UK. http://www.fta.co.uk/export/sites/fta/_galleries/downloads/air_freight/the-role-of-air-freight-in-the-UK.pdf

Gnadt A., 2018. Technical and Environmental Assessment of All-Electric 180-Passenger Commercial Aircraft; S.M. Thesis, Massachusetts Institute of Technology, 2018.

Gnadt, A., Speth, R., Sabnis, J. and Barrett, S., 2018. Technical and Environmental Assessment of all-electric 180-seater aircraft. Progress in Aerospace Sciences, 105, 1-30.

Graver, B. & Rutherford, D., 2018. Transatlantic Airline Fuel Efficiency Ranking, 2017. ICCT White paper. https://theicct.org/sites/default/files/publications/Transatlantic_Fuel_Efficiency_Ranking_20180912_v2.pdf.

Hansen, M., 2002. Micro-lvel analysis of airport delay externalities using deterministic queueing models: a case study. Journal of Air Transport Management, 8, 73-87.

Hao, E., 2014. Ancillary Revenues in the Airline Industry: Impacts on Revenue Management and Distribution Systems. MIT Masters' thesis, June 2014. https://dspace.mit.edu/bitstream/handle/1721.1/89854/890140266-MIT.pdf?sequence=2

Heathrow Airport, 2011. Air Quality Strategy 2011-2020. https://www.heathrow.com/file_source/Company/Static/PDF/Communityandenvironment/air-quality-strategy_LHR.pdf

Hepperle, M., 2012. Electric flight – potential and limitations. AVT-209 Workshop on Energy Efficient Technologies and Concepts Operation, Lisbon, Portugal, 2012, 1-30.

Hoogwijk, M., Faaij, A., de Vries, B. and Turkemburg, W., 2009. Exploration of regional and global cost-supply curves of biomass energy from short-rotation crops and abandoned cropland and rest land under four IPCC SRES land-use scenarios. *Biomass and Bioenergy*, Vol. 33 (1), pp. 26-43

IATA, 2007. Estimating air travel demand elasticities. https://www.iata.org/whatwedo/Documents/economics/Intervistas_Elasticity_Study_2007.pdf

ICAO, 2009. Available capacity and average passenger mass. ICAO Working Paper STA/10-WP/5. https://www.icao.int/Meetings/STA10/Documents/Sta10_Wp005_en.pdf

ICAO, 2014. ICAO Annual Report, 2014: Appendix 1. https://www.icao.int/annual-report-2014/Documents/Appendix_1_en.pdf

ICAO, 2016a. Resolution A39-3. Consolidated statement of continuing ICAO policies and practices related to environmental protection. http://www.icao.int/environmental-protection/Documents/Resolution_A39_3.pdf

ICAO, 2016b. ICAO Annual Report, 2016. http://www.icao.int/about-icao/Pages/annual-reports.aspx

ICAO, 2017. ICAO Engine Emissions Databank. https://www.easa.europa.eu/easa-and-you/environment/icao-aircraft-engine-emissions-databank

ICCT (2019). CO2 emissions from commercial aviation, 2018. ICCT Working Paper 2019-16. https://theicct.org/sites/default/files/publications/ICCT_CO2-commercl-aviation-2018_20190918.pdf

IEA, 2016. Energy prices and taxes online data service. http://www.iea.org/statistics/monthlystatistics/monthlyoilprices/

IEA, 2017. World Energy Statistics, 2016. http://www.iea.org/statistics/.

INFRAS/IWW, 2000. External Costs of Transport: Accident, Environmental and Congestion Costs of Transport in Western Europe, Karlsruhe/Zurich/Paris.

Intervistas, 2007. Estimating Air Travel Demand Elasticities. https://www.iata.org/en/iata-repository/publications/economic-reports/estimating-air-travel-demand-elasticities---by-intervistas/

IPCC, 2001. *Climate Change 2001—The Scientific Basis* (eds. J. T.Houghton, Y.Ding, D. J.Griggs, M.Noguer, P. J.Van Der Linden and D.Xiaoxu). Cambridge University Press, Cambridge.

Jones, K and Cadoux, R., 2009. Metrics for Aircraft Noise. CAA ERCD Report 0904. http://publicapps.caa.co.uk/docs/33/ERCD0904.pdf

Kar, R, Bonnefoy, P. & Hansman, R. J., 2010. Dynamics of Implementation of Mitigating Measures to Reduce CO_2 Emissions from Commercial Aviation. https://www.researchgate.net/publication/268425966_Dynamics_of_Implementation_of_Mitigating_Measures_to_Reduce_CO_2_Emissions_from_Commercial_Aviation

Krammer, P., Dray, L. and Köhler, M., 2013. Climate-neutrality versus carbon-neutrality for aviation biofuel policy. Transportation Research Part D, 23, 64-72.

Larson, R., and Odoni, A. R., 1981. Urban Orperations Research. Prentice-Hall, NJ.

Lissys, 2017. The PIANO X Aircraft Performance Model. www.piano.aero.

Marenco, A., Thouret, V., Nedelec, P., Smit, H., Helten, M., Kley, D., Karcher, F., Simon, P., Law, K., Pyle, J., Poschmann, G., Von Wrede, R., Hume, C. and Cook, T., 1998. Measurement of ozone and water vapour by Airbus in-service aircraft: The MOZAIC airborne program, an overview. Journal of Geophysical Research, 103(D19), 25631-25642.

Morrell, P. and Dray, L., 2009. Environmental aspects of fleet turnover, retirement and life cycle. Final report for the Omega consortium. http://bullfinch.arct.cam.ac.uk/documents/FleetTurnover_CranfieldCambridge.pdf

NOAA, 2008a. Integrated Surface Database (ISD). http://www.ncdc.noaa.gov/oa/climate/isd/index.php.

NOAA, 2008b., Integrated Global Radiosonde Archive. http://www.ncdc.noaa.gov/oa/climate/igra/.

O'Neill, B. C., Kriegler, E., Riahi, K., Ebi, K., Hallegatte, S., Carter T. R. et al. 2013. A new scenario framework for climate change research: The concept of shared socio-economic pathways. Climatic Change, 122(3), 387-400.

Oum, T., Waters, W. & Yong, J.-S., 1992. Concepts of priceelasticities of transport demand andrecent empirical estimates. Journal of Transport Economics and Policy, 26(2), 139-154.

Poll, D. I. A., 2018. On the relationship between non-optimum operations and fuel requirement for large civil transport aircraft, with reference to environmental impact and contrail avoidance strategy. The Aeronautical Journal, 122 (1258), 1827-1870.

RDC, 2017. RDC Aviation airport and enroute charges databases. http://www.rdcaviation.com/.

Reynolds, T., Barrett, S., Dray, L., Evans, A., Köhler, M., Vera-Morales, M., Schäfer, A., Wadud, Z., Britter, R., Hallam, H., Hunsley, R., 2007. Modelling Environmental and Economic Impacts of Aviation: Introducing the Aviation Integrated Model- ling Tool. In: Proceedings of the 7th AIAA Aviation Technology, Integration and Operations Conference, Belfast, 18–20 September 2007, AIAA-2007-7751.

Reynolds, T. G., 2009. Development of flight inefficiency metrics for environmental performance assessment of ATM. 8th USA/Europe Air Traffic Management Research and Development Seminar, Napa, CA, June 29 - July 2.

Sabre, 2017. Market Intelligence passenger demand, routing and aircraft schedule databases. https://www.sabreairlinesolutions.com.

Sausen, R., Isaksen, I., Grewe, V., Huaglustaine, D., Lee, D. S., Myhre, G., Köhler, M. O., Pitari, G., Schumann, U., Stordal, F. and Zerefos, C., 2005. Aviation radiative forcing in 2000: an update on IPCC(1999). Meteorologische Zeitschrift, 14(4), 555-561.

Schäfer, A., Evans, A. D., Reynolds, T. and Dray, L. M. Costs of Mitigating CO2 Emissions from Passenger Aircraft. *Nature Climate Change*, Vol. 6, 2016, pp. 412-417.

Searle, S. and Malins, C., 2015. A reassessment of global bioenergy potential in 2050. *GCB Bioenergy*, Vol. 7 (2), pp. 328-336.

Shine, K. P., Fuglestvedt, J. S., Hailemariam, K., and Stuber, N., 2005. Alternatives to the global warming potential for comparing climate impacts of emissions of greenhouse gases. Climatic Change, 68(3), 281-302.

Simone, N. W., Stettler, M. E. J., and Barrett, S. R. H., 2013. Rapid estimation of global civil aviation emissions with uncertainty quantification. Transportation Research Part D, 25, 33-41.

Stettler, M. E. J., Boies, A. M., Petzold, A. and Barrett, S. R. H., 2013. Global civil aviation black carbon emissions. Environmental Science and Technology, 47, 10397-10404.

Summers, R., Heston, A. and Kravis, I., 2016. Penn World Tables. http://cid.econ.ucdavis.edu/pwt.html

Sustainable Aviation, 2015. The SA Noise Roadmap. http://www.sustainableaviation.co.uk/wp-content/uploads/2015/09/SA-Noise-Road-Map-Report.pdf.

Timmis, A., Hodzic, A., Koh, L., Bonner, M., Schäfer, A., and Dray, L., 2015. Environmental impact assessment of aviation emissions reduction through implementation of composite materials. International Journal of Life Cycle Assessment, 20(2), 233-243.

Torija, A. J., Self, R. H. and Flindell, I. H., 2016. On the CO_2 and noise emissions forecast in future aviation scenarios in the UK. Proceedings of inter.noise 2016, Hamburg.

Torija, A. J. , Self, R. H. and Flindell, I. H., 2016. Evolution of noise metrics in future aviation scenarios in the UK. 23rd International Congress on Sound and Vibration, Athens, 10-14 July 2016.

Torija, A.J., Self, R. H. and Flindell, I. H., 2017. A model for the rapid assessment of the impact of aviation noise near airports. Journal of the Acoustical Society of America 141(2), 981-995.

Wadud, Z., 2009. A systematic review of literature on the valuation of local environmental externalities of aviation. Final report for the Omega consortium.

Wang, B., O'Sullivan, A., Dray, L., Al Zayat, K. and Schäfer, A., 2017. Modelling the Pass-Through of Airline Operating Costs on Average Fares in the Global Aviation Market. 21st ATRS conference, Antwerp, 5-8 July 2017.

Wang, B., O'Sullivan, A., Dray, L. and Schäfer, A., 2018. Modelling airline cost pass-through within regional aviation markets. Transportation Research Record, accepted.

Wayson, R. L., Fleming, G. G. and Iovinelli, R. (2009). Methodology to estimate particulate matter emissions from certified commercial aircraft engines. Journal of the Air and Waste Management Association, 59(1); 91-100.

White, S., Ollerhead, J. B., Cadoux, R. E. and Smith, M. J. T., 2003. Quota Count Validation Study: Noise Measurements and Analysis. CAA ERCD Report 0205. https://publicapps.caa.co.uk/docs/33/ERCD0205.PDF

Wilkerson, J. T., Jacobson, M. Z., Malwitz, A., Balasubramanian, S., Wayson, R., Fleming, G., Naiman, A. D., Lele, S. K., 2010. Analysis of emission data from global commercial aviation: 2004 and 2006. Atmos. Chem. Phys., 10, 6391-6408.

Wolfe, P. J., Yim, S. H. L., Lee, G., Ashok, A., Barrett, S. R. H. and Waitz, I. A., 2014. Near-airport distribution of the environmental costs of aviation. Transport policy, 34, 102-108.

Wood, E.C., Herndon, S. C., Timko, M. T., Yelvington, P. E. and Miake-Lye, R.C., 2008. Speciation and chemical evolution of nitrogen oxides in aircraft exhaust near airports. Environmental Science and Technology, 2008, 42(6), 1884-1891.

World Bank, 2016. Global air transport data. http://data.worldbank.org/indicator/IS.AIR.PSGR

Yim, S. H. L., and Barrett, S. R. H., 2014. Rapid Dispersion Code (RDC): a technical note. Available from http://lae.mit.edu.

Yim, S. H. L., Lee, G. L., Lee, I. H., Allroggen, F., Ashok, A., Caiazzo, F., Eastham, S. D., Malina, R. and Barrett, S. R. H., 2015. Global, regional and local health impacts of civil aviation emissions. Environmental Research Letters, 10(3), 034001.

Zschocke, A. High biofuel blends in aviation. ENER/C2/2012/420-1, 2012. http://www.hbba.eu/study/index.html

Appendix 1: OD demand model, main parameters

For further discussion of these parameters, their sources and/or estimation, see Dray et al. (2014). Note that two income and two population terms are used in the demand equation (Section 3.1.1). Therefore the income and population elasticities are double the parameter used in the equation. Note also that the income elasticity terms are derived from Intervistas (2007) and are not part of the estimated model: the R^2 values refer to the estimated model only. Generalised cost elasticities are typically slightly larger (more negative) than fare elasticities estimated on the same data. A further discussion of the differences is given in Dray et al. (2014).

Route group	Distance, statute miles	Income elasticity	Population elasticity	Generalised cost elasticity	R^2
Intra North America	< 500	1.6	0.86 (0.04)	-2.04 (0.08)	0.53
	500 - 1000	1.7	0.84 (0.02)	-2.61 (0.07)	0.77
	> 1000	1.8	0.86 (0.02)	-2.61 (0.06)	0.57
Intra Europe	< 500	1.3	0.75 (0.05)	-1.24 (0.09)	0.47
	500 - 1000	1.4	0.85 (0.05)	-1.27 (0.08)	0.47
	> 1000	1.5	0.75 (0.03)	-1.08 (0.05)	0.47
Intra Asia	< 500	1.8	0.80 (0.06)	-0.62 (0.16)	0.66
	500 – 1000	1.8	0.95 (0.06)	-0.89 (0.13)	0.66
	> 1000	2.0	0.83 (0.05)	-1.00 (0.11)	0.66
Intra Central/ South America	< 500	1.8	0.87 (0.05)	-0.58 (0.19)	0.74
	500 – 1000	1.8	1.16 (0.10)	-1.65 (0.43)	0.74
	> 1000	2.0	1.18 (0.10)	-0.98 (0.26)	0.74
Intra Africa	All	1.8	1.18 (0.13)	-0.98 (0.24)	0.70

Intra Middle East	All	1.5	0.43 (0.15)	-1.60 (0.32)	0.75
North Atlantic	All	2.0	1.40 (0.09)	-2.45 (0.18)	0.76
South Atlantic	All	2.2	0.99 (0.08)	-1.93 (0.22)	0.76
Pacific	All	2.0	0.55 (0.09)	-1.69 (0.24)	0.59
North – Central/ South America	All	2.0	0.80 (0.18)	-1.37 (0.63)	0.71
Europe – Middle East	All	1.5	0.66 (0.11)	-2.58 (0.17)	0.65
Europe - Africa	All	2.0	0.82 (0.10)	-1.92 (0.13)	0.46
Other routes	All	2.0	0.78 (0.05)	-0.42 (0.07)	0.45

Appendix 2: Itinerary choice model, main parameters

For further discussion of this model and the parameters included, see section 3.1.2. Pax_{origin} and Pax_{dest} refer to the parameters for total airport passenger numbers in the previous year. Note that this model has been updated for version 9 of AIM; previously it used origin and destination airport fixed effects. Major route groups are shown below but parameters for all route groups can be found in the data file *Elasticities.csv*.

Route group	Intercept	Fare	Time	Frequency	N_{legs}	Pax_{origin}	Pax_{dest}	R^2
Intra North America	0.86 (0.004)	-3.9e-03 (5.9e-05)	-5.5e-03 (4.6e-05)	0.74 (0.004)	-1.99 (0.01)	2.75e-08 (4.1e-10)	2.79e-08 (4.1e-10)	0.59
Intra Europe	0.76 (0.006)	-5.1e-03 (8.6e-05)	-2.8e-03 (4.4e-05)	0.84 (0.004)	-3.43 (0.02)	3.9e-08 (8.8e-10)	4.0e-08 (9.0e-10)	0.65
Intra Asia	0.95 (0.01)	-2.1e-03 (1.1e-04)	-1.3e-03 (4.7e-05)	0.82 (0.009)	-3.51 (0.02)	3.5e-08 (9.9e-10)	3.6e-08 (1.0e-09)	0.58
Intra South America	0.81 (0.02)	-8.2e-03 (4.1e-04)	-1.5e-03 (1.9e-04)	0.88 (0.02)	-2.50 (0.06)	1.2e-07 (6.7e-09)	1.1e-07 (6.7e-09)	0.60
Intra Central America	0.91 (0.03)	-2.2e-03 (5.4e-04)	-1.7e-03 (1.2e-04)	0.48 (0.03)	-1.84 (0.08)	1.4e-07 (1.1e-08)	1.3e-07 (1.1e-08)	0.43
Intra Middle East	0.67 (0.04)	-3.4e-03 (4.8e-04)	-2.7e-03 (2.4e-04)	0.60 (0.03)	-2.88 (0.08)	5.2e-08 (4.6e-09)	5.2e-08 (4.5e-09)	0.91
Intra Africa	0.97 (0.03)	-1.6e-03 (1.5e-04)	-3.6e-04 (6.6e-05)	0.53 (0.03)	-1.30 (0.07)	3.9e-07 (4.0e-08)	3.5e-07 (4.3e-08)	0.85
North America - Europe	0.84 (0.006)	-8.5e-04 (4.3e-05)	-3.7e-03 (4.8e-05)	0.72 (0.006)	-2.24 (0.02)	8.2e-08 (9.7e-10)	8.1e-08 (9.8e-10)	0.91
North America - Asia	1.13 (0.01)	2.7e-04 (4.6e-05)	-2.6e-03 (5.5e-05)	0.78 (0.02)	-2.47 (0.03)	2.4e-08 (1.2e-09)	2.2e-08 (1.3e-09)	0.80
Europe - Asia	1.00 (0.01)	-5.7e-04 (3.6e-05)	-2.3e-03 (3.4e-05)	0.79 (0.009)	-2.36 (0.02)	1.9e-08 (9.2e-10)	2.1e-08 (9.6e-10)	0.90
North - South America	0.76 (0.01)	-3.2e-04 (5.2e-05)	-3.4e-03 (7.8e-05)	0.76 (0.01)	-1.81 (0.03)	8.7e-08 (2.1e-09)	8.4e-08 (2.1e-09)	0.92
Europe - Middle East	0.94 (0.01)	-2.2e-03 (7.8e-05)	-2.5e-03 (6.5e-05)	0.72 (0.09)	-2.58 (0.03)	5.6e-08 (1.8e-09)	5.6e-08 (1.8e-09)	0.91
Asia - Middle East	0.91 (0.15)	-1.8e-04 (1.2e-04)	-2.6e-03 (7.0e-05)	0.69 (0.17)	-1.91 (0.03)	3.2e-08 (2.0e-09)	3.3e-08 (1.9e-09)	0.93
Africa - Europe	1.01 (0.01)	-7.9e-04 (4.9e-05)	-1.6e-03 (3.7e-05)	0.66 (0.01)	-2.27 (0.03)	6.3e-08 (2.3e-09)	6.6e-08 (2.5e-09)	0.74
South - Central America	0.85 (0.02)	-7.25e-06 (1.5e-04)	-4.8e-03 (1.3e-04)	0.46 (0.02)	-1.01 (0.07)	1.7e-07 (9.5e-09)	1.2e-07 (9.2e-09)	0.82

Appendix 3: Fare model, main parameters

As discussed in Section 3.1.3, the fare model has many input parameters. A full set of parameters for all world regions is given in the file Elasticities.csv. Only a selection of parameters for the largest route groups are given here. A more comprehensive discussion of the fare model, the meaning of the different parameters and its validation can be found in Wang et al (2017; 2018). Note that most variables are in log form, as shown in Section 3.1.3.

Route group	Intercept	FuelCost/ pax	Nonfuel Cost/flight	Nonfuel cost/pax	Frequency	Pax	CUI	R^2
Intra North America	2.08 (0.07)	0.21 (0.004)	0.14 (0.004)	0.13 (0.01)	-0.007 (0.002)	-0.06 (0.002)	0.01 (0.002)	0.55
Intra Europe	2.48 (0.08)	0.20 (0.01)	0.18 (0.01)	-0.03 (0.01)	0.064 (0.003)	-0.07 (0.003)	0.006 (0.003)	0.64
Intra Asia	2.37 (0.16)	0.38 (0.01)	0.18 (0.01)	0.11 (0.02)	-0.053 (0.003)	-0.001 (0.003)	0.07 (0.004)	0.88
Intra South America	-1.70 (0.38)	0.23 (0.02)	0.38 (0.03)	0.78 (0.05)	-0.022 (0.01)	-0.03 (0.01)	0.04 (0.01)	0.89
Intra Central America	1.63 (0.31)	0.098 (0.02)	0.16 (0.02)	0.26 (0.04)	0.018 (0.01)	-0.08 (0.01)	0.15 (0.01)	0.87
Intra Middle East	-6.73 (1.09)	0.093 (0.05)	0.60 (0.06)	1.51 (0.14)	0.095 (0.02)	-0.09 (0.01)	0.02 (0.03)	0.81
Intra Africa	1.55 (0.59)	0.22 (0.02)	0.29 (0.02)	0.17 (0.04)	-0.02 (0.01)	-0.07 (0.01)	0.10 (0.02)	0.91
North America - Europe	1.09 (0.23)	0.15 (0.02)	0.23 (0.02)	0.071 (0.02)	0.077 (0.005)	-0.07 (0.005)	0.03 (0.01)	0.55
North America - Asia	0.64 (0.32)	0.14 (0.03)	0.27 (0.03)	0.20 (0.02)	0.043 (0.01)	-0.07 (0.004)	0.14 (0.02)	0.62
Europe - Asia	3.31 (0.19)	0.32 (0.02)	0.13 (0.02)	0.10 (0.01)	0.081 (0.004)	-0.08 (0.003)	0.10 (0.01)	0.81
North - South America	2.00 (0.44)	0.25 (0.03)	0.24 (0.04)	-0.21 (0.04)	-0.003 (0.01)	-0.06 (0.01)	0.03 (0.02)	0.73
Europe - Middle East	0.82 (0.34)	0.09 (0.03)	0.35 (0.03)	0.051 (0.03)	0.13 (0.01)	-0.10 (0.01)	0.02 (0.02)	0.82
Asia - Middle East	3.26 (0.25)	-0.03 (0.02)	0.30 (0.02)	-0.13 (0.03)	0.004 (0.01)	-0.05 (0.004)	0.02 (0.01)	0.88
Africa - Europe	3.63 (0.28)	0.16 (0.02)	0.27 (0.02)	0.075 (0.02)	0.066 (0.007)	-0.09 (0.006)	0.06 (0.01)	0.89
Europe – South America	1.06 (0.46)	0.37 (0.04)	0.19 (0.04)	0.097 (0.02)	0.13 (0.01)	-0.03 (0.01)	0.05 (0.01)	0.70

Appendix 4: Aircraft size choice model, main parameters

A full specification of the aircraft size choice model is given in Section 3.2.1. Choice parameters between the nine different aircraft size classes are estimate for travel within each world region and for travel between all world regions. A full set of parameters is given in the file AircraftData_params.csv. Example parameters for flights within Europe, within North America, within Asia and between regions are given below.

Size class	Intercept	Distance	Origin hub	Dest. hub	Pax	Load factor	Origin runway	Dest. runway	NLCC	HHI
Intra-Europe										
2	-6.74	0.0028	0.43	0.42	7.3e-06	-0.35	0.00061	0.00062	0.02	0.67
3	-10.50	0.0036	0.35	0.33	1.2e-05	3.64	0.00059	0.00058	-0.07	1.24
4	-11.24	0.0046	0.48	0.46	1.3e-05	3.73	0.00041	0.00042	0.01	1.72
5	-11.67	0.0048	0.22	0.19	1.5e-05	6.28	0.00016	0.00015	-0.06	1.91
6	-14.59	0.0060	1.00	1.01	1.6e-05	0.37	5.8e-05	0.00011	0.12	1.87
7	-15.41	0.0059	1.49	1.42	1.8e-05	0.45	0.00020	0.00022	-0.08	2.10
8	-17.65	0.0061	0.41	0.38	1.8e-05	-1.21	0.00062	0.00062	-0.03	1.75
9	-17.16	0.0054	-1.23	-1.33	1.9e-05	2.67	0.00058	0.00065	-0.61	-1.19
Between all world regions										
2	-4.29	0.0008	-0.93	-0.91	8.6e-06	-0.45	0.00038	0.00033	0.10	1.43
3	-4.82	0.0019	-0.75	-0.75	8.3e-06	0.93	0.00032	0.00023	-0.04	0.07
4	-7.14	0.0022	-1.44	-1.46	1.2e-05	1.42	0.00055	0.00048	0.06	0.87
5	-6.60	0.0024	-0.72	-0.76	1.3e-05	1.82	0.00030	0.00024	0.06	1.09
6	-19.55	0.0034	-1.33	-1.23	1.4e-05	2.28	0.0014	0.0013	-0.08	1.05
7	-17.01	0.0034	-0.97	-0.93	1.7e-05	1.86	0.0012	0.0011	-0.33	0.61
8	-23.22	0.0037	-1.06	-1.08	1.9e-05	1.62	0.0016	0.0015	-0.04	1.71
9	-27.95	0.0037	-0.59	-0.59	2.0e-05	2.10	0.0019	0.0018	-0.21	1.41
Intra North America										
2	-1.71	0.0011	-0.073	-0.07	4.2e-06	-0.93	-4e-05	-5e-05	0.047	-0.35
3	-4.37	0.0017	-0.23	-0.21	7.0e-06	-1.44	-1e-07	-1e-05	0.006	1.91
4	-2.05	0.0022	-0.53	-0.52	8.1e-06	-6.64	0.00019	0.00017	-0.04	2.94
5	-9.48	0.0026	-0.26	-0.25	8.1e-06	-0.73	0.00034	0.00033	0.07	3.82
6	-21.35	0.0038	-1.03	-1.29	6.7e-06	4.94	0.00037	0.00044	0.40	2.80
7	-19.14	0.0035	-0.44	-0.52	8.6e-06	1.28	0.00055	0.00059	0.11	5.14
8	-23.55	0.0038	-0.94	-0.87	8.7e-06	-2.53	0.00081	0.00097	0.43	7.13
9	-10.88	0.0053	-0.26	-0.20	1.4e-05	-3.71	-0.002	-0.002	0.03	2.81
Intra Asia										
1	-7.20	0.0047	-0.43	-0.39	3.5e-06	1.27	0.00033	0.00034	-0.26	0.02
2	-5.05	0.0056	0.36	0.33	3.5e-06	0.82	4.0e-05	6.5e-05	-0.10	-0.87
3	-7.54	0.0057	0.79	0.74	3.6e-06	1.53	0.00044	0.00047	-0.00	-0.32
4	-6.31	0.0057	0.57	0.53	4.1e-06	0.70	0.00046	0.00049	-0.12	-0.90
5	-18.59	0.0068	0.81	0.80	4.3e-06	2.70	0.0012	0.0012	-0.00	-0.91
6	-11.28	0.0066	1.80	1.76	4.5e-06	2.22	0.00038	0.00039	-0.16	-0.64
7	-10.88	0.0068	2.00	1.94	4.6e-06	2.10	4.5e-05	6.8e-05	-0.03	-0.91
8	-16.96	0.0069	1.59	1.61	4.8e-06	-0.84	0.0012	0.0012	-0.19	-5.09

Appendix 5: Fleet turnover model parameters

For further discussion of these parameters, see section 3.4.2, Dray (2013) and Morrell and Dray (2009). Parameters for retirement curves are given below. Note that average age at retirement (as given by the steepest part of the retirement curve) is given by $-\varphi_1/\varphi_2$.

Model	φ_1	φ_2	R^2
Narrowbody	5.10 (0.28)	-0.184 (0.011)	0.88
Widebody	6.64 (0.55)	-0.230 (0.022)	0.95
Regional Jet	3.98 (0.27)	-0.135 (0.012)	0.73
Turboprop	3.78 (0.21)	-0.114 (0.008)	0.94
Executive Jet	5.02 (0.36)	-0.124 (0.013)	0.80
< 100 seats (1960-64)	4.12 (0.58)	-0.214 (0.028)	0.97
< 100 seats (1965-71)	4.19 (0.48)	-0.161 (0.019)	0.95
< 100 seats (> 1972)	5.03 (0.41)	-0.165 (0.018)	0.92
100-190 seats (1960-64)	4.20 (0.55)	-0.192 (0.024)	0.95
100-190 seats (1965-71)	4.36 (0.52)	-0.136 (0.018)	0.94
100-190 seats (> 1972)	6.03 (0.52)	-0.211 (0.022)	0.97
190-300 seats	5.42 (0.47)	-0.140 (0.018)	0.81
> 300 seats	6.73 (0.55)	-0.242 (0.022)	0.94

Parameters for the freighter conversion model are given below.

Model	ω_1	ω_2	R^2
Narrowbody	-3.02 (0.18)	0.068 (0.007)	0.51
Widebody	-3.17 (0.11)	0.110 (0.011)	0.70
Turboprop	-1.53 (0.12)	0.048 (0.005)	0.39
Executive Jet	-5.80 (0.13)	0.129 (0.017)	0.65
100-190 seats	-3.01 (0.23)	0.037 (0.010)	0.65
190-300 seats	-4.80 (0.38)	0.165 (0.018)	0.71
> 300 seats	-2.27 (0.14)	0.079 (0.010)	0.55

Appendix 6: Default technology assumptions

The default technology parameters used in AIM are derived from Schäfer et al. (2014) and Dray et al. (2018). Both of these papers review the technologies, operational strategies and fuels which are projected to become available for aircraft over the next 50 years, including estimates of their costs, applicability and fuel use. The tables below give the assumptions used for: future generations of conventional technology aircraft; alternative aircraft technologies; retrofits to existing aircraft; and operational measures. Biofuel modelling is discussed in Appendix 7. Values in brackets give the range considered when modelling technology uncertainty. The technology data file is designed to be configurable to the study in question, so different versions may exist.

Technology	**Size class**	**Available from**	**Capital cost, million US$(2015)**	**Change in non-fuel yearly cost, million US$ (2015)**	**Change in block fuel use, %**
Next generation conventional	1	2020 (2018-2025)	40.9 (35.7-46.1)	-0.35 (- 0.3 - -0.47)	16 (15-21)
	2	2020 (2018-2025)	53.6 (46.8-60.4)	-0.4 (-0.35 - -0.55)	16 (15-21)
	3	2019 (2018-2020)	69.6 (64.7-74.6)	-	20 (15 – 22)
	4	2016	75.8 (70.4-81.3)	-	20 (15 – 22)
	5	2018 (2017-2019)	88.9 (82.5-95.2)	-	20 (15 – 22)
	6				
	7	2020 (2018-2022)	211 (189 – 233)	-0.026	12 (10 – 14)
	8	2020 (2018-2022)	251 (233-270)	-0.35 (0 – 0.07)	21 (17.5 – 23.7)
	9	2020 (2017-2022)	305 (284-323)	-0.2 (0 – 0.4)	4
Subsequent generation conventional	1	2040 (2033-2050)	41 (36-46)	-0.35 (- 0.3 - -0.47)	28 (25 – 32)
	2	2040 (2033-2050)	54 (47-60)	-0.4 (-0.35 - -0.55)	28 (25 – 32)
	3	2039 (2031-2045)	75 (68 – 82)	-	30 (26 – 34)
	4	2036 (2031-2041)	83 (75 – 90)	-	30 (26 – 34)
	5	2038 (2032-2044)	97 (87 – 106)	-	30 (26 – 34)
	6	2032 (2027-2037)	123 (114 – 132)	-	14 (12 – 14)
	7	2040 (2033-2047)	211 (188 – 233)	-0.026	24 (22 – 24)
	8	2040 (2032-2047)	251 (233 – 270)	-0.35 (0 – 0.07)	31 (29 – 33)
	9	2042 (2039-2045)	306 (284 – 324)	-0.2 (0 – 0.4)	17 (15 – 17)

Technology	Size class	Available from	Capital cost, million US$(2015)	Change in non-fuel yearly cost, million US$ (2015)	Change in block fuel use, %
Advanced Turboprop	1	2030 (2025-2035)	22 (19 – 24)	1.7 (0.9 – 2.6)	43 (37 – 46)
	2	2030 (2025-2035)	28 (24 – 31)	1.7 (0.9 – 2.6)	43 (37 – 46)
Optimised CRP	3	2035 (2030-2040)	73 (61 – 85)	0.4 (0.2 – 0.5)	41 (40 – 45)
	4	2035 (2030-2040)	98 (82 – 115)	0.4 (0.2 – 0.6)	41 (40 – 45)
	5	2035 (2030-2040)	99 (83 – 116)	0.4 (0.2 – 0.6)	41 (40 – 45)
Blended- Wing Body	6	2040 (2035-2045)	217 (180 – 289)	-0.3 (-0.2 - -0.5)	30 (15 – 40)
	7	2040 (2035-2045)	233 (194 – 310)	-0.3 (-0.2 - -0.5)	30 (15 – 40)
	8	2040 (2035-2045)	249 (207 – 332)	-0.3 (-0.2 - -0.5)	30 (15 – 40)
	9	2040 (2035-2045)	364 (303 – 485)	-0.3 (-0.2 - -0.5)	30 (15 – 40)

Technology	Size class	Available from	Capital cost, million US$(2015)	Change in non-fuel yearly cost, million US$ (2015)	Change in fuel use, %
Blended winglets	3 – 7	2015	0.85 – 1.9	-	3 (2 – 4)
Surface Polish	1 – 7	2015	0.03 – 0.13	0.03 – 0.16	1 (0.5 – 1.5)
Carbon Brakes	1 – 9	2015	-	0.015 – 0.045	0.15 (0.1 – 0.2)
Engine Upgrade Kit	1 – 7	2015	0.5 – 1.8	-	1 (0.5 – 1.5)
Re-engining	1 – 7	2015	7.1 – 16.6	-	12.5 (10 – 15)
Electric Taxi	1 – 9	2018	0.3 – 4	-	2.8 (1.8 -3.8)
Cabin Weight Reduction	1 – 9	2015	0.2 – 2.3	-	1.2 (1.2 – 2.1)

Measure	Size class	Available from	Cost, million US$(2015)	Change in fuel use, %, relevant flight phase
Surface congestion management	1 – 9	2015	0.015 – 0.06	15 (10 – 20)
Single engine taxi	1 – 9	2015	0 – 0.06	30 (20 – 40)
Optimize departures	1 – 9	2015	0.2 – 0.6	20 (10 – 30)
Reduce cruise inefficiency	1 – 9	2015	0.07 – 0.13	5.5 (2.8 – 8)
Optimize approach	1 – 9	2015	0.2 – 0.6	40 (15 – 50)
Reduced fuel reserves	1 – 9	2015	0 – 0.5	0.01 – 0.4
Reduced tankering	1 – 5	2015	0	0.26 (0.34 – 0.27)
Increased engine maintenance	1 – 9	2015	0.001 – 0.002	2.4 (1 – 4)
Increased aerodynamic maintenance	1 – 9	2015	0.001 – 0.002	1 (0.2 – 1.5)
Engine wash	1 – 9	2015	-0.1 – 0.09	0.75 (0.25 – 1)
Increased LF / reduced frequency	1 – 5	2015	0.2 – 7.6	0[g]
Increased turboprop use	1 – 2	2015	2.6	30 (25 – 32)

Appendix 7: Biofuel modelling

Biofuels can be included in AIM in several different ways, depending on the information available. The type of biofuel scenario that is run is governed by the input variable *BiofuelScenario* in *AIMRunParameters.csv*. These scenarios are detailed in the input file *BioFuelCharacteristics.csv*, which gives characteristics such as the year of initial availability, the time to full production, relative fuel lifecycle emissions in comparison to fossil Jet A and the type of cost modelling. The cost modelling parameter can take values as follows:

- CostModelType = 0. In this case, a price threshold is also set in BioFuelCharacteristics.csv. If the price of fossil Jet A is below this threshold, the biofuel price is held constant at the threshold value. If the price of fossil Jet A rises above the threshold, the biofuel price is modelled as being infinitesimally below the fossil Jet A price (including typical carbon price). This accounts for the profit-maximising behaviour of fuel producers. In this case the global availability of biofuel is limited only by the maximum blend variable ('*MaxBiofuelBlend*' in *AIMRunParameters.csv*).
- CostModelType = 2. In this case, the price is assumed to always be infinitesimally below the price of fossil Jet A (including carbon price). This explores the case in which biofuel adoption is as high as theoretically possible, but no cost data is available. Because the price is close to that of Jet A, no system changes due to increased or reduced airline costs are modelled. As above, supply is limited only by the maximum blend with fossil Jet A allowed.
- CostModelType = 3. In this case, a cost curve model is used to estimate costs and availability on a regional basis. Cost curves are derived from Hoogwijk et al. (2009), adjusted as in Searle & Malins (2015). The variation over time is scaled as for North America in DoE (2011). These cost curves give the cost of biomass; to get the cost of fuel, transport, plant investment and operations and maintenance costs are also needed. Here we assume as a central case $3.6/gallon in 2020 (year 2015 US dollars), falling to $1.8 ($1.3-$2.3) per gallon in 2050. Example cost curves for the central case over time are given in Figure 29. It is assumed that aviation has priority access to biofuels, i.e. we do not consider how much of the biomass available may be used by other sectors. However, uptake is still limited by the maximum blend variable. This is the model used for biofuel cost and availability in Dray et al. (2018).

Various assumptions can be made for the maximum biofuel blend. It can be used to limit uptake based on biomass supply assumptions and the use of biomass by other sectors (in particularly electricity generation). It can also be used to reflect current technical limits on biofuel blends. As discussed in Zschoke (2012), certified biofuels are currently limited to a 50% blend with Jet A to maintain a high enough aromatic content in the blended fuel for continued functioning of seals. Therefore under current regulation *MaxBiofuelBlend* should be no higher than 0.5. However, this constraint could be relatively easily lifted in future by adding aromatics to higher blends. Note that within the code the proportion of biofuel use for a given segment is the product of two factors: the available blend (e.g. *bioBlend*), which is limited by certification requirements and supply, and the uptake of fuel at that blend, which is affected by costs relative to Jet A and the uptake of other technologies that are incompatible with biofuels.

All fuels are assumed to be drop-in biofuels and typically a cellulosic biomass feedstock is assumed, as this has favourable cost and scalability characteristics and relatively little impact on food production. For further discussion of the biofuel modelling, see Dray et al. (2018). Note that where supply estimates in GJ or EJ are given, these refer to final totals after accounting for conversion losses during the fuel production process (see e.g. Searle & Malins, 2015).

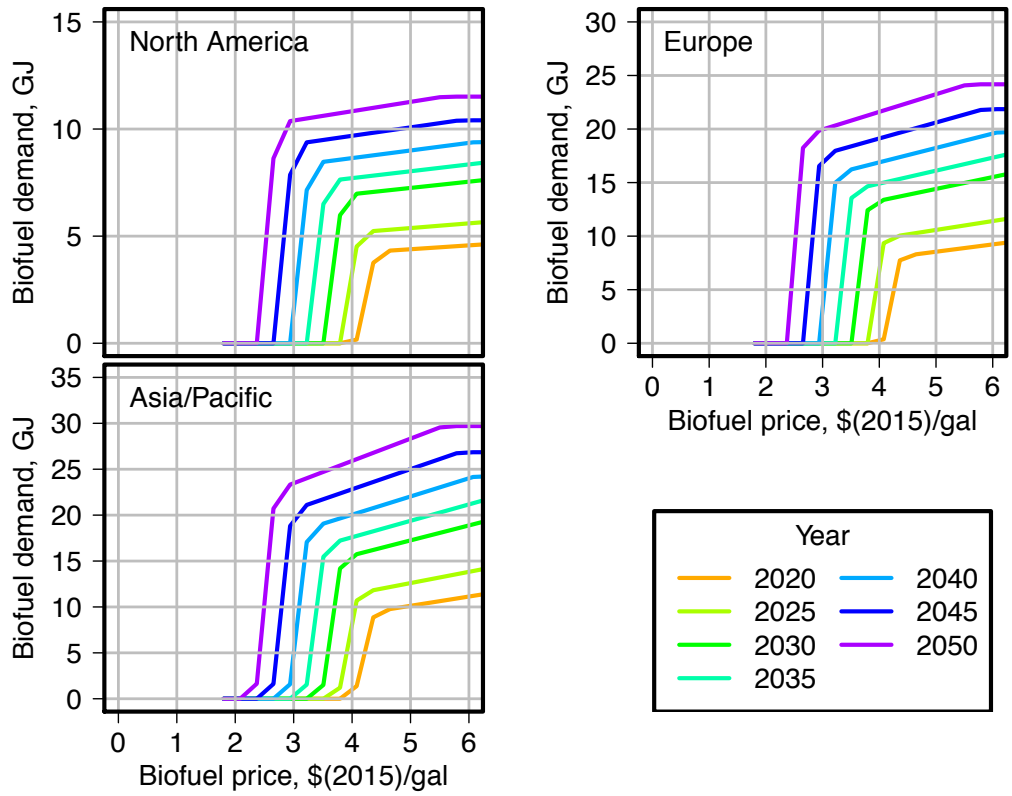

Figure 29. Biofuel cost curves used in the current version of AIM: central lens, North America, Europe and Asia/Pacific.

Appendix 8: Adding new technologies

Data on technology characteristics (including new aircraft types, retrofits and some operational measures) is stored in the input file *TechnologyMeasureData.csv*. New technologies can be simulated either by editing existing technologies in the file or by adding extra entries at the bottom. Note that if you change the number of technologies in this file you also need to: change the variable *numMeasures* in *DimensionsAndSolutionParameters.csv;* and add an extra column for compatibility with other measures in *TechnologyMeasureData.csv.*

The variables needed per line in the technology file are as follows (most important ones **bolded**):

- **MeasureName: identifying name for the technology (string, e.g. "ElectricAircraft")**
- Index: identifying number for the technology (int, e.g. 1)
- Level: gives whether these characteristics are central values (1) or reflect the pessimistic or optimistic lens assumptions (2 or 0).
- AircraftSize: applicable aircraft size class (0-8).
- **RunMeasure: 1 to run, 0 to exclude. This allows runs with different technology availability (as well as excluding size class/technology combinations that are not compatible).**
- StartYear: the year the technology first becomes available, for a given lens, size class and technology (e.g. 2018).
- EndYear: The year the technology stops becoming available (e.g. because a given retrofit is assumed to be standard on new aircraft models).
- ApplicabilityForRetrofit: gives the proportion of the fleet which are assumed to be able to retrofit this option (0 if not a retrofit, 0.2 if 20% of existing fleet are eligible). Applicability may be limited by, for example, this measure already being available on some of the fleet.
- ApplicabilityForNew: gives the proportion of new aircraft in this size class which could use this option (e.g. 1 for 100%). Note that applicability limits due to limited range are dealt with separately and should not be included here.
- **ApplicabilityTrend: gives the time period over which the S-curve model for uptake should be applied for technologies that are sufficiently different from current ones that there is likely to be a distinction between early and late adopters (see e.g. Kar, Bonnefoy & Hansman, 2010). E.g. 10 for 10 years.**
- AgeThreshold: if this technology can only be applied to aircraft above a certain age (e.g. if it is to mitigate age-based deterioration) then this gives the threshold in years (e.g. 20 for 20 years).
- **EnergyGate, EnergyTaxiOut, EnergyTakeoff etc. These variables give the change in energy use per flight phase from the reference aircraft without this technology in each size class. For example, EnergyTakeoff = -0.3 means that this technology uses 30% less energy than the reference aircraft in taking off (typically this also means 30% less fuel, but it is encoded as energy use because of aircraft that use different energy carriers). Note that for climbout, cruise and approach values are specified at two reference stage lengths, to capture technologies where benefits are dependent on stage length.**

- EINOxGate, EINOxTaxiOut, EINOx takeoff, etc. These variables capture how NOx emission index (i.e. NOx emitted per amount of fuel used) changes per phase when using this technology, relative to the reference aircraft, when this technology is used. E.g. -0.3 for 30% decrease. Note that this is often assumed 0 (i.e. NOx decreases because less fuel is used but emission index stays the same).
- EIPMGate, EIPMTaxiOut, EIPM takeoff, etc. These variables capture how PM emission index changes for the new technology relative to the reference aircraft, similarly to the NOx variables described above.
- UpfrontCosts: For new aircraft models, the estimated purchase price of the aircraft (including typical discounts from list price; note these may be 30-50% or more). For other technologies, the initial implementation cost. Year 2015 US dollars.
- YearlyCostsVol, YearlyCostsRoute, YearlyCostsLand, YearlyCostsMaint, YearlyCostsCrew: change in yearly (non-fuel/carbon, non-finance) costs by category when using this technology, relative to the reference aircraft without the technology installed. Year 2015 US dollars.
- CruiseSpeed: Indicates any change in cruise speed from the reference aircraft that might be expected using this technology (e.g. -0.1 = 10% decrease).
- **AssessmentMethodology: Set to 1 to assess using NPV (e.g. for new aircraft technologies). Set to 0 to assess using payback period (e.g. retrofits, drop-in fuels). Set to 2 to automatically assume adopted with no change in non-fuel costs (e.g. if you do not know what the costs of the technology are but want to assess its benefits).**
- Reversible: 1 if this technology can be easily stopped if no longer cost-effective (e.g. operational measures), 0 otherwise.
- AgeDependent: 1 to flag measures where the benefits change depending on aircraft age (e.g. measures to mitigate deterioration over time), 0 otherwise.
- DeltaLiquidFuelPrice: multiplicative factor for fuel price when using this technology. This applies only to stopping tankering, otherwise this should be set to 1.
- Flags: this variable flags particular types of technology measures so that they can be turned on or off together. For example Flags = 5 for ATM-based measures and 6 for alternative fuels.
- ForceBest: If applying a policy where airlines are mandated to use a particular 'best-practice' technology, this can be set to 1 for those technologies. Otherwise 0.
- LoadFactorImpact: Indicates how this measure affects average load factor (e.g. 0.05 for 5% increase, 0 for no change).
- AircraftSizeImpact: Indicates how this measure affects number of seats per size class (e.g. 0.05 for 5% increase).
- PassOnFuelBurn: Indicates whether the stock model should pass on calculated fuel burn to the LTO ops model. For example, if the main benefits come from a change in flight frequency, passing on fuel burn changes would lead to double-counting. 1 to pass on, 0 to not pass on.
- DCheckInstallOnly: 1 indicates a (retrofit) measure which would typically only be installed at a major maintainance check (roughly one opportunity every 6 years). 0 otherwise.

- ChangeInTurnaroundTime: absolute change in minimum turnaround time from using the measure, in minutes. E.g. 10 if minimum turnaround time would increase by 10 minutes.
- CompatibleWithMeasure0, CompatibleWithMeasure1, etc.: These variables capture whether this measure can be applied at the same time as the other measures in the file. Therefore there needs to be one column per measure. For example, single engine taxi is not compatible with electric taxi, and different new aircraft models are not compatible with each other. 1 if compatible, 0 if not.
- MinimumRunwayLength: Minimum runway length (m) needed to use this technology. This only needs to be set if the technology needs a substantially longer runway than the reference aircraft to take off. Otherwise set to 0.
- MaximumStageLengthIntroYear_nm: Maximum stage length in the technology introduction year, for technologies which have a range limitation. Nautical miles. Only needs to be set of the range limitation is substantially different to the reference aircraft, otherwise use a dummy large value (e.g. 100,000).
- MaximumStageLengthTimestep_years: For technologies with a range limitation, gives the timestep over which that range limitation might improve (e.g. 3 years). This might apply in the case of electric aircraft where battery technologies are continually improving. Otherwise set to dummy large value (e.g. 100).
- MaximumStageLengthPerStep_Increase: For technologies with a range limitation, gives the likely improvement in maximum range (in nautical miles) per timestep (e.g. 90). Otherwise set to 0.

Note that each combination of measure, level and size class has its own line in the file regardless of whether or not the measure can be used at that size class – if it cannot be used then runMeasure is always 0 and the remainder of the parameters take dummy values.

In interpreting outcomes, several features are worth noting. Total global emissions are aggegates over all aircraft types, sizes, stage lengths and flight phases. For example, technologies which are substantially different from existing aircraft models are assumed to have an S-curve type adoption pattern over a user-specified number of years to account for early/late adopters (see above), and fleet turnover timescales can be of order 30 years. This means that most radical new technologies will only have small impacts in the first few years after they become available. Assessing the potential of a new aircraft model may require modelling at least 10-20 years beyond its introduction date. Similarly, a technology which is highly successful in reducing emissions for a particular aircraft size class or distance may have a minor impact on global emissions if there are not also corresponding emissions reductions for other size classes and distances. Figure 30 shows how year-2015 flight departures, LTO NOx, RPK and fuel use vary with distance flown. Around half of flights are under 1,000 km and around half of fuel use is on flights under 3,000 km. Thus (broadly) emissions are divided into roughly equal halves shorter-haul/single aisle type aircraft and longer-haul/twin-aisle type aircraft. A new single-aisle design in multiple sizes which halved fuel use for comparable missions would therefore lead roughly to a 25% decrease in emissions if fully adopted. Technologies which are specifically range-limited will also only be able to realise benefits up to the proportion of global flights under that range (absent substantial changes in routing/hubbing structure).

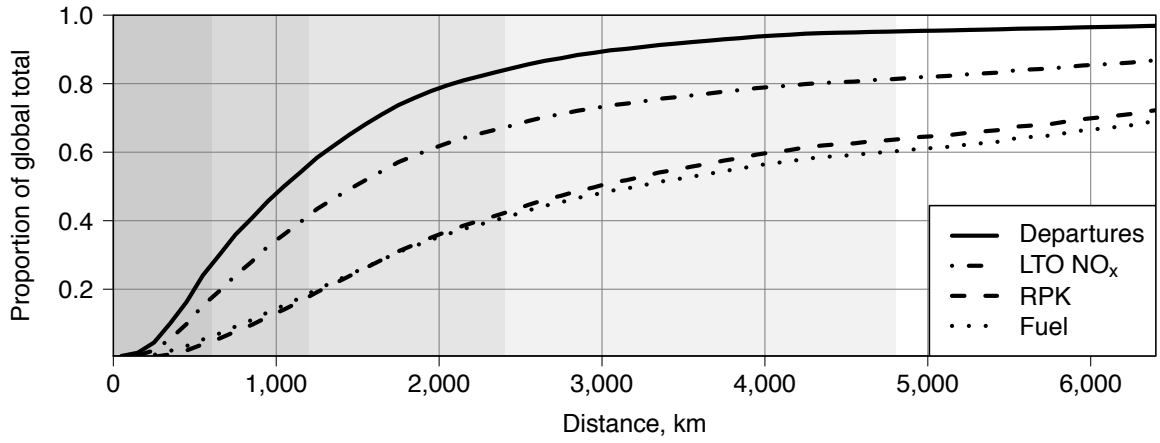

Figure 30. Global cumulative distribution of year-2015 scheduled flight departures, LTO NOx, RPK and fuel use by flight distance.

Similarly, emissions are aggregates over all flight phases. Figure 31 shows the proportion of total fuel attributed to different flight phases for different aircraft size classes and stage lengths, for an assumed 0.8 passenger load factor. 'Other' includes takeoff, landing, taxi and holding emissions. Although cruise is usually (apart from very short-haul flights) the highest-emissions phase, for a typical single-aisle flight the aggregate of other flight phase emissions is as large or larger. This means that technologies which are very successful at reducing cruise emissions, but less successful at addressing emissions in other phases, may seem to underperform. For example, a single-aisle technology which reduces cruise emissions by 40% but other phase emissions by only 20% will actually only deliver reductions of around 30% in practice.

Finally, as discussed above, the benefits of all alternative technologies are measured against a year-2015 typical technology baseline (e.g. the A320 rather than A320neo). The newest models of conventional aircraft already use 15-20% less fuel than this baseline, and (as discussed in Appendix 6 and Dray et al. (2018)), subsequent generations of conventional-technology aircraft will improve on this further. Thus the difference between radical changes in technology and the best-available conventional technology at the time may be smaller than anticipated.

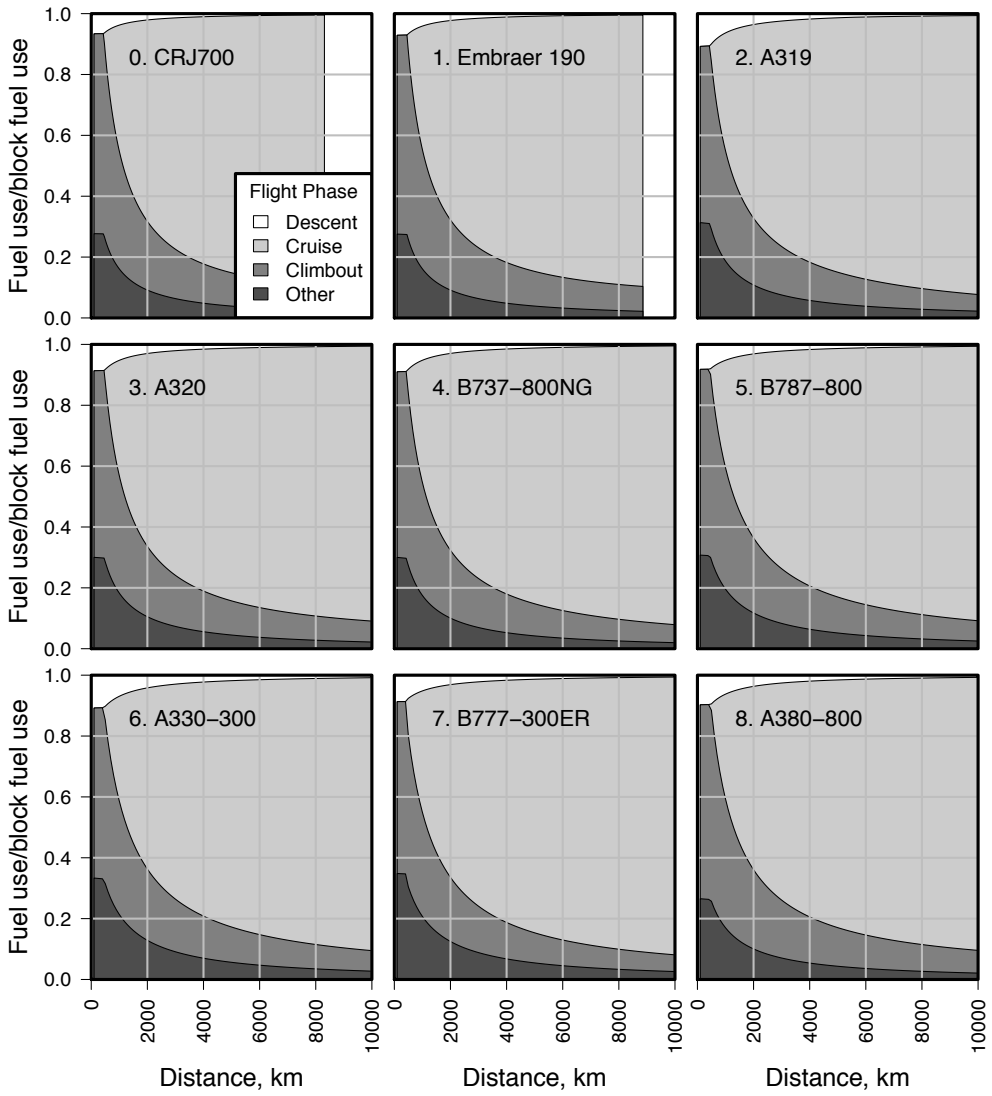

Figure 31.Distribution of fuel use to different flight phases by stage length for 0.8 assumed passenger load factor.

These effects together can often make radical new technologies appear to underperform. If a technology does not seem to be producing the benefits expected, it can be worth checking (in the output *FleetData* file) what proportion of the fleet is the new technology in each size class; and (in the input *TechnologyMeasureData* file), which size classes the technology is applicable to and how benefits differ per flight phase.